Description and phylogenetic relationships of a new species of *Torvoneustes* (Crocodylomorpha, Thalattosuchia) from the Kimmeridgian of Switzerland (#80581)

First revision

Guidance from your Editor

Please submit by **19 Mar 2023** for the benefit of the authors .

Structure and Criteria
Please read the 'Structure and Criteria' page for general guidance.

Custom checks
Make sure you include the custom checks shown below, in your review.

Raw data check
Review the raw data.

Image check
Check that figures and images have not been inappropriately manipulated.

Privacy reminder: If uploading an annotated PDF, remove identifiable information to remain anonymous.

Files

Download and review all files from the materials page.

1 Tracked changes manuscript(s)
1 Rebuttal letter(s)
20 Figure file(s)
3 Table file(s)
5 Other file(s)

Custom checks

New species checks

- Have you checked our new species policies?
- Do you agree that it is a new species?
- Is it correctly described e.g. meets ICZN standard?

Structure and Criteria

Structure your review

The review form is divided into 5 sections. Please consider these when composing your review:

1. **BASIC REPORTING**
2. **EXPERIMENTAL DESIGN**
3. **VALIDITY OF THE FINDINGS**
4. General comments
5. Confidential notes to the editor

You can also annotate this PDF and upload it as part of your review

When ready submit online.

Editorial Criteria

Use these criteria points to structure your review. The full detailed editorial criteria is on your guidance page.

BASIC REPORTING

- Clear, unambiguous, professional English language used throughout.
- Intro & background to show context. Literature well referenced & relevant.
- Structure conforms to PeerJ standards, discipline norm, or improved for clarity.
- Figures are relevant, high quality, well labelled & described.
- Raw data supplied (see PeerJ policy).

EXPERIMENTAL DESIGN

- Original primary research within Scope of the journal.
- Research question well defined, relevant & meaningful. It is stated how the research fills an identified knowledge gap.
- Rigorous investigation performed to a high technical & ethical standard.
- Methods described with sufficient detail & information to replicate.

VALIDITY OF THE FINDINGS

- Impact and novelty not assessed. *Meaningful* replication encouraged where rationale & benefit to literature is clearly stated.
- All underlying data have been provided; they are robust, statistically sound, & controlled.
- Conclusions are well stated, linked to original research question & limited to supporting results.

Standout reviewing tips

The best reviewers use these techniques

Tip	*Example*
Support criticisms with evidence from the text or from other sources	*Smith et al (J of Methodology, 2005, V3, pp 123) have shown that the analysis you use in Lines 241-250 is not the most appropriate for this situation. Please explain why you used this method.*
Give specific suggestions on how to improve the manuscript	*Your introduction needs more detail. I suggest that you improve the description at lines 57- 86 to provide more justification for your study (specifically, you should expand upon the knowledge gap being filled).*
Comment on language and grammar issues	*The English language should be improved to ensure that an international audience can clearly understand your text. Some examples where the language could be improved include lines 23, 77, 121, 128 – the current phrasing makes comprehension difficult. I suggest you have a colleague who is proficient in English and familiar with the subject matter review your manuscript, or contact a professional editing service.*
Organize by importance of the issues, and number your points	*1. Your most important issue* *2. The next most important item* *3. …* *4. The least important points*
Please provide constructive criticism, and avoid personal opinions	*I thank you for providing the raw data, however your supplemental files need more descriptive metadata identifiers to be useful to future readers. Although your results are compelling, the data analysis should be improved in the following ways: AA, BB, CC*
Comment on strengths (as well as weaknesses) of the manuscript	*I commend the authors for their extensive data set, compiled over many years of detailed fieldwork. In addition, the manuscript is clearly written in professional, unambiguous language. If there is a weakness, it is in the statistical analysis (as I have noted above) which should be improved upon before Acceptance.*

Description and phylogenetic relationships of a new species of *Torvoneustes* (Crocodylomorpha, Thalattosuchia) from the Kimmeridgian of Switzerland

Léa C Girard [Corresp., 1, 2], **Sophie De sousa oliveira** [2], **Irena Raselli** [1, 3], **Jeremy E Martin** [4], **Jérémy Anquetin** [1, 3]

[1] Department of Geosciences, University of Fribourg, Fribourg, Fribourg, Switzerland

[2] Géosciences Rennes, Université Rennes I, Rennes, Bretagne, France

[3] Jurassica Museum, Porrentruy, Jura, Switzerland

[4] Laboratoire de géologie de Lyon, terre, planète, environnement, UMR CNRS 5276 (CNRS, ENS, université Lyon 1), Ecole Normale Supérieure de Lyon, Lyon, Rhône-Alpes, France

Corresponding Author: Léa C Girard
Email address: lea.girard@unifr.ch

Metriorhynchids are marine crocodylomorphs found all across Jurassic and Lower Cretaceous deposits of Europe and Central and South America, often as isolated and fragmentary remains. Despite being one of the oldest fossil family named in paleontology, the phylogenetic relationships within Metriorhynchidae have been subject to many revisions over the past fifteen years. Herein, we describe a new metriorhynchid from the Kimmeridgian of Porrentruy, Switzerland. The material consists of a relatively complete, disarticulated skeleton preserving pieces of the skull, including the frontal, prefrontals, right postorbital, nasals, maxillae, right premaxillae and nearly the entire mandible and many remains of the axial and appendicular skeleton such as cervical, dorsal, and caudal vertebrae, ribs, the left ischium, the right femur, and the right fibula. This new specimen is referred to the new species *Torvoneustes jurensis* **sp. nov.** as part of the large-bodied macrophagous tribe Geosaurini. *Torvoneustes jurensis* presents a unique combination of cranial and dental characters including a smooth cranium, a unique frontal shape, acute ziphodont teeth, an enamel ornamentation made of numerous apicobasal ridges shifting to small ridges forming an anastomosed pattern toward the apex of the crown, and an enamel ornamentation touching the carina. The description of this new species allows to take a new look at the currently proposed evolutionary trends within the genus *Torvoneustes* and provides new information on the evolution of this clade.

Description and phylogenetic relationships of a new species of Torvoneustes (Crocodylomorpha, Thalattosuchia) from the Kimmeridgian of Switzerland.

Léa C. Girard[1,2], Sophie De sousa oliveira[2], Irena Raselli[3,1], Jeremy E. Martin[4], Jérémy Anquetin[3,1]

[1] Department of Geosciences, University of Fribourg, 1700 Fribourg, Switzerland
[2] Université de Rennes 1, Rennes 35000, France
[3] Jurassica Museum, 2900 Porrentruy, Switzerland
[4] Laboratoire de géologie de Lyon, terre, planète, environnement, UMR CNRS 5276 (CNRS, ENS, université Lyon 1), École normale supérieure de Lyon, 69364 Lyon cedex 07, France

Corresponding Author:
Léa Girard[1,2]
Chemin du Musée 6, 1700 Fribourg, Switzerland
Email address: lea.girard@unifr.ch

Abstract

Metriorhynchids are marine crocodylomorphs found all across Jurassic and Lower Cretaceous deposits of Europe and Central and South America, often as isolated and fragmentary remains. Despite being one of the oldest fossil family named in paleontology, the phylogenetic relationships within Metriorhynchidae have been subject to many revisions over the past fifteen years. Herein, we describe a new metriorhynchid from the Kimmeridgian of Porrentruy, Switzerland. The material consists of a relatively complete, disarticulated skeleton preserving pieces of the skull, including the frontal, prefrontals, right postorbital, nasals, maxillae, right premaxillae and nearly the entire mandible and many remains of the axial and appendicular skeleton such as cervical, dorsal, and caudal vertebrae, ribs, the left ischium, the right femur, and the right fibula. This new specimen is referred to the new species *Torvoneustes jurensis* sp. nov. as part of the large-bodied macrophagous tribe Geosaurini. *Torvoneustes jurensis* presents a unique combination of cranial and dental characters including a smooth cranium, a unique frontal shape, acute ziphodont teeth, an enamel ornamentation made of numerous apicobasal ridges shifting to small ridges forming an anastomosed pattern toward the apex of the crown, and an enamel ornamentation touching the carina. The description of this new species allows to take a new look at the currently proposed evolutionary trends within the genus *Torvoneustes* and provides new information on the evolution of this clade.

Introduction

Thalattosuchia Fraas, 1901 is a clade of mostly marine crocodylomorphs that existed from the Early Jurassic to the Early Cretaceous and had a global distribution from the eastern margins of the Tethys, the opening Atlantic Ocean, down to the coasts of South America, China and north of Africa (Fraas, 1901, 1902; Andrews, 1913; Gasparini & Iturralde-Vinent, 2001; Fara *et al.*,2002; Frey *et al.*, 2002; Buchy *et al.*, 2006b; Herrera *et al.* 2015b; Johnson *et al.*, 2020b; Young *et al.*, 2020a; Wilberg *et al.*, 2022). Thalattosuchians are subdivided into the more coastal Teleosauroidea Geoffroy Saint-Hilaire, 1831, and the exclusively pelagic Metriorhynchoidea Fitzinger, 1843. Among archosaurs, ~~metriorhynchoids, and in particular~~ Metriorynchidae Fitzinger, 1843, show the most developed morphological adaptations to life at sea, including: limbs transformed into flippers with a great reduction of the forelimbs and a simplification of the pelvic girdle; lengthening of the body; loss of osteoderms; a smooth skin; a hypocercal tail; a slender and lighter skull; hypertrophied salt glands; orbits placed laterally and overhung by the prefrontals; loss of the mandibular fenestra (Fraas, 1902; Andrews, 1913; Vignaud, 1995; Frey *et al.*, 2002; Gandola *et al.*, 2006; Pierce *et al.*, 2009; Young & Andrade, 2009; Young *et al.*, 2010, 2020a, 2020b; Herrera *et al.*, 2013a, 2015; Foffa *et al.*, 2018c; Sachs *et* al., 2021; Spindler *et al.*, 2021; LeMort *et al.*, 2022). ~~This association of characteristics gives metriorhynchids a unique morphology.~~

Metriorhynchids include two subclades. Metriorhynchinae Lydekker, 1889 are usually characterized by a slender body, an elongated snout, and a higher count of poorly ornamented teeth (Parrilla-Bel *et al.*, 2013; Sachs *et al.*, 2021). In contrast, Geosaurinae Lydekker, 1889 are more robust macrophagous predators with shorter snouts and a reduced number of large, often ornamented, ziphodont teeth (Young *et al.*, 2012b, 2015). During the Middle Jurassic, each of these groups saw the emergence of the more derived tribes Rhacheosaurini and Geosaurini, respectively (Young *et al.*, 2013a, b, Foffa and Young, 2014b, Foffa *et al.*, 2018a). The diversity of metriorhynchids has long been underestimated, but intensives revisions in the last two decades and the description new material significantly improved the knowledge of the group and its inner phylogenetic relationship (Frey *et al.*, 2002; Wilkinson *et al.*, 2008; Pierce *et al.*, 2009; Young & Andrade, 2009; Andrade *et al.*, 2010; Wilberg, 2012; Young *et al.*, 2010, 2020a, 2020b; Cau and Fanti, 2011).

Compared to their counterparts in England or Germany, the late Jurassic metriorhynchid fossil record of Switzerland is relatively poor. Most of the fossils of swiss thalattosuchians belongs to teleosauroids (Krebs, 1967; Guignard & Weidmann, 1977; Rieppel, 1981) with rare occurrence of metriorhynchoids (Schaefer *et* al., 2018; Abel *et al,* 2020; Young *et al.*, 2020b). In addition to the specimen described herein, several specimens of Thalattosuchia have been excavated in the canton of Jura in the past 20 years. They are mainly represented by isolated teeth, but a few well preserved teleosaurid skulls and skeletons are known (Schaefer, 2012; Schaefer *et al.*, 2018). Unidentified remains of metriorhynchids have been found in the canton of Jura in the form of a nasal, frontal, femur and vertebrae, as well as a single tooth of *Dakosaurus* Quenstedt, 1856 (Schaefer *et al.*, 2018). A metriorhynchid anterior rostrum is also known from the lower Tithonian of Bern representing an indeterminate Rhacheosaurini (Rieppel, 1979, Young *et al.*,

2020b). Here we describe a new specimen from the upper Kimmeridgian of the Jura Canton of Switzerland (Fig. 1). It consists of a relatively complete, associated skeleton with many cranial and postcranial bones preserved. This specimen is identified herein as a new species of the genus *Torvoneustes* Andrade, *et al*, 2010 and located in the phylogenetic context of Metriorhynchidae. This material also allowss a reassessment of the evolutionary trends previously proposed for the genus.

Materials & Methods

Material

MJSN BSY008-465 is a disarticulated metriorhynchid skeleton (Fig. 2). The specimen was initially collected by the Pal A16 on a large block of limestone. Bones were prepared directly on the surface and kept on pedestals of rock. This initial phase of preparation, especially the acid preparation, was poorly controlled and resulted in damages of the more fragile bony elements such as some cranial and mandibular elements. More recently, all bones were completely removed from the block to facilitate scientific study. The preserved remains of MJSN BS008-465 include cranial and mandibular elements as well as material from the axial and appendicular skeleton. Many elements are fragmented and show evidence of deformation.

The preserved elements of the cranium include the frontal, prefrontals, right postorbital, nasals, maxillae, right premaxillae. The mandible is almost complete and preserve both angulars, surangulars, articulars, splenials, and dentaries. Many isolated teeth are also preserved. The postcranial elements include cervical, dorsal, and caudal vertebrae, ribs, the left ischium, the right femur, and the right fibula. Numerous bone fragments are not identifiable.

Geological setting

Between 2000 and 2011, controlled paleontological excavations were conducted by the Pal A16 before the construction of the A16 Transjurane highway in the Canton of Jura (Fig. 1). They revealed the presence of several rich fossiliferous horizons of marls and limestones, as well as many dinosaurs tracksites in the Ajoie region around the city of Porrentruy (Marty *et al.*, 2003). During the Late Jurassic, this region was part of a carbonate platform with diversified shallow depositional environments such as lagoons, reefs, channels and littoral zones forming layers rich in marine fossils (Colombié and Strasser, 2005; Comment *et al.*, 2015).

MJSN BSY008-465 was found in 2008 on the hardground level 4000 of the Lower *Virgula* Marls (Fig. 3) in the locality Courtedoux-Bois de Sylleux, Switzerland (Fig. 1). The Lower *Virgula* Marls belong to the Chevenez Member of the Reuchenette Formation. They dateto the late Kimmeridgian and correspond to the end of the *Mutabilis* ammonite zone and beginning of the *Eudoxus* ammonite zone (Comment *et al.*, 2015). These marls are notably characterized by the abundance of the small oyster *Nanogyra virgula* Koppka, 2015, which gives them their name. The hardground level 4000 is rich in invertebrates, notably encrusted and benthic bivalves and brachiopods. Vertebrates are mostly represented by isolated material, to the exception of the metriorhynchid MJSN BSY008-465 described herein, a partial teleosauroid skeleton

provisionally referred to *Steneosaurus* cf. *bouchardi*, now combined as *Proexochokefalos* cf. *bouchardi* (Schaefer *et al.*, 2018; Johnson *et al.*, 2020b), and a relatively complete shell of the thalassochelydian turtle *Thalassemys bruntrutana* Puntener, Anquetin, and Billon-Bruyat, 2015 (Püntener *et al.*, 2015).

Phylogenetic analyses

The phylogenetic analyses were conducted using the data matrix and procedure of Young *et al.* (2020a), which were derived from Young *et al.* (2020b). The original matrix includes 179 taxa coded for 574 characters. The outgroup is *Batrachotomus kupferzellensi*s Gower, 1999. The matrix was modified with Mesquite 3.61 (Maddison & Maddison, 2019) to include MJSN BSY008-465 as a new operational taxonomic unit (see Suplementary data). The latter was scored for 204 characters. The analytical procedure strictly follows the one described by Young *et al.* (2020a). The parsimony analyses were conducted using TNT 1.5 (No taxon limit) (Goloboff *et al.*, 2008 ; Goloboff & Catalano, 2016) with the RAM increased to 900 Mb. The analysis used the scripts provided by Young *et al.* (2020a) and consisted of an unweighted analysis followed by seven different extended implied weighting analyses (k=1, 3, 7, 10, 15, 20 and 50). The main script (EIW.run) runs an initial "new technology" search (xmult:hits 10 replications 100 rss css xss fuse 5 gfuse 10 ratchet 20 drift 20; sec:drift 10 rounds 10 fuse 3; ratchet:numsubs 40 nogiveup; drift:numsubs 40 nogiveup) holding 20,000 trees per analysis, then runs a "traditional methods" search (bbreak:TBR) on the saved trees. The script then computes the descriptive statistics, the strict consensus tree, the majority rule consensus tree, and the maximum agreement subtree (for more details, see Young *et al.*, 2020a).

The Bayesian analysis was conducted using MrBayes3.2.7 (Ronquist *et al.*, 2012), again following the procedure described by Young *et al.* (2020a). The sampling model is a Markov Chain Monte Carlo with only variable characters scored and a Gama distribution (Mkv+G model). Five independent analyses are run, each with 10 chains for 10 million generations with a sampling every 5000 generations and a burn-in of 40% (for more details, see Young *et al.*, 2020a). At the end of the analysis, the consensus tree is saved.

Imaging

Each element of the cranium of MJSN BSY008-465 was individually scanned with a portable surface scanner (Artec Space Spider). The scans were treated with the software Artec Studio 13 to produce textured 3D models. The elements were assembled in Blender 2.8 in order to reconstruct the skull of MJSN-BSY008-465 in 3D (De Sousa Oliveira *et al.*, in press). This technique helped the description ~~and comprehension~~ of the specimen and highlighted lost contacts between the bones. The 3D models of each individual element, as well as the reconstructed skull and mandible are made openly available in De Sousa Oliveira *et al.* (in press).

The microscopic observation and detailed photographs of the teeth of MJSN BSY008-465 were realized with a digital microscope (Keyence VHX-970F).

Institutional abbreviations

BSPG, Bayerische Staatssammlung für Paläontologie und Geologie, Munich, Germany; CAMSM, Sedgwick Museum, Cambridge, UK; IGM, Colección Nacional de Paleontología, Instituto de Geología, México, Mexico; MANCH, Manchester Museum, Manchester, UK; NHMUK, Natural History Museum, London, UK; NHMW, Naturhistorisches Museum Wien, Vienna, Austria; MHNG, Muséum d'Histoire Naturelle, Genève, Switzerland; MJML, Museum of Jurassic Marine Life, Dorset, UK; MJSN, Jurassica Museum (formerly Musée Jurassien des Sciences Naturelles), Porrentruy, Switzerland; NKMB, Naturkunde Museum Bamberg, Bamberg, Germany; MUDE, Museo del Desierto, Saltillo, Mexico; OUMNH, Oxford University Museum of Natural History, Oxford, UK; SMNS, Staatliches Museum für Naturkunde Stuttgart, Baden-Württemberg, Germany; YORYM, Yorkshire Museum, York, UK.

Results

Systematic palaeontology

CROCODYLOMORPHA Hay, 1930

THALATTOSUCHIA Fraas, 1901

METRIORHYNCHIDAE Fitzinger, 1843

GEOSAURINAE Lydekker, 1889

GEOSAURINI Lydekker, 1889

Torvoneustes Andrade, Young, Desojo & Brusatte, 2010

Diagnosis: see in Young *et al*., 2013b

Type species: *Dakosaurus carpenteri* Wilkinson, Young and Benton., 2008

Included valid species: *Torvoneustes coryphaeus* Young, Andrade, Etches and Beatty, 2013b; *Torvoneustes mexicanus* (Wieland, 1910); *Torvoneustes jurensis* sp. nov.

Occurrence: Kimmeridgian of Mexico (Barrientos-Lara *et al.*, 2016); Kimmeridgian of Dorset, UK (Grange and Benton, 1996; Wilkinson *et al.*, 2008, Young *et al.* 2013b); middle Oxfordian to

Tithonian of Oxfordshire, UK (Young, 2014); middle Oxfordian of Yorkshire (Foffa *et al.*, 2018b); late Kimmeridgian of Canton Jura, Switzerland (Schaefer *et al.*, 2018); upper Valanginian of Moravian-Silesian Region, Czech Republic (Madzia *et al.*, 2021).

Torvoneustes jurensis sp. nov.
urn:lsid:zoobank.org:act:5DEFCF6F-D7EF-4711-9CB6-A7219F612ECB
Figs 2 and 4–16

Diagnosis: *Torvoneustes jurensis* sp. nov. is identified as a member of *Torvoneustes* by the following combination of characters: robust teeth lingually curved, conical crown, bicarinate with a prominent keel; enamel ornamentation made of conspicuous subparallel apico-basal ridges on the basal two thirds of the crown shifting to short, low-relief ridges forming an anastomosed pattern on the apex; carinae formed by a keel and true microscopic denticles forming a continuous row on the distal and mesial carinae; enamel ornamentation extending up to the carinae near the crown apex; inflexion point on the lateral margin of the prefrontals directed posterolaterally in dorsal view, at an angle of approximately 70 ° from the anteroposterior axis of the skull; acute angle (close to 60°) between the posteromedial and the lateral processes of the frontal. *Torvoneustes jurensis* differs from the other species of *Torvoneustes* by the following combination of characters: presence of a distinct angle between the anteromedial and the lateral processes of the frontal; smoother overall ornamentation of the skull bones. *Torvoneustes jurensis* also differs from *To. carpenteri* in: lacking "finger-like" projections on the posterior margin of the prefrontal; angle of 142° in average between the anterior and lateral processes of the frontal; and having a long anteromedial process of the frontal reaching the same level as the anterior margin of the prefrontals (shorter process in *To. carpenteri*). *Torvoneustes jurensis* is also clearly distinct from *To. coryphaeus* in having: a tooth enamel ornamentation extending up to the carinae; prefrontals with a rounded distal margin (forming an acute angle in *To. coryphaeus*); and a supraorbital notch of 90° (45° in *To. coryphaeus*). The slender morphology, acuteness, and great number of teeth of *Torvoneustes jurensis* nov. sp. differs from both *To. coryphaeus* and *To. carpenteri*. *Torvoneustes jurensis* differs from *To. mexicanus* in having irregular denticle basal length (120–200µm, mean: 160µm) and distribution (density up to 40 denticles/5mm in the upper middle part of the crown and down to 30 denticles/5mm in the base and apex) on the carinae (regular basal length of 142 µm and density of 30 denticles/5mm in *To. mexicanus*).

Etymology: The species is named after the Jura, which corresponds to both the mountain range and the Swiss canton ~~from~~ where the holotype was found. The complete name could therefore be translated from Latin as “savage swimmer from Jura”.

Holotype: MJSN BSY008-465, a relatively complete disarticulated skeleton including the frontal, prefrontals, right postorbital, nasals, maxillae, right premaxillae, angulars, surangulars, articulars, splenials, dentaries, several isolated teeth, cervical, dorsal, and caudal vertebrae, ribs, the left ischium, the right femur, and the right fibula (Fig. 2 and Fig. 4–16).

Type horizon and locality: Courtedoux-Bois de Sylleux, Ajoie, Canton of Jura, Switzerland (Fig. 1). Lower Virgula Marls, Chevenez Member, Reuchenette Formation, late Kimmeridgian (Eudoxus ammonite zone), Late Jurassic (Fig. 3; Comment *et al.*, 2015).

DESCRIPTION

Cranium

Cranial elements are disarticulated except for the frontal preserving its contact with the left prefrontal. The preserved elements of the cranium are exclusively part of the skull roof and snout. Many pieces are fractured, incomplete, and/or deformed. As a result, the general shape and size of most of the skull fenestrae and apertures, such as the preorbital fossae, orbits, and supratemporal fenestrae cannot be clearly determined. Based on the skull reconstruction (Fig. 4), the skull total length is estimated at 88 cm, and the rostrum length (nasals and maxillae) is about 49 cm (55.7% of the total skull length), corresponding to the mesorostrine condition as defined by Young *et al.* (2010). The skull width-to-length ratio is 0.28. The supratemporal fenestrae are greatly enlarged and the orbits are facing laterally (Fig. 4).

Premaxillae.

An incomplete right premaxilla is preserved. Its anterior part is severely damaged and the posterior part, including the contact with the maxilla, is missing. The external nares aperture is partly conserved, oblong, moderate in width and formed entirely by the premaxilla (Fig. 5d, 5e). A complete, laterally located alveolus is visible in ventral view. In dorsal view, the external surface of the bone is smooth except for a few superficial pits. The bone thickens on the external edge of the narial opening and close to the alveolus, but it thins posteriorly. The alveolar orientation suggests a tooth implantation directed anteroventrally (Fig. 4c).

Maxillae.

Both maxillae are preserved. The right maxilla is almost complete, only missing its anteriormost part and the posterior end of the tooth row (Fig. 6). This element is heavily fractured and deformed, especially in its anterior part where the bone was broken in several parts and glued back together. This anterior part, is deformed and stretched anteriorly. The remaining matrix prevents the observation of the medial side of the right maxilla. The left maxilla is incomplete and broken in four parts. Some of the fragments are severely damaged. Both maxillae contact with a posteromedial process which is probably formed by the palatine. As preserved, the right maxilla is 49.8 cm long. In ventral view, it widens in its posterior region. In lateral and dorsal view, the bone surface is smooth with only pitting ornamentation on its anterior half (Fig. 6). Shallow grooves extend a few millimeters posterior to some of the foramina but are barely visible and can only be spotted on the 3D model (see Supplementary material). Most other members of the Geosaurini subclade with known maxillae present conspicuous surface bone ornamentation made of grooves and ridges, often with a unique pattern (Young *et al.*, 2013b).

Plesiosuchus manselii and *To. coryphaeus* both have maxillae ornamented with grooves and raised ridges, while *Dakosaurus maximus* has additional pits to this ornamentation pattern (Young *et al.*, 2012a; Young *et al.*, 2013b). The incomplete maxilla of cf. *Torvoneustes* (MANCH L6459) shows a similar pattern to *To. coryphaeus* with moderate to strong grooves and a raised edge aligned with the sagittal axis of the skull but lack posteroventral foramina (Young, 2014). *Torvoneustes carpenteri* has a pattern of pits and grooves on the lateral edge of its maxilla (Grange and Benton, 1996; Wilkinson *et al.*, 2008). In contrast, MJSN BSY008-465 has an ornamentation pattern closer to the one seen in *Geosaurus giganteus*, or *Purranisaurus potens* (Young & Andrade, 2009; Young *et al.*, 2013b, Herrera *et al.*, 2015a).

The alveoli are set on a slightly more dorsal plane than the palatal surface of the maxilla. The medial margin of the palatal plate of the right maxilla bears a longitudinal furrow that likely corresponds to the maxillary palatal groove. Each maxilla preserves at least 15 alveoli, which is more than the estimated number of 14 (with 11 strictly preserved alveoli) for *To. carpenteri* (Grange and Benton, 1996; Wilkinson *et al.*, 2008; Young *et al.*, 2013b) and less than the estimated alveolar count of 17-19 for *To. coryphaeus* (Young *et al.*, 2013b). However, there is at least one or two missing alveoli on MJSN BSY008-465 considering the dentary alveolar count. None of the specimens referred to the genus *Torvoneustes* preserves a complete maxilla, therefore this character should be treated carefully (see Discussion). Among derived Geosaurini, maxillary alveolar count is usually estimated to be lower than 16 (Table 1; Wilkinson *et al.*, 2008; Young & Andrade, 2009; Young *et al.*, 2012b). The alveoli are large, overall homogeneous in size, slightly anteriorly oriented and subcircular with a slightly longer anteroposterior axis than their mediolateral axis, which differentiates MJSN BSY008-465 from the members of the informal 'E-clade' taxa whose members show the opposite condition (Abel *et al.*, 2020). The interalveolar space is homogeneously narrow, being less than a quarter the length of the adjacent alveoli. Tooth enlargement and interalveolar space reduction are characteristics shared among several members of the Geosaurini subclade (Herrera *et al.*, 2015b) like *Dakosaurus, Plesiosuchus* (Young *et al.*, 2012b), *P. potens* (Herrera *et al.*, 2015a) some members of the 'E-clade' (Abel *et al.*, 2020) and *Torvoneustes* (Grange and Benton, 1996; Wilkinson *et al.*, 2008; Young *et al.*, 2013b; Young, 2014). The maxillary sutural surfaces with the nasal and premaxilla are visible asslopes of the bone in lateral view. In medial view, the maxilla is concave to accommodate the nasal cavity and thicker around the tooth row. A notch between the 5th and 6th alveoli (Fig. 6a) on the right maxilla is a reception pit but is the only one on the fossil and therefore does not support a tooth-on-tooth vertical interlocking as seen in *Dakosaurus* (Young *et al.*, 2012a) or *Tyrannoneustes lythrodectikos* (Foffa and Young, 2014). In addition, there is no evidence for a maxillary overbite as seen in *Geosaurus giganteus* (Young & Andrade, 2009). It is ~~therefore~~ likely that the tooth occlusion of MJSN BSY008-465 follows the same interdigitated pattern as in *To. mexicanus* (Barrientos-Lara *et al.*, 2016).

Nasal

Both nasals are present as symmetrical, unfused elements (Fig 5a, 5b). The right nasal is the best preserved, most complete and less deformed of the two. The nasals are flattened by taphonomy, the left one more so than the right one. The anterior process of the right nasal is curved upward due to postmortem deformation. The posterior part of the right nasal has been fractured then glued back but is not perfectly aligned. This same part is lost in the left nasal. The anterior part of the left nasal is broken and bent laterally. The bone surface is smooth. Only a few elliptical pits are present along the anterolateral parts (Fig. 5a, 5b). This ornamentation pattern differs from the one seen in *To. coryphaeus* (Young *et al.*, 2013b), *P. manselii*, *D. maximus* (Young *et al.*, 2012b), and cf. *Torvoneustes* (MANCH L6459) (Young, 2014). However, it is consistent with other species of Geosaurini with smooth and pitted nasals such as *To. carpenteri* (Grange and Benton, 1996), *G. grandis, G. giganteus* (Young & Andrade, 2009), and *Dakosaurus andiniensis* (Pol and Gasparini, 2009). The end of the dorsoposterior process, which should contact the lacrimal, is lost in both nasals. Overall, the nasals are triangular in shape, with the anterior part being elongate and acute. This shape is found in most metriorhynchoids (Andrews, 1913; Lepage *et al.*, 2008) including rhacheosaurines such as *Cricosaurus* Wagner, 1858 (Fraas, 1902.; Herrera et al., 2013; Parrilla-Bel and Canudo, 2015, Sachs *et al.*, 2019; 2021), derived geosaurins like *Dakosaurus, Plesiosuchus, Torvoneustes, Purranisaurus* (Wilkinson *et al.*, 2008; Pol & Gasparini, 2009; Young *et al*., 2012b, 2013b; Herrera et al., 2015a) and basal ~~M~~etriorhynchoid ~~like~~ *Pelagosaurus typus* Bronn, 1841 (Pierce & Benton, 2010). Based on ~~the sutural contacts with the maxillae and~~ the skull reconstruction (Fig. 4), ~~it appears that~~ the nasals do not reach the premaxillae anteriorly. The posteromedial, posterolateral, and anterolateral sutural surfaces of the nasal with the frontal, the prefrontal, and the maxilla, respectively, are well preserved. On the median edge, a subtle angle marks the limit between the nasal-frontal and the median nasal sutures. The two nasals would contact on the midline of the skull, the medial concavity of the nasals in dorsal aspect suggests the presence of the longitudinal depression at their contact, a metriorhynchoid apomorphy (Young *et al.*, 2012).

Prefrontal

Both prefrontals are preserved, but the anterior parts and the descending processes are missing. The left prefrontal is still connected with the frontal (Fig. 7) while the right one is found apart (Fig. 5c). The right prefrontal seemingly suffered more damage than the left one, with the bone surface being partially flaked off and the bone flattened and stretched. It has also been broken and glued back together. The left prefrontal shows little deformation but is raised in its anterior part above the level of the frontal during taphonomy. The posterior part of the descending process on both prefrontals is barely preserved as a thin, concave structure. In dorsal view, the prefrontal is large, laterally extended, and it partially overhangs the orbit (Fig. 4a), a feature common within Metriorhynchidae (Fraas, 1902; Andrews, 1913; Herrera *et al.*, 2015a; Young *et al.*, 2010). The bone surface is smooth with numerous round or elliptical pits, as in *P. potens* (Herrera *et al.*, 2015a), more densely distributed on the anteromedial part (Fig. 5c, 7). As in most metriorhynchids, the posterolateral corner of the prefrontal is rounded in MJSN BSY008-

465 (Andrews, 1913; Lepage *et al.*, 2008), which differs from the geosaurines *To. coryphaeus* (Young *et al.*, 2013b) and *D. maximus* (Young *et al.*, 2012a, Pol and Gasparini, 2009) in which the posterolateral corner is angular. The inflection point of this corner is directed posteriorly and forms with the midline of the skull an angle of about 70°, which is found in other Geosaurinae such as *To. carpenteri, D. maximus*, and *D. andiniensis*. A posteriorly directed inflection point of the prefrontal of 70° or less is an apomorphy of the tribe Geosaurini (Cau and Fanti, 2011). If they share a similar shape, the posterior edge of the prefrontals in MJSN BSY0008-465 lacks the "finger-like" projections described in *To. carpenteri* (Young *et al.*, 2013b).

Frontal

The frontal is mostly complete but somewhat flattened during taphonomy (Fig. 7). It consists of a single unpaired element without external sign of a medial suture. Only the anterior most part of the anteromedial process and portions of both intratemporal flanges are missing. The medioventral part of the left lateral process is extended in ~~the~~ posteromedial direction (Fig. 7). Remaining matrix prevents the observation of the ventral side of the frontal. The anteromedial process of the frontal is broad, triangular in shape and extends anteriorly between the nasals. Considering the nasals geometry and preserved sutural contacts (Fig. 4), it is likely that the anterior process of the frontal ended in an acute tip, almost reaching the level of the anterior margin of the prefrontals as seen in cf. *Torvoneustes* (MANCH L6459) and *To. coryphaeus* (Young *et al.*, 2013b; Young, 2014). This differs from the shorter process of *To. carpenteri* (Grange and Benton, 1996; Wilkinson *et al.*, 2008), but the crushing of the specimen might ~~induce an observation bias of~~ this character. Posteriorly, the frontal has two lateral processes forming the anterior margin of each supratemporal fenestrae, and a posterior process forming the anterior part of the intertemporal bar. The opening between the posterior and the lateral processes form an angle of approximately 60°, which is commonly found among geosaurines whereas metriorhynchines typically show an angle of about 90° (Wilkinson *et al.*, 2008). The posterior process is straight with a constant width of 23 mm~~. At its posterior end, where the contact with~~ the parietal ~~takes place, two deep grooves form~~ a M-shaped, strongly digitated suture (Fig. 7). The intratemporal flanges (*sensu* Buchy, 2008) extend ventrally from the posterior and lateral processes. They form a triangular area with faint pitting inside the anterior corner of the supratemporal fenestrae. The anterior outline of the supratemporal fossa suggests that it was longer than wide and ovoid in shape, which is a common feature among geosaurines (Buchy, 2008). The supratemporal fenestrae extend far anteriorly and almost reach the level of the interorbital minimal distance (Fig. 7). This condition is seen in both *To. carpenteri* and *To. coryphaeus* as well as within *G. grandis* (Foffa and Young, 2014, fig. 9). In dorsal view, the external surface of the frontal is smooth with occasional pitting on the center of the bone, mostly concentrated on the anterior part of the posterior process. This differs from the ornamented frontal of *To. coryphaeus* (Young *et al.*, 2013b), as well as from the anteroposteriorly aligned grooves and ridges observed in the frontal of cf. *Torvoneustes* (MANCH L6459; Young, 2014). In contrast, it resembles the description of *To. carpenteri* (Grange and Benton, 1996; Wilkinson

et al., 2008). In *To. carpenteri* and *To. coryphaeus,* the anterior and lateral processes of the frontal form an almost straight line or a slight concavity (Young *et al.*, 2013b), whereas in MJSN BSY008-465 there is a clear angle of 142° between the processes, measured on the better preserved left side (Fig. 7b). The inflection point is probably located at the meeting point between the frontal, nasal and prefrontal.

Postorbital

Only the part forming the anterolateral margin of the supratemporal fossa of the right postorbital is preserved (Fig. 8a-c). It is broken around its middle and was glued back together. The ventrolateral part, that should make a major contribution to the postorbital bar, is missing. The posterior portion of the postorbital curves slightly laterally but this is probably the result of postmortem deformation. Two processes are distinguishable on what is preserved of the postorbital. The anterior process is anteromedially oriented in dorsal view, making most of the curve of the lateral edge of the supratemporal fossa, and was in contact with the frontal. The posterior process is almost straight, slightly posteromedially oriented, and was in contact with the squamosal. The contact with the lateral process of the frontal is V-shaped, as described in several other metriorhynchids like *Ty. lithrodectikos* (Andrews, 1913; Foffa and Young, 2014). In the posterior part, the postorbital becomes a thin raised ridge that forms the anterior part of the postorbital-squamosal ridge. Posteriorly, the postorbital-squamosal suture is not readily observable but a change in the bone texture on the medial surface of the bone could match with a similar change on the anterior part of the right squamosal. In medial view, a deep incision in the postorbital marks the contact with the frontal (Fig. 8b), which agrees with observations made on complete skulls of other Metriorhynchidae (Andrews, 1913; Young *et al.*, 2013b). This contact marks the point where the postorbital extends medioventrally to take part in the intratemporal flange. Based on the skull reconstruction, the postorbital likely extended further laterally than the prefrontal, resulting in an enlarged supratemporal fossa as usually seen in metriorhynchids (Wilkinson *et al.*, 2008; Foffa and Young, 2014). The bone surface is unornamented except for one elliptical foramen on the anterior process. There might be another foramen at the corner of the "V-shaped" suture but it is hard to discern due to poor bone preservation.

Squamosal

Both squamosals are present but only their dorsal portion is preserved. The descending process, which participated to the occipital region, is lost. The right squamosal is the better preserved than the left. In dorsal view, the medial part of the right squamosal is concave (Fig 8f), forming a characteristic "L-shape" (Andrews, 1913; Foffa and Young, 2014; Pol and Gasparini, 2009). The anterior part was in contact with the postorbital. This suture is not readily visible, but a change in bone texture could match with the one seen on the postorbital (see above). A marked ridge separates the squamosal in a medial and a lateral half consisting in a vertical descending surface forming the squamosal flat surface. This ridge forms the posterior part of the postorbital-squamosal ridge, whose postorbital-squamosal contact would be an area of muscle attachment

(Holliday & Witmer, 2007, 2009; Young *et al.*, 2013b) This ridge is present in all Metriorhynchidae but significantly lower among Metriorhynchinae compared to Geosaurinae (Andrews, 1913; Lepage *et al.*, 2008; Pol and Gasparini, 2009; Young *et al.*, 2012b; 2013b; Young & Andrade, 2009). The median process of the squamosal forms the posterolateral corner of the supratemporal fossa and was probably in contact with the lateral process of the parietal, this contact however isnot preserved. The posterior edge of the lateral process curves slightly upwards. The squamosal flat surface, a structure described in many metriorhynchids (Pol and Gasparini, 2009; Herrera *et al.*, 2013, 2015a; Parrilla-Bel *et al.*, 2013) is not as well expressed as the one described for *To. coryphaeus* (Young *et al.*, 2013b) but does resemble the one seen in *D. andiniensis* and *Cricosaurus araucaniensis* (Pol and Gasparini, 2009). On both medial and lateral sides there is a foramen in the middle of the bone. In ventral view, the squamosal presents several concavities, identical on both elements that may correspond to portions of the cranioquadrate canal and otic aperture, but they cannot be identified with certainty due to poor preservation.

Parietal

The parietal is a single unpaired element, as usual in crocodylomorphs (Fig. 8d, 8e; Pol & Gasparini, 2009; Leardi *et al*., 2017). The medial part of the parietal is well preserved, whereas its lateral processes are lost. Like the squamosal, only the dorsal part is preserved. The parts that should connect ventrally with the prootic and the laterosphenoid are missing. Upon discovery, the parietal and frontal were still articulated with one another (Fig. 2), but this contact was lost during extraction and preparation. Anteriorly, the parietal is of equal width with the posterior process of the frontal. It then gradually narrows posteriorly to an extreme degree until it only appears as a raised sagittal ridge (Fig. 4, 8e). This narrowing is more pronounced in MJSN BSY008-465 than in *To. coryphaeus* (Young *et al.*, 2013b) and is at least as strong as in *To. carpenteri* (Grange and Benton, 1996), if not more. The anterior process of the parietal forms the posterior part of the intertemporal bar. Ventrally, the parietal widens to form the posteromedial corner of the supratemporal fossae. When complete, the parietal would be “T-shaped” in dorsal view with widely extended lateral processes as in other metriorhynchids (Andrews, 1913; Young *et al.* 2013b; LeMort *et al*., 2022). In lateral view, the anterior process of the parietal slopes down posteriorly, starting from the point where the ridge is thinnest. From this point, the ridge widens again and forms a triangular area facing dorsally as in other Metriorhynchidae (Herrera *et al.*, 2015a). The contact with the supraoccipital is not preserved. In ventral view, the posterior part of the parietal is hollow and has one or two foramina on its deepest point.

Mandible

Both mandibular rami are preserved (Fig. 4b). They are relatively complete, but some parts are fractured, eroded, and deformed. Some elements of the mandible are not articulated anymore. The mandible is represented by several main parts: two ensembles made of the angular, surangular, articular and prearticular; the disarticulated splenials; and the dentaries (preserved in

several pieces). The coronoids are lost. The notable absence of a mandibular fenestra is an apomorphy of the Metriorhynchidae (Fraas, 1902; Andrews, 1913; Vignaud, 1995; Young *et al.*, 2010). The total length of the mandible is about 815 mm with the anterior end missing. The general shape of the mandible is similar to the one described for *Ty. lythrodectikos* and Geosaurini with the coronoid process located higher than the plan of the tooth row and lower than the retroarticular process, indicating an increase in gape (Young *et al.*, 2012a, 2012b, 2013a, Foffa and Young 2014).

Dentary

Both dentaries are preserved but not equally well. The left dentary is ~~is~~ almost complete but broken into three parts (Fig. 9), only missing its anteriormost portion. The right dentary is broken into two pieces but is highly damaged and deformed. Its ventral and medial parts are completely lost, whereas the posterior part is crushed and deformed. The latter now lies more dorsally and medially compared to the anterior part. The damages are partly due to taphonomic conditions, but also to the poorly controlled acid treatment of the fossil. The left dentary is about 45 cm long, 4.5 cm high and 2.6 cm wide. The right dentary preserves two teeth, including one on its most deformed part with the alveolus deformed and projected inward (Fig. 4b). The left dentary preserves one tooth in the middle of the rostrum (Fig. 9). In dorsal view, the dentary is a long and thick bone. It narrows posteriorly where it was in contact with the angular and surangular. The dentary widens anteriorly starting from the posteriormost alveolus, which is smaller than the one immediately in front. The anterior part of the dentary, including the three anteriormost visible alveoli, shortly curves inward, this bending of the dentary seems natural. There are at least 16 clearly identifiable alveoli, potentially 17, that are overall homogeneous in size. The alveoli are enlarged, subcircular, and slightly longer than wide. The three anteriormost alveoli are larger than the others and lie slightly more dorsally. Overall, the more anterior are the alveoli the more anterodorsally they are oriented. The remaining tooth on the left dentary is anterodorsally directed while the one on the undeformed part of the right dentary is dorsally oriented. As in the maxillae, the interalveolar space is uniform and greatly reduced, being less than half of the anteroposterior length of the adjacent alveoli (see above). In lateral view, the lateral margin of the alveoli lies slightly lower than the medial margin except for the three anteriormost alveoli where the lateral and medial margins are on the same plane (Fig. 9b, d). The surangular-dentary groove is visible (Fig, 9b), and does not end anteriorly with a foramen as is the case in *Dakosaurus* (Pol and Gasparini, 2009). A pitting pattern is present on the lateral and ventral surfaces of the dentaries. However, there is no heavy grooving as described in *To. carpenteri* (Wilkinson *et al.*, 2008). At least eight alveoli are adjacent to the symphysis. This count is higher than the four observed in *Dakosaurus maximus* (Young *et al.*, 2012b) but close to estimated height in the indeterminate Geosaurini (SMNS 80149) from the informal E-clade(Abel *et al.*, 2020; Young *et al.*, 2020a) and *Geosaurus* (Young *et al.*, 2012b); as well as the nine of *Pl. manselii* (Young *et al.*, 2012b), but lower than the 10-13 of the early Geosaurini *Ty. lythrodectikos* (Young *et al*., 2013a; Waskow *et al.*, 2018). No reception pits for maxillary teeth

are observed on the dentaries, indicating that there was no overbite creating a scissor-like occlusion mechanism like in *G. giganteus* nor any tooth-on-tooth interlocking as seen in *Dakosaurus maximus* (Young *et al.*, 2012a; Young & Andrade, 2009).

Splenial

The left splenial is better preserved than the right one. The two splenials have been flattened and both their anterior and posterior ends are broken off. The left splenial is about 37 cm long. In dorsal view, each splenial is narrow on its anterior and posterior ends and thicker in the middle. The lateral edge is straight, but the medial edge is slightly convex (Fig. 10c). The lateral aspect of the splenial is overall concave, with raised ridges forming the sutural contacts with the angular and dentary ventrally, and with the dentary and surangular dorsally (Fig. 10a). Anteriorly, the splenial likely reaches the fifth or sixth alveoli, but this observation might be ~~biased due to the preservation of the specimen~~. In *Pl. manselii* (Young *et al.*, 2012b), the splenial anteriorly reaches alveoli six anteriorly and alveoli seven or eight in *Ty. lythrodectikos* (Foffa & Young, 2014; Waskow *et al.*, 2018) and in Rhacheosaurini such as *Cricosaurus bambergensis* or *C. albersdoerferi* it is clearly posterior to the 10th alveoli (Sachs *et al.*, 2019, 2021; LCG, pers.obs). The medial surface of the splenial is slightly convex. The ventral edge of the bone is thicker and participates to the ventral edge of the mandible itself. The bone surface is smooth. On the medial surface, a foramen is visible posterior to the thickened part of the bone. The splenials would contact one another along the symphysis and the remains of the contact is visible on the anterior third of the splenial, ~~materialized~~ by a rougher surface of the bone (Fig. 10b, 10d).

Angular and surangular

The angular and surangular are preserved on both sides. They are missing their anterior part and show signs of crushing, erosion, and deformation, especially on the left mandibular ramus. The angular and surangular are strongly sutured along their entire length. They respectively form the ventral and dorsal halves of the posterior part of the mandibular ramus (Fig. 11). In lateral view, the surangular-dentary groove is well expressed. This groove is present in all Metriorhynchidae, albeit not always visible due to deformation, and it is especially deep in the members of the Geosaurini tribe (Pol and Gasparini, 2009; Young & Andrade, 2009; Young *et al.*, 2012b, 2013b;). This groove is associated with the passage of the mandibular nerve (Holliday and Witmer, 2007; Young & Andrade, 2009; George and Holliday, 2013) and its posterior end is marked by a foramen. Two other smaller foramina, more or less aligned with the one on the surangular-dentary groove, are found on the posterior part of the surangular, following the upward curve of the bone. The dorsal margin of the surangular rises slightly posteriorly before sloping down after reaching the coronoid process. The coronoid process is located on the anterodorsal half of the surangular. The coronoid process is higher than the tooth row, but lower than the retroarticular process. In dorsal view, the coronoid process narrows posteriorly and forms a ridge. In medial view, the surangular medial ridge for the coronoid is visible. The medial surface of the angular and surangular is concave, especially on their anterior part where they would form the lateral

wall of the Meckelian groove and contact the splenial and the coronoid,. The large foramen that connects with the surangular-dentary groove in the lateral surface of the ramus is present below the coronoid process. The angular is thicker than the surangular and forms the ventral margin of the mandible. The posterior part of the angular curves upward towards the retroarticular process atan angle of approximately 30° with the ventral surface of the angular. Posteriorly, the angular extends beyond and rises higher than the glenoid fossa to form the ventral part of the retroarticular process as on other Geosaurini (Young *et al.*, 2012b; Herrera *et al.*, 2015).

Prearticular

Only the right prearticular is well preserved. The prearticular is absent in many crocodylomorphs (Iordansky, 1973; Ruebenstahl *et al*., 2022) but is present in metriorhynchoids as well as in a few teleosaurids such as *Machimosaurus* (Andrews, 1913; Martin & Vincent, 2013; Young *et al.*, 2014a; Martin *et al.*, 2015) Its presence is therefore considered a symplesiomorphy of Thalattosuchia (Andrews, 1913; Martin *et al.*, 2015). The prearticular is a triangular-shaped bone only visible in medial view of the ramus (Fig. 11a, 11b). It contacts the angular ventrally, the surangular laterally, and the articular posterodorsally.

Articular

The articular is well preserved only on the right mandibular ramus. It contacts the prearticular anteroventrally, the angular posteroventrally, and the surangular laterally. The articular projects far medially. The glenoid fossa, which accommodates the articular condyle of the quadrate, is deep and rounded, and is oriented anterodorsally. . The glenoid fossa is divided in two concavities by a low ridge similar to the condition in *To. coryphaeus* and *Ty. lithrodectikos* (*Young et al.*, 2013b; Foffa & Young, 2014) but different to what is seen in *Pl. manselii* where there is no separation (Young *et al.*, 2012b). The glenoid fossa is separated from the retroarticular process by a raised ridge similar to the one seen in *To. coryphaeus, Ty lithrodectikos* or "*Metriorhynchus*" *brachyrhynchus* which forms "ridge-and-concavity" morphology to accommodate the "sulcus-and-condyle" of the quadrate (Andrews, 1913; Young *et al.*, 2012b, 2013b; Foffa & Young, 2014). The dorsal surface of the retroarticular process is a triangular smooth posterodorsally oriented concavity, which curves medially in dorsal view. The retroarticular process extends laterally beyond the glenoid fossa and slopes downward in medial view. The medial end of the bone is a rugose surface. This overall matches the usual metriorhynchid condition (Andrews, 1913; Young *et al.*, 2012b, 2013b; Foffa & Young, 2014). The tip of the retroarticular process is broken off, but it would rise higher than the rest of the articular.

Dentition

At least fifteen isolated teeth were found closely associated with the skeleton MJSN BSY008-465. Nine of these isolated teeth are complete, or almost complete, and preserve both the crown

and the root. Three additional teeth are still in place on the dentaries and two more on the left maxilla (see above).

Teeth

Based on macroscopic observation, the teeth correspond to the typical metriorhynchid morphology. They are caniniform, conical, and single-cusped (Massare, 1987; Vignaud, 1997). The teeth are large, robust and bicarinate with the carinae on the anteroposterior axis running continuously from the crown base to the apex. There is no basal constriction of the crown, but the crown-root junction is clearly visible from color and texture (Fig. 12). The length of each tooth roots is at least twice the height of each crown. In cross section, the base of the crown is sub-circular to ovoid with the labial face thicker than the lingual one. The tooth roots are ovoid in cross-section. Closer to the apex, the mediolateral compression of the teeth is increasing. Most tooth crowns are over 20 mm high, but the tooth height is not uniform. The average crown height is 21.94 mm with a standard deviation of 4.38. This calculation includes all of the 15 teeth. It is to be noted that some of them have their apex broken but not enough to significantly affect the crown height. The shortest tooth crown is 13.23 mm high and the highest is 29.28 mm. The average width at the tooth base is 10 mm (standard deviation 0.9) for a length of 11.36 in average (standard deviation 0.87). The average difference between the width and the length is 1.36 mm (standard deviation 0.93), but the minimal value is 0.3 mm and the maximal value is 3.67 mm with no correlation to the crown height. The teeth are curved lingually and posteriorly. The morphology of the alveoli and the teeth still in place, especially the anterior ones, indicate that teeth were implanted slightly forward in the jaws. Crowns are heavily ornamented with long longitudinal subparallel ridges on at least the basal two thirds of the teeth. Ridges are denser on the lingual face than on the labial one. On the apex, the ornamentation becomes low, short ridges forming an anastomosed pattern of drop-shaped ornaments (Figs. 12, 13). This peculiar ornamentation pattern has only been described in other *Torvoneustes* species (Andrade *et al.*, 2010; Young *et al.*, 2013b; Barrientos-Lara *et al.*, 2016; Foffa *et al*., 2018b, Young *et al.*, 2019;) as well as in the machimosaurids *Machimosaurus* von Meyer, 1837 and *Lemmysuchus obtusidens* Andrews, 1909 (Johnson *et al.*, 2017). As seen in *To. carpenteri, To. mexicanus* and isolated *Torvoneustes* teeth (Andrade *et al.*, 2010; Young *et al.*, 2013b, 2014, 2019; Barrientos-Lara *et al.*, 2016; Foffa *et al*., 2018b; Madzia *et al.*, 2021) , the enamel ridges on the upper part of the teeth shift and bend toward the carinae. The carina is well developed, as in other *Torvoneustes* specimens. The developed keel and the shift of enamel ridges toward the carinae are both autapomorphies of *Torvoneustes* (Andrade *et al.*, 2010; Young *et al.*, 2013b, 2014, 2019; Barrientos-Lara *et al.*, 2016; Foffa *et al*., 2018b; Madzia *et al.*, 2021). On the basal two thirds of the crown, the carinae are serrated with no involvement of the enamel ornamentation. On the apical third of the crown, there is a clear shift in the enamel ornamentation pattern, and the enamel ridges bend toward the carinae and touch the serrated keel (Fig. 13a). The serration is present from the base of the carinae to the apex and is high, especially on the apical half of the crown. Both of these features are also found in *Torvoneustes* (Andrade *et al.*, 2010; Young *et al*.,

2013b, 2014, 2019; Barrientos-Lara *et al*., 2016; Foffa *et al.*, 2018b; Madzia *et al.*, 2021). The serration is only faintly visible on macroscopic observation. The tooth apex is sharp, similar to what is described for *Torvoneustes mexicanus* and different from the blunter tooth tips of *To. carpenteri*, *To. coryphaeus* and and *Torvoneustes* teeth from the UK(Wilkinson *et al.*, 2008; Andrade *et al.*, 2010; Young *et al.*, 2013b, 2019; Barrientos-Lara *et al.*, 2016; Foffa *et al.* 2018b; Madzia *et al.*, 2021). In an unpublished work on isolated thalattosuchian teeth from the Pal A16 collection, Schaefer (2012) already noted the resemblance of the teeth of MJSN BSY008-465 with the ones of *To. carpenteri*, while pointing out the greater sharpness of the former. Observed with optic aids, the serration of the carinae is formed by a continuous row of poorly isomorphic, isolated denticles weakly affecting the keel height (poorly developed incipient denticles). This serration corresponds to the microziphodont condition as defined by Andrade *et al.* (2010) with the denticles all smaller than 300 µm in height and length. The denticles base length varies between 120 and 200 µm with an average of 160 µm (Fig. 13), differing from the regular and 142-µm-long (average) denticles of *To. mexicanus* (Barrientos-Lara *et al.*, 2016). The denticle density (amount of denticles/5mm, following Andrade *et al.*, 2010) ranges from 31 to 40 depending on the area on the teeth with an average of 35, which is higher than the average measured on *To. mexicanus* (Barrientos-Lara *et al.*, 2016) and *G. grandis*, but corresponds to the number found on *Geosaurus* indet. (SMNS 81834; Andrade *et al.*, 2010). The denticle density increases in the middle of the tooth crown and decreases at the apex, making the denticles more densely packed and narrower on the part where the carina is the highest. At the apex, the enamel ornamentation joins the carina (Fig. 13a, 13b), similar to the condition in *To. carpenteri* and *To. mexicanus* (Andrade *et al.*, 2010; Barrientos-Lara *et al.*, 2016) and contrary to what is observed in *To. coryphaeus* (Young *et al.*, 2013b; Foffa *et al.*, 2018a). The denticles are harder to discern in this region. This false-ziphodont condition (Prasad and de Lapparent de Broin, 2002) is found in *Torvoneustes* but also in *Machimosaurus* (Andrade *et al.*, 2010; Young *et al.*, 2014b). However, the combination of true and false ziphodonty, as defined by Andrade *et al.*, 2010, is only known in *To. carpenteri, To. mexicanus,* and *Torvoneustes* sp. (OUMNH J.50061 and OUMNH J.50079-J.50085) (Young *et al.*, 2013b; Young *et al.*, 2019; Barrientos-Lara *et al.*, 2016). The base of the carina around the upper middle of the tooth shows structures resembling the “inflated base” seen in *To. carpenteri* (Fig. 13b; Andrade *et al.*, 2010). MJSN BSY008-465 does not present the faceted teeth of *Ieldraan* and *Geosaurus* (Young *et al.*, 2013a; Foffa *et al.*, 2018a), nor the macroscopic denticles of *Dakosaurus* (Andrade *et al.*, 2010; Pol and Gasparini, 2009), nor the characteristic flanges on the side of the carinae seen in *Plesiosuchus* (Owen, 1883; Young *et al.*, 2012b).

Tooth count

The holotype of *To carpenteri* (BRSMG Ce17365) is the only other specimen referred to *Torvoneustes* that has a maxilla as complete as MJSN BSY008-465 (Grange and Benton, 1996; Wilkinson *et al.*, 2008). The paratype of *To. carpenteri* (BRSMG Cd7203) preserves a dentary, yet just a few fragments and not a complete piece, in contrast to MJSN BSY008-465. On the

right maxilla of MJSN BSY008-465, there are at least 15 preserved alveoli (13 on the left one) while there are at least 16 to 17 alveoli on the left dentary and possibly 17 alveoli on the more poorly preserved right dentary. The dentary tooth count is usually lower than the maxillary count. This might indicate at the very least one to two missing alveoli on the right maxilla. Metriorhynchids bear three teeth on the premaxilla (Andrews, 1913; Wilkinson *et* al., 2008; Young & Andrade, 2009). Therefore, this would indicate a dental formula for MJSN BSY008-465 of three premaxillae teeth, 16 to 18 maxillary teeth and 16 to 17 dentary teeth (3+16-18/16-17) for a minimal count, but it is likely that the maxillary tooth count could be even higher. It is therefore closer to the 3+17-19/15-17 estimated for *To. coryphaeus* than the 3+14/14 formula estimated for *To. carpenteri* (Young *et al.*, 2013b). However, it must be noted that no *Torvoneustes* species was found with complete maxillae. Moreover, the skull of *To. carpenteri* (BRSMG Ce17365) is damaged, so the estimated tooth count might be underestimated, especially considering that, in *To. coryphaeus*, the maxillary tooth row reaches beyond the anterior margin of the orbit. This is also observed in other geosaurines such as *D. andiniensis, G. giganteus* and potentially *P. manselii* (Young *et al.*, 2013b). Comparison with *To. carpenteri* and MJSN BSY008-465 are limited because the contour of the orbits is completely lost in both.

Tooth wear

In addition to postmortem fractures, the teeth of MJSN BSY008-465 present signs of macroscopic wear. Several teeth have their apex broken resulting in a flattened and smoothed tip. This type of wear was described in *To. coryphaeus* as an indication of repeated impact against hard surfaces. Some teeth also present signs of enamel spalling wear, mainly represented by triangular facets of broken enamel on the labial face. This type of wear was interpreted as resulting from tooth-food abrasion and was also described in *To. coryphaeus*, *To. carpenteri* and *D. maximus* (Grange and Benton, 1996; Andrade *et al.*, 2010; Young *et al.*, 2012a, 2012b, 2013b).

Postcranial elements

From the postcranial skeleton, many vertebrae and ribs are preserved as well as a few elements of the pelvis and hindlimbs. Despite the number of postcranial elements, no osteoderms were found. The absence of osteoderms is an apomorphy of Metriorhynchidae (Fraas, 1902; Andrews, 1913; Young *et al.*, 2010).

Vertebrae

MJSN BSY008-465 was found with 22 of its vertebrae including three cervicals, nine dorsals and 10 caudals (Fig. 14). The atlas-axis complex is missing as well as the sacral vertebrae. The vertebrae suffered different level of damage and deformation. Some show stretching, with the centrum deflected from its natural, vertical plane and the apophyses not aligned anymore, or crushing with no preferential direction of deformation. This is mainly the case in the dorsal vertebrae. All vertebrae are amphicoelous, as in all metriorhynchids (Fraas, 1902; Pierce &

Benton, 2006; Cau & Fanti, 2011; Young *et al.*, 2013a; Parrilla-Bel & Canudo, 2015). The concavity is shallow and similarly developed in the anterior and posterior articular surfaces.

Cervical vertebrae

Three post-axis cervical vertebrae are preserved. The number of post-axis cervical vertebrae is considered to be five among Metriorhynchidae, with the fifth cervical closely resembling the first dorsal (Fraas, 1902; Wilkinson *et al*., 2008; Young *et al.*, 2013a; Parrilla-Bel & Canudo, 2015; Sachs *et al*., 2021). The cervical vertebrae of *To. jurensis* look similar to one another,we can therefore assume that the preserved vertebrae are all mid cervicals. Two of them are well preserved, including one complete (Fig 14a, 14b). The centrum is subcircular to ovoid, with the length of the vertebra subequal to the centrum height and width, which is typical for geosaurines (Parrilla-Bel and Canudo, 2015). The neural spine is shorter than the centrum height. As in all thalattosuchians, the cervical vertebrae are amphicoelous (Fraas, 1902; Wilkinson *et al*., 2008; Pierce & Benton, 2006; Cau & Fanti, 2011; Young *et al.*, 2013a; Parrilla-Bel & Canudo, 2015; LeMort *et al*., 2022). The parapophysis is low on the centrum, ventrally directed, without reaching lower than the ventral margin of the centrum (Fig. 14). A low parapophysis not associated with the neural arch is what characterizes cervical vertebrae in metriorhynchids (Andrews, 1913; Young *et al.*, 2013a; Parrilla-Bel and Canudo, 2015). The parapophysis ends with a concave articular facet. This facet articulates with the cervical rib. The diapophysis is also low, starting just above the neural arch-centrum suture, and ventrally oriented, reaching below the suture. The neurocentral sutures are not closed. On the ventral margin, at the edges of the articulation surfaces of the centrum, discrete ridges are a sign of muscle attachments (Parrilla-Bel and Canudo, 2015). There is a deep concavity between the parapophysis and diapophysis. This strong constriction has also been noted in *Maledictosuchus riclaensis* (Parrilla-Bel and Canudo, 2015). In ventral view, there are two shallow concavities between the parapophyseal processes and the centrum ventral margin, creating a medial keel also described on the cervical vertebrae of *D. maximus* and *Ma. riclaensis* (Fraas, 1902; Parrilla-Bel & Canudo, 2015). The ventral margin of the centrum is concave in lateral view. The parapophyses project below this margin in the middle of the centrum, but they do not extend more ventrally than the ventral margin of the articular facets. The zygapophyses are well developed, separated, and extended beyond the centrum. The postzygapophyses are wider than the prezygapophyses, but the latter extend further from the centrum. The articular surfaces of the zygapophyses are ovoid and flat. The morphology of the cervical vertebrae is consistent with the ones described for *To. carpenteri*, *Ma. riclaensis* and other metriorhynchids (Fraas, 1902; Andrews, 1913; Wilkinson *et al.*, 2008; Young *et al.*, 2013a; Parrilla-Bel and Canudo, 2015; LeMort *et al*., 2022).

Dorsal vertebrae

At least nine dorsal vertebrae are preserved, none of them with a complete neural spine nor complete diapophyseal processes. All of them are deformed to some extent. In metriorhynchids, the first dorsal vertebra is the one where the parapophysis is no longer on the centrum but on the

neural arch (Young *et al.*, 2013a; Parrilla-Bel and Canudo, 2015). The dorsal vertebrae of MJSN BSY008-465 follow the trend observed by Fraas (1902) with a constriction of the middle of the centrum giving it an hourglass shape. The centrum is higher than wide. Its length is subequal to its height. The vertebrae are amphicoelous, with both articular faces overall equally concave, unlike what had been noted in *Ty. lythrodectikos* and *To. carpenteri* (Wilkinson *et al.*, 2008; Young *et al.*, 2013a; Parrilla-Bel & Canudo, 2013). On the neural arch, the spine extends vertically in the posterior half of the centrum length. The parapophysis joins the diapophysis on the neural arch to form the anterior extension, like a little step, of the transverse apophysis, as typically observed within Metriorhynchidae (Fig.14c, 14d; Andrews, 1913, fig. 62; Parrilla-Bel & Canudo, 2015). The transverse apophysis extends greatly beyond the centrum on each side. It is overall straight with a slight ventral concavity. The zygapophyses are well developed, but not as much as the ones on the cervical vertebrae. As in *Ty. lythrodectikos* and the E-clade member PSHME PH1, they project slightly beyond the centrum (Parrilla-Bel and Canudo, 2015; Abel *et al*., 2020). Among the dorsal vertebrae of MJSN BSY008-465, some of them show unfused suture between the centrum and neural arch, indicating a specimen which did not achieved full maturity (a sub-adult; Brochu, 1996, Herrera *et al.*, 2013). As seen on the cervical vertebra, on the ventral margin of the caudal vertebra the edges of the articulation surfaces of the centrum, discrete ridges are a sign of muscle attachments.

Caudal vertebrae

In MJSN BSY008-465, only ten caudal vertebrae are preserved. The number of caudal vertebrae can differ greatly between metriorhynchid species but it is usually over 30 (Fraas, 1902; Andrews, 1913; Parrilla-Bel and Canudo, 2015; De sousa oliveira, in press). The size and shape of the preserved vertebrae vary greatly, which suggests that they originate from different parts of the tail (Fig. 14e–h). However, none of them can be associated with the bend of the tail fluke. Three vertebrae with reduced apophysis are associated with the anterior part of the tail (Fig. 14e, f). These caudal vertebrae are hourglass shaped, but the constriction is not as strong as in the cervical and dorsal vertebrae. Their centrum presents a ventral keel. The centrum length of the vertebrae is subequal to their width. The neural spine is overall rectangular in shape and oriented posterodorsally. The general shaoe of the caudal vertebra of MJSN BSY008-465 is similar to *To. carpenteri* and E-clade member PSHME PH1 (Wilkinson *et al*., 2008; Abel *et al.,* 2020). The other caudal vertebrae does not all preserve the neural spine.These vertebrae are greatly reduced for some of them, and are interpreted as more posterior in the caudal serie. The zygapophyses are not preserved. The articular surfaces of the centra are rounded and slightly concave. On the caudal vertebrae, the suture between the centrum and neural arch is closed.

Ribs

Cervical ribs.

Three cervical ribs are identified. They form short, slender ribs directed posteriorly with an acute end (Fig. 15a-c). The external face forms a ridge starting from the tuberculum and capitulum. The medial face is concave. The roughly triangular mid-shaft cross section. In lateral view, the ribs are "V-shaped". This correspond to the typical condition in Metriorhynchidae (Andrews, 1913; Wilkinson *et al.*, 2008; Abel *et al.*, 2020)

Dorsal ribs

There are 15 preserved, but incomplete, dorsal ribs from MJSN BSY008-465. The dorsal ribs are long and slender, ovoid or round in cross section (Fig. 15d, e). They are arched, having a flat medial surface, whereas the lateral surface is rounded.. There is a ridge on the posterior surface running down from the tubercular (diapophyseal process). The proximal two thirds are flat on the medial side. In its distal third in lateral view, the rib narrows to form a ridge. On the medial side this part shows a sutural surface. This shift might mark the limit between the vertebrocostal part to the intercostal part of the rib, but no intercostal is sufficiently preserved to give a better description. Tuberculum and capitulum are not preserved in available ribs. The ribs overall resemble the dorsal ribs of *To. carpenteri* and other metriorhynchids (von Arthaber, 1906; Andrews, 1913; Wilkinson *et al.*, 2008, Herrera *et al*., 2013, fig. 7N).

Chevron

At least one chevron is preserved, probably from the posterior part of the tail considering its small size (Fig. 15f, g). In lateral view it is Y-shaped, and in dorsal view it presents two lateral and one medial branches, which corresponds to what has been described in other Metriorhynchidae (Andrews, 1913; Sachs *et al*., 2019, 2021).

Appendicular skeleton

Ischium

The left ischium is badly preserved, lacking a major portion of its ventral part where the bone would widen the most (Fig. 16c). The proximal part is also missing, as well as the anterior process it should be bearing (Andrews, 1913; Herrera *et al.*, 2013; Young *et al.*, 2013b; Wilkinson *et al.*, 2008). Like in other metriorhynchids, theneck of the ischium is narrow and thick, measuring 2.5 cm wide. The ischium widens and flattens distally in an overall triangular wing with a thickness of about two millimeters only. The partly preserved wing is similar to the classic metriorhynchid morphology as seen in *To. carpenteri, C. araucanensis* (Andrews, 1913; Wilkinson *et al.*, 2008; Herrera *et al, 2013;* LeMort *et al*., 2022.) The surface of the wing is covered by striations corresponding to muscular attachment marks on both sides but better expressed on the lateral one.

Femur

The right femur of MJSN BSY008-465 lacks both proximal and distal ends (Fig. 16a, b). It has the sigmoidal shape typically found in Thalattosuchia (Andrews, 1913; Wilkinson *et al.,* 2008; Herrera *et al.*, 2013; Young *et al.*, 2013b; Sachs *et al*., 2021) but with the curves not as pronounced as in *Enaliosuchus macrospondylus* Koken, 1883 or *Ty. lythrodectikos* (Young *et al.*, 2013b; Sachs *et al*., 2020). The bone is about 24 cm long and 3 cm wide, a similar size to *Ty. lythrodectikos* (Young *et al.*, 2013b). It is slightly narrower in the middle than at the ends. The medial side is almost flat, whereas the lateral side is convex. The bone flattens toward the distal end. As in *Ty. lythrodectikos* and *C. araucanensis,* the femur widens toward the distal end (Herrera *et al.*, 2013; Young *et al.*, 2013b; Sachs *et al*., 2021). The proximal end, despite the damages it suffered, shows on both sides the rugose surface for muscle attachment commonly found in metriorhynchids (Andrews, 1913; Lepage *et al.*, 2008; Wilkinson *et al.*, 2008; Herrera *et al.*, 2013; Young *et al.*, 2013b).

Fibula

The right fibula is a slender bone about a third of the preserved femur length (Fig. 16d), the same proportion as found in *Ty. lythrodectikos* and *C. suevicus* and *C. araucanensis* (Andrews, 1913; Herrera *et al.*, 2013; Young *et al.*, 2013b). This ratio is affected by the missing ends of the femur, as well as the missing part of the fibula. The hindlimb proportion in metriorhynchids are often measured with the femur and tibia. The tibia length being 30 to 40% of the femoral length is the general trend found among metriorhynchids while a ratio below 30% is distinctive of derived metriorhychins (Andrews, 1913; Wilkinson *et al*., 2008; Young & Andrade, 2009; Cau & Fanti, 2011; Young *et al.*, 2013b; Foffa *et al.*, 2019). The distal end of the fibula is not preserved. The proximal end is damaged but shows a single convex condyle as usual in Metriorhynchidae (Andrews, 1913; Herrera *et* al., 2013; Sachs *et al.*, 2019, 2021) . The inner side is flatter than the outer one, like what is seen in the femur. The bone is one centimeter wide at mid length and enlarged toward both ends, being 2 cm wide at the proximal end.

Phylogenetic analysis

Following the methodological protocol of Young *et al.* (2020b), the eight parsimony analyses resulted in eight strict consensus topologies with lengths ranking from 2417 steps for the unweighted analysis to 2033 steps for the weakly downweighted topologies (k=20 and k=50; see Table 2). The complete eight strict consensus trees are provided as supplementary material, while descriptive statistics for each of these trees are presented in Table 2. Focusing on the internal relationships of Geosaurinae, four distinct topologies are recovered (Fig. 17). They all have a similar structure, except for the position of *Tyrannoneustes lythrodectikos*, *Ieldraan melkshamensis*, *Geosaurus lapparenti*, "*Metriorhynchus*" *westermanni*, and "*Metriorhynchus*" *casamiquelai*.

In all of the strict consensus trees, *Torvoneustes jurensis* is included in a polytomous clade with all terminal taxa assigned to *Torvoneustes* (Fig. 17). This clade forms a polytomy with the E-

clade and *Purranisaurus potens*. In the unweighted analysis, this group made of *Torvoneutes*, the E-clade and *P. potens* forms a polytomy with *Ty. lythrodectikos* and a clade consisting of Geosaurina + Plesiosuchina (Fig. 17a). These taxa form together the Geosaurini. In the strongly downweighted analyses (k = 1 and k = 3), "*M.*" *westermanni* and "*M.*" *casamiquelai* assume more basal positions outside of geosaurines (Fig. 17b). *Tyrannoneustes lythrodectikos* is sister group to the E-clade, which corresponds to the 'subclade T' of Foffa *et al.* (2018a). Within Geosaurina, *I. melkshamensis* and *G. lapparenti* switch positions. The moderately downweighted analyses (k = 7 and k = 10) result in a topology overall consistent with that of the strongly downweighted analyses, except that "*M.*" *westermanni* and "*M.*" *casamiquelai* regain a basal position among geosaurines (Fig. 17c). In the moderately to weakly downweighted analyses (k = 15, k = 20, and k = 50), *I. melkshamensis* and *G. lapparenti* switch back to the positions they have in the strict consensus of the unweighted analysis (Fig. 17d). Overall, the results of our parsimony analyses are consistent with those of Young *et al.* (2020b) and Abel *et al.* (2020), except our strict consensus for the unweighted analysis that is less well resolved (subclade T only recovered by the weighted analyses).

To improve the resolution of relationships, unstable taxa were pruned a posteriori from the consensus trees to produce a maximum agreement subtree for each of the parsimony analysis (see Material and methods). For the unweighted analysis, a total of 13 OTUs, including eight geosaurines ("*Metriorhynchus*" *brachyrhynchus*, *Tyrannoneustes lythrodectikos*, *Geosaurus lapparenti*, *Purranisaurus potens*, Druegendorf merged, English rostrum, *Torvoneustes* sp., *Torvoneustes mexicanus*), are pruned from the original set of 180 OTUs. In contrast, 33 OTUs, including 12 geosaurines ("*Metriorhynchus*" *brachyrhynchus*, *Neptunidraco ammoniticus*, *Purranisaurus potens*, Druegendorf merged, English rostrum, Mr Passmore's specimen, Chouquet cf hastifer, *Torvoneustes* sp., *Torvoneustes mexicanus*, *Geosaurus grandis*, *Geosaurus giganteum*, and *Ieldran melkshamensis* or *Geosaurus lapparenti*), are pruned for the weighted analyses. The four new topologies obtained for relationships within Geosaurinae are presented in Figure 18.

All maximum agreement subtrees suggest that *Torvoneustes* sp. and *Torvoneustes mexicanus* are unstable taxa. This is probably the result of the partial nature of these terminals represented by single specimens consisting of an incomplete occipital region and a portion of rostrum, respectively. The pruning of these taxa reveals the internal relationships of the *Torvoneustes* clade. *Torvoneustes coryphaeus* is recovered as the most basal taxon in a sister group relationship with a clade consisting of cf. *Torvoneustes* and *To. jurensis* + *To. carpenteri* (Fig. 18). From a more general perspective, the internal relationships of the E-clade and Geosaurina are also identified as unstable.

The Bayesian analysis results in a resolved, but poorly supported tree (Fig. 19). *Torvoneustes jurensis* is resolved as the sister taxon of *To. carpenteri*. These two species form the most derived clade within the clade *Torvoneustes*. *Torvoneustes mexicanus* is found as the sister taxon of *To. jurensis* + *To. carpenteri*, whereas *To. coryphaeus* appears as the most basal form. Most nodes in the *Torvoneustes* clade and the E-clade are weakly supported. The Bayesian topology

for Geosaurini is similar to the one obtained by Young *et al.* (2020b), with only two exceptions: 1) the position of cf. *Torvoneustes* and *Torvoneustes* sp. are switched; 2) *To. mexicanus* and *To. carpenteri* are no longer sister taxa. In our analysis, the node supports within subclade T is slightly lower, which can be explained by the inclusion of *To. jurensis* as a new terminal. The different phylogenetic analyses performed as part of the present study all consistently find *To. jurensis* (MJSN BSY008-465) nested within a *Torvoneustes* clade, supporting our identification. Both the Bayesian analysis and the maximum agreement subtrees of the parsimony analyses support a close relationship between *To. jurensis* and *To. carpenteri*.

Discussion

MJSN BSY008-465 assigned to Geosaurinae

The absence of mandibular fenestrae, the orbits facing laterally and overhung by the prefrontals, and the absence of osteoderms (despite the preservation of numerous postcranial remains) unambiguously place MJSN BSY008-465 among Metriorhynchidae (Fraas, 1901, 1902; Andrews, 1913; Young *et al.*, 2010). In this section, we discuss the assignment of this specimen to Geosaurinae.

The dental characteristics of the Late Jurassic metriorhynchids allow to discriminate the Geosaurini from the Metriorhynchinae. The latter usually have smooth to faintly ornamented teeth, uncarinated or with low, non-serrated carinae, whereas Geosaurini have smooth to heavily ornamented teeth with high, serrated carinae (Table 1). The presence of prominent serrated carinae appears to be restricted to the Geosaurini tribe (Andrade *et al*., 2010; Young *et al*. 2011). Metriorhynchids genera, can even be identified based on teeth only and within Geosaurini, teeth can be used for species identification, (Young & Andrade, 2009; Andrade *et al.*, 2010; Schaefer, 2012; Young *et al.*, 2013a, 2013b; Barrientos-Lara *et al.*, 2016; Foffa *et al.*, 2018a, 2018b; Schaefer *et* al., 2018; Madzia *et al.*, 2021). MJSN BSY008-465 shares with *Torvoneustes* the presence of conspicuous apicobasal ridges on the first two-thirds of the crown shifting to an anastomosed pattern on the apex, as well as the bending of the enamel ridges toward the carinae. The teeth of some Metriorhynchinae (*Cricosaurus* spp., *Maledictosuchus nuyiviianan*) resemble those of *Torvoneustes* with conspicuous apicobasal ridges on the first two-thirds of the crown, but in their case the apex is smooth and the carinae are low and non-serrated (Sachs *et al.*, 2019; Table 1).

Derived geosaurines, such as *Plesiosuchus*, *Dakosaurus*, *Torvoneustes*, *Geosaurus*, *Purranisaurus* and the E-clade, show an extreme reduction in interalveolar space associated with a reduction of the tooth count and a moderateenlargement of the teeth (Young *et al.*, 2012b, 2013a, 2013b; Herrera *et al.*, 2015a; Abel *et al.*, 2020). Metriorhynchines, including those with a low tooth count such as *'Cricosaurus' saltillensis* (see below), have large and variable interalveolar spaces (Buchy *et al.*, 2013; Young *et al.*, 2020a; Herrera *et al.*, 2021a, 2021b). The only exception is *Gracilineustes leedsi* in which reduced interalveolar spaces are associated with a high tooth count (+30 per maxilla; Young *et al.*, 2013b). MJSN BSY008-465 has reduced interalveolar spaces associated with moderately enlarged teeth, which corresponds to the

condition in derived geosaurines. In addition, the teeth of MJSN BSY008-465 are on average larger than the typical height observed for metriorhynchine teeth, which are usually shorter than two centimeters (Wilkinson *et al.*, 2008; Herrera *et al.*, 2021b).

The tooth count is often used to differentiate geosaurines from metriorhynchines (Young *et al.*, 2013), but it should be noted that the absolute tooth count is known only in a limited number of species (Table 1). Geosaurini are usually considered to have 16 or less teeth per maxilla (Cau and Fanti, 2011). With this in mind, the estimated tooth count for MJSN BSY008-465 (17–18 or more, see above) may seem high for a Geosaurini, especially when some non-rhacheosaurin metriorhynchines, such as "*C.*" *saltillensis* and "*C.*" *macrospondylus*, present comparable tooth counts (Table 1; Buchy *et al.*, 2013; Aiglstorfer *et al.*, 2020). However, this relatively low tooth count in some racheosaurins seems to be linked to a pronounced shortening of the skull. On the other hand, it appears that the tooth count is poorly estimated in *Torvoneustes* because no complete maxilla is known, and some species have a comparable tooth count as MJSN BSY008-465. For example, *To. coryphaeus* is estimated to have up to 19 alveoli per maxilla (Young *et al.*, 2013b), which also falls into the range of other geosaurines such as Chouquet's "*Metriorhynchus*" cf. *hastifer* and its at least 20 maxillary teeth (Lepage *et al.*, 2008). Therefore, the tooth count for *Torvoneustes* is maybe underestimated for the moment based on the available material. It is also possible that the tendency toward the great reduction in the number of teeth is restricted to the clade uniting Geosaurina, Dakosaurina, and Plesiosuchina. In any case, it appears that tooth count, as a tool for identification, should be handled with care, especially when based on estimations.

MJSN BSY008-465 shares with Geosaurinae the presence of an acute angle of about 60° between the medial and lateral processes of the frontal. This angle is closer to 90° in most Metriorhynchinae, to the exception of *Cricosaurus* and *Maledictosuchus* in which this angle is around 45-50° (Wilkinson *et al*., 2008; Cau & Fanti, 2011; Buchy *et al.*, 2013, Parrilla-Bel *et al.*, 2013; Foffa & Young, 2014). The new specimen described herein shares several additional cranial and mandibular features with the macrophagous predators of the Geosaurini tribe: an inflection point of the prefrontals relative to the skull midline of 70° or less; a high glenoid fossa and retroarticular process; a strongly expressed surangular-dentary groove (Young & Andrade, 2009; Young *et al.*, 2012b; Young *et al.*, 2013b; Foffa and Young, 2014). In addition to some dental characteristics discussed above, MJSN BSY008-465 also has some cranial features that may recall the metriorhynchine *Cricosaurus*. MJSN BSY008-465 notably has a smooth and unornamented cranial surface, but this is also the case of *D. andiniensis* and *P. potens* (Pol & Gasparini, 2009; Herrera *et al.*, 2015a). The frontal of MJSN BSY008-465 differs in shape from that of other geosaurines and somewhat resembles that of *"C." saltillensis* (Buchy *et al.*, 2013), but there is a great diversity of frontal shapes among metriorhynchids (Foffa and Young, 2014, fig. 10; Herrera, 2015). Despite these few similarities, MJSN BSY008-465 lacks some cranial characters that are typical of *Cricosaurus*, such as the presence of a bony septum on the premaxillary and the presence of reception pits on the maxilla (as seen in *C. bambergensis* and *C. albersdoerferi*; Sachs *et al.*, 2019, 2021). Therefore, the craniomandibular characters, like the

dental characters, indicate that MJSN BSY008-465 should be assigned to Geosaurinae and suggest that the resemblances with *Cricosaurus* are only superficial.

The total body length of MJSN BSY008-465 is estimated to be around four meters (De Sousa Oliveira *et al.*, in press), which exceeds the sizes typically measured and estimated for *Rhacheosaurus* (157 cm), *Cricosaurus* (200 cm), and *Geosaurus* (270 cm), but falls in the range of large-bodied geosaurines such as *Suchodus dubroviensis* Lydekker, 1890 (410 cm), *D. andiniensis* (430 cm); *To. coryphaeus* (370 cm) and *To. carpenteri* (400-470 cm) (Young *et al.*, 2010, 2019). Because this specimen is one of the few metriorhynchids found with a significant part of its postcranium (see also Sachs *et al.*, 2019; LeMort *et al.*, 2022),, some remarks relative to the assignment of the specimen should be made also on this part of the skeleton.

Geosaurinae (*Neptunidraco ammoniticus*, "*M.*" *brachyrhynchus*, *Ty. lythrodectikos*, *To. carpenteri*, *Geo. lapparenti*, *D. maximus*) and MJSN BSY008-465 share a centrum length subequal to centrum width on cervical vertebrae, whereas in other Metriorhynchidae (*Thalattosuchus superciliosus*, *Rhacheosaurus gracilis*, *C. araucanensis*, *C. suevicus*, *C. bambergensis*, *C. albersdoerferi*) the centrum is shorter than wide (see character 423 of the phylogenetic matrix; Parrilla-Bel and Canudo, 2015). In MJSN BSY008-465, the neural length spine of the dorsal vertebrae is about half the length of the centrum and its dorsal margin is rounded. This is markedly different from *C. suevicus* and *C. albersdoerferi* in which the neural spine of the dorsal vertebrae is wide and rectangular with a flat dorsal margin and subequal in length to the length of the centrum (Sachs *et al.*, 2021). The centrum of the dorsal vertebrae is also distinctly longer than high in *C. albersdoerferi* and Creraceous metriorhynchids (Sachs *et al.*, 2020, 2021), whereas the centrum length is subequal to its height in MJSN BSY008-465 as in E-clade member PSHME PH1 and *N. ammoniticus* (Cau & Fanti, 2011; Abel *et al.*, 2020).

In metriorhynchids there is a drastic reduction of the length of the tibia and fibula compared to the femur (Fraas, 1902; Andrews, 1913; Foffa *et al.*, 2019). The tibia of MJSN BSY008-465 is not preserved, but the fibula is usually subequal or slightly longer than the tibia in metriorhynchids and can therefore be used as a proxy (Sachs *et al.*, 2019). As preserved, knowing that each bone is missing parts of the articular heads, the fibula of MJSN BSY008-465 is about 30% of the femoral length, which corresponds to the proportions usually observed in metriorhynchids. Members of the tribe Rhacheosaurini appear to be an exception because their tibia is less than 30% of the femur length (Andrews, 1913; Wilkinson *et al*., 2008; Young & Andrade, 2009; Cau & Fanti, 2011; Foffa *et al.*, 2019). However, this character (see #518 in the phylogenetic matrix, Supplementary data in Foffa *et al.*, 2019) can only be scored in a small number of metriorhynchids, and its repartition should be further investigated, especially in derived geosaurines such as *Dakosaurus*. Although not as diagnostic as the dental and cranial characters, the postcranial characters of MJSN BSY008-465 tend to suggest an affinity of this specimen with geosaurines rather than with non-metriorhychine metriorhynchid and to exclude a relationship with rhacheosaurins such as *Cricosaurus*.

Taxonomic diversity in the geosaurine genus *Torvoneustes*.

The genus *Torvoneustes* is a member of Geosaurinae and is currently represented by three valid species: the type species *To. carpenteri* from the upper Kimmeridgian, a skull heavily crushed and not described in many details, and some postcranial remains from a second specimen (Grange and Benton, 1996; Wilkinson *et al.*, 2008; Andrade *et al.*, 2010); *To. coryphaeus* from the lower Kimmeridgian, a 3D preserved skull missing the anterior part of the rostrum (Young *et al.*, 2013b); and *To. mexicanus,* likely from the Kimmeridgian, represented by a piece of a rostrum (Barrientos-Lara *et al.*, 2016). Other specimens were referred to the genus and include several isolated teeth form the Oxfodian (BRSMG Cd5591, Cd5592; CAMSM J.13305J, 13309, J.13310, YORYM:2016.306–2016.309; OUMNH J.52428, J.47587a, J.47560; Foffa *et al*., 2018b); three specimens referred to *Torvoneustes sp.* (MJML K1707) from the Upper Kimmerigian; OUMNH J.50061 and OUMNH J.50079-J.50085 from the lower Tithonian (Young *et al.*, 2019); cf. *Torvoneustes* (MANCH L6459) from the middle Oxfordian (Young, 2014), and *Torvoneustes*? (NHMW 2020/0025/0001) an isolated tooth crown from the upper Valanginian. All specimens are from England, except *To. mexicanus* and *Torvoneustes*?, which are from Mexico and Czech Republic respectively (Table 1).

Based on the three valid species, the genus *Torvoneustes* is defined by the following characteristics (Wilkinson *et al.*, 2008; Andrade *et al.*, 2010; Young *et al.*, 2013b; Barrientos-Lara *et al.*, 2016): great reduction of the interalveolar space; acute angle (around 60°) between the medial and lateral processes of the frontal; inflexion point on the lateral margin of the prefrontals directed posterolaterally at an angle of ~70° from the anteroposterior axis of the skull; circular to subcircular tooth cross section; carina formed by a keel and a contiguous row of poorly defined microscopic denticles difficult to observe even under SEM observation; conspicuous enamel ornamentation consisting of subparallel apicobasal ridges on the first two thirds of the crown shifting to short, low relief tubercles on the apex. The new specimen described herein closely follows this definition, but also presents significant differences with each of the recognized species.

The frontal of MJSN BSY008-465 is shaped differently than those of *To. carpenteri* and *To. coryphaeus*. In *To. carpenteri*, the frontal is shorter than in *To. coryphaeus* and MJSN BSY008-465. *Torvoneustes coryphaeus* has an ornamented frontal while in *To. carpenteri* and MJSN BSY008-465 the frontal is smooth. Finally, MJSN BSY008-465 is characterized by a clear angle between the anterior and posterolateral processes of the frontal, at the meeting point of the frontal, nasals and prefrontals. In the aforementioned two species, there is no visible angle and the processes are aligned in an almost straight line. Variation in shape of the frontals in the genus *Torvoneustes* is not well known, as only two described specimens preserve this element in addition to the new material described herein. Within metriorhynchids, we can note the great interspecific variation in the shape of the frontal (Foffa and Young, 2014). For example in *Cricosaurus*, there is a great variation of the frontal shape, as seen in *C. araucanensis* (Herrera, 2015).

MJSN BSY008-465 cannot be compared with *Torvoneustes* sp. (MJML K1707). The latter consists of an incomplete occipital region and this part is completely lost in our specimen.

However, MJSN BSY008-465 can be distinguished from all other English specimens. *Torvoneustes jurensis* differs from the type species *To. carpenteri* based on the following characters: smooth maxillae without grooves; anterior process of the frontal reaching the anterior margin of the prefrontals; posterolateral edges of the prefrontals lacking "fringer-like" projections; teeth more slender, curved, and with a sharp apex. MJSN BSY008-465 also differs from *To. coryphaeus* in having: a smooth skull; rounded posterolateral edges of the prefrontals (no acute angle); slender teeth with sharp apex; tooth ornamentation touching the carina in the upper part of the crown. Isolated *Torvoneustes* sp. teeth from the UK (BRSMG Cd5591, Cd5592; CAMSM J.13305J, 13309, J.13310, YORYM:2016.306–2016.309; OUMNH J.52428, J.47587a, J.47560, J.50061, J.50079-J.50085) preserve tooth crowns and roots very similar to *To. carpenteri*, As noted above, MJSN BSY008-465 has slender teeth. Finally, MJSN BSY008-465 is different from cf. *Torvoneustes* MANCH L6459 by its smooth cranium.

Torvoneustes mexicanus is only known by a single specimen that consists of a fragment of snout with preserved teeth. The species diagnosis is based only on the teeth with the following characters: conical, lingually curved, bicarinate, and more slender than in other *Torvoneustes* species; sharp apex; microziphodont condition with well-defined isomorphic denticles; crown enamel ornamentation consisting of apicobasally aligned ridges on the basal two-thirds of the crown and shifting to short drop-shaped tubercles meeting the carina on the apex (Barrientos-Lara *et al.*, 2016). On macroscopic observation, the teeth of MJSN BSY008-465 and *To. mexicanus* are very similar, but they differ on microscopic features. The denticles of *To. mexicanus* are well defined, regular in shape, size and distribution with a denticle basal length of about 142 µm and a denticle density (#denticles/5mm) of 30 (Barrientos-Lara *et al.*, 2016). The crown height seems to range between 1 and 2.5 cm. In MJSN BSY008-465, the basal length and distribution of denticles are irregular; on the tooth total length, the base of the denticles can vary from 120 to 200 µm in length with an average of 160 µm measured on four different teeth; denticles are also more densely packed in the upper middle of the tooth with a density reaching 40 while they can drop to 30 on the basal most part of the carina and the tooth apex. These observations are homogenous on the four observed teeth. It is to be noted however that denticles are sometimes hard to discern, because of their shape and size but also due to areas where they are worn or where the carina is broken. We compared these results with measurements based on formerly published SEM photographs of teeth of *To. carpenteri* (Young *et al.*, 2013a). In this species, the denticle basal length varies between 120 and 220 µm, with most measured denticles having a basal length between 160 and 200 µm. Unfortunately, denticle density cannot be determined. Again based on published SEM photographs (Madzia *et al.*, 2021), the denticles of *Torvoneustes*? (NHMW 2020/0025/0002) range in size from 200 to 270 µm in basal length and have a density of 19.

Previous studies showed that the denticle density is variable between geosaurines species such as *Dakosaurus* and *Geosaurus* (Andrade *et al.*, 2010). Measurements took in the middle of the carina gives the following densities for the microziphodont specimens: 28.1 in *Geosaurus* indet. (NHM R.486), and 33.3 for the mesial carina and 41.7 for the distal carina in *G. grandis.* These

results suggest possible interspecific variations in denticles density for a same tooth morphotype among geosaurines and that these variations should not be overlooked for systematic purposes (Andrade *et al.*, 2010). In this study however, the density of denticles is only measured on one tooth. The intraspecific and the individual variation, which were documented in other studies on crocodylomorphs teeth (Prasad and de Lapparent de Broin, 2002), were not explored in this case. However, the observations on MJSN BSY008-465, in addition to previous studies on metriorhynchid teeth, support the idea that microscopic dental characteristics in metriorhynchids have a potential to be used in systematics and should be further investigated.
From the above discussion and taking into account that *To. mexicanus* is only known by a very incomplete specimen of uncertain stratigraphical origin, it seems reasonable to conclude that MJSN BSY008-465 represents a different species, which we name here *Torvoneustes jurensis*. Future discoveries of more complete fossil specimens of *To. mexicanus* will allow a better understanding of the differences between these species.

Macroevolution trends in *Torvoneustes*

Young *et al.* (2013b, 2019) discussed macroevolutionary trends in the genus *Torvoneustes.* They first noted a reduction of the maxillary tooth count with time from “relatively high” in cf. *Torvoneustes* (MANCH L6459; Young *et al.*, 2019) and 17–19 in *To. coryphaeus* (Young *et al.*, 2013b), to 14 in *To. carpenteri* (Wilkinson *et al.*, 2008). However, it should be noted that no complete maxilla is known for any specimen referred to *Torvoneustes*, so these tooth counts represent estimations (see above). Another trend noted in *Torvoneustes* is a decrease in dermocranial external ornamentation, with the upper Kimmeridgian *To. carpenteri* having a smoother skull than the older representatives *To. coryphaeus* and cf. *Torvoneustes* MANCH L6459 (Grange and Benton, 1996; Wilkinson *et al.*, 2008; Young *et al.*, 2013b; Young, 2014). Concerning the tooth morphology, the following macroevolutionary trends were proposed: increasing enamel ornamentation; blunter crown apices; tooth crown losing the lingual curvature; and crown cross section becoming subconical (Young *et al.*, 2019). These trends are interpreted to be linked to an increasingly durophagous diet (Young *et al.*, 2013b; 2019; Foffa *et al.*, 2018c). *Torvoneustes coryphaeus*, *To. carpenteri, Torvoneustes?* (NHMW 2020/0025/0001) and *Torvoneustes* sp. (OUMNH J.50061 and OUMNH J.50079-J.50085) fit relatively well into this proposed evolutionary trend. However, that is not the case of *To. mexicanus* which has more slender teeth than *To. coryphaeus* and *To. carpenteri,* as well as more curved teeth than the latter. The teeth of *To. mexicanus* are also sharper than those of *To. coryphaeus, To. carpenteri* and *Torvoneustes* sp. OUMNH J.50061 and OUMNH J.50079-J.50085.
The acquisition of false serration (false ziphodont dentition; Prasad and de Lapparent de Broin, 2002; Young & Andrade, 2009; Andrade *et al.*, 2010) is another macroevolutionary trend proposed for *Torvoneustes* (Young *et al.*, 2019). *Torvoneustes coryphaeus* is the only species lacking the false ziphodont dentition and is also the oldest specimen whose teeth are known. The other specimens preserving teeth (*To. carpenteri*; *Torvoneustes* sp., OUMNH J.50061 and OUMNH J.50079-J.50085; *Torvoneustes*?, NHMW 2020/0025/0001; *To. mexicanus*) all present

the false ziphodont condition. Therefore, the authors propose the acquisition of the false ziphodont condition in all species younger than *To. coryphaeus* (Young *et al.*, 2019).
The discovery of the occipital region of a *Torvoneustes* specimen of great size from the Tithonian of England led Young *et al.* (2019) to propose an increase of body size as a possible evolutionary trend within *Torvoneustes*. This specimen is estimated to be around 6 meters long while other *Torvoneustes* specimens are estimated to be between 3.70 and 4.70 meters long (Young *et al.*, 2011, 2019). And finally, Young *et al.* (2019) also suggested that the increase in length of the suborbital fenestrae leading to an enlarged pterygoid musculature and the ventralization of basioccipital tuberosities would be another evolutionary trend of *Torvoneustes*. However, because this part of the cranium is not preserved in *To. jurensis*, this trend will not be further discussed below.
Torvoneustes jurensis fits relatively well with some of the aforementioned macroevolutionary trends. First, *To. jurensis* is younger than *To. coryphaeus* and indeed presents the false ziphodont condition on its teeth. However, it should be noted that in the current state of knowledge the distribution of this character does not per se corresponds to an evolutionary trend, especially considering the observation of this character among Oxfordian isolated teeth (Foffa *et al*., 2018b),older than *To. coryphaeus*. Therefore, false ziphodont condition may be a synapomorphy uniting *Torvoneutes* species but lost in *To. coryphaeus*.
Torvoneustes jurensis, which is from the early late Kimmeridgian, has an even smoother cranium than *To. carpenteri*. Dermocranial ornamentation appears early during ontogeny in crocodylomophs, usually developing in specimens with a skull longer than 200 mm (de Buffrénil, 1982; de Buffrénil *et al.*, 2015). This indicates that the smooth cranium of *To. jurensi* is not linked to its ontogenic stage and fits into the evolutionary trend proposed by Young *et al.* (2019). Within Thalattosuchia, the trend toward smoother dermocranial bones is believed to improve hydrodynamic efficiency (Young *et al.*, 2013b) and overall follows the idea that pelagic species have less ornamented skulls than semi-aquatic one (comparing metriorhynchids and pelagic teleosauroids to non-pelagic teleosauroids for example; Clarac *et al.*, 2017, Foffa *et al*., 2019). This trend is also present in *Dakosaurus* with *D. andiniensis*, the geologically younger species, showing smoother cranial bones than *D. maximus* (Pol and Gasparini, 2009; Young *et al.*, 2012a). However, the functional role of bone ornamentation remains controversial in crocodylomorphs (de Buffrénil *et al.*, 2015). Clarac *et al.* (2017) presented evidence that the evolution of ornamentation in pseudosuchians is influenced by both natural selection and Brownian motion. The study shows that heavy ornamentation is present in pseudosuchians with semi-pelagic lifestyle and linked to basking for animals with low mobility, these results are backed by finding from Pochat-Cottilloux *et al.* (2022). Therefore, the loss of ornamentation in Thalattosuchia may rather be linked to an increasingly pelagic lifestyle than directly to hydrodynamic efficiency. The loss of ornamentation of the cranium and osteoderms was also observed by Foffa *et al*., 2019 in ~~Teleosauroid~~ and similarly linked it to adaptation to pelagic lifestyle.

The description of *To. jurensis* contradicts some aspects of the other proposed evolutionary trends. *Torvoneustes jurensis* presents slenderer and shaper teeth than the other *Torvoneustes* species, except *To. mexicanus*. In their description, Barrientos-Lara *et al.* (2016) raised the question of whether the slender and sharp teeth of *To. mexicanus* could be linked to ontogeny, but the lack of data to characterize ontogenic changes within *Torvoneustes* teeth led them to consider the differences between *To. mexicanus* and other *Torvoneustes* as specific characters. The teeth of *To. jurensis* are very similar to those of *To. mexicanus*. However, the skull length of the holotype of *To. jurensis* is similar to that of the holotype of *To. carpenteri*. Their body length is estimated to be close to 4.0 m for *To. jurensis* and between 4.0 and 4.70 m for *To. carpenteri* (Grange and Benton, 1996; Wilkinson *et al.*, 2008; Young *et al.*, 2011; De Sousa Oliveira *et al.*, in press). Therefore, ontogeny cannot explain the differences in tooth morphology between these species. The sharp and slender teeth of *To. jurensis* and *To. mexicanus* may instead represent a diverging tooth morphotype within the genus. It might indicate that *To. mexicanus* and *To. jurensis* are less specialized than species with more robust teeth. They might be opportunist feeders with durophagous tendencies. This would be consistent with the Kimmeridgian environment of the Jura platform: *Torvoneustes jurensis* was found in a carbonate platform environment where remains of teleosauroids (*Sericodon jugleri* Von Meyer, 1845; *Proexochokefalos* cf. *bouchardi* Sauvage, 1872 and another durophagous genus *Machimosaurus hugii* Meyer, 1837) are abundant, as well as many coastal marine turtles (Thalassochelydia) and hard scale fishes (e.g., *Scheenstia* sp., Figure 20).

The maxillary tooth count of *To. jurensis* is estimated to be at least 16 or 17, but probably higher. Therefore, it seems like the reduction of maxillary tooth count is not a homogenous trend in the genus. However, it should be stressed once more that no definitive maxillary tooth count is known at the moment for any specimen referred to *Torvoneustes*. It is then possibly too early to conclude on any trend for this character.

Regarding the increase in body size, it should be noted that crocodilians continue to grow well into adulthood (Sebens, 1987; Grigg and Kirshner, 2015) and that only a handful of specimens are known for *Torvoneustes*. In these circumstances, any conclusion on size evolutionary trends must therefore be taken with care. As noted above, the holotype specimens of *To. carpenteri* and *To. jurensis* are roughly of comparable total length, which could agree with the proposed evolutionary trend as the two species are roughly of the same age. However, many isolated teeth showing similar characteristics as those of MJSN BSY008-465 were found in the same stratigraphical layers during the excavation on the A16 highway, along with teeth of *Sericodon, , Proexochokefalos, Machimosaurus* and *Dakosaurus* (Schaefer, 2012; Schaefer *et al.*, 2018) : teeth with sub-circular to ovoid cross-section, bicarinate with micro-ziphodont condition, enamel ornamentation composed of sub parallel apicobasal ridges on the basal two thirds of the crown shifting into low relief drop-shaped ridges forming an “anastomosed pattern” on the remaining upper third of the crown. These teeth show a great variation of height and base length (Schaefer, 2012; LCG, pers. obs.). One of these teeth in particular (MJSN TCH007-91) shows a base length 31% longer than the largest tooth associated with MJSN BSY008-465. The great variation in

crown size of isolated teeth indicates that specimens of various sizes (and potentially ages) visited the area, including specimens significantly larger than MJSN BSY008-465. Considering there is only a few *Torvoneustes* specimens known between the middle Oxfordian and the Tithonian, it seems premature to consider size increase as an evolutionary trend in *Torvoneustes* for the moment.

Conclusions

The holotype of *Torvoneustes jurensis* is the most complete skeleton of the genus and the first specimen to preserve both extensive cranial and postcranial material. This new species is distinct from the other species on the basis of cranial morphology, dental characters, and geographic distribution. The phylogenetic analysis tends to confirm these observations. The distinction between *To. jurensis* and *To. mexicanus* remains difficult due to the fragmentary nature of the Mexican specimen. While future discovery of more specimens of *To. mexicanus* might help to get a better understanding of the differences between these two taxa, the dental characters allow us to discriminate them as two distinct species. It is interesting to note also that the genera *Cricosaurus* and *Dakosaurus* are as well found in the Kimmeridgian deposits of Europe, Mexico and South America, but that they are represented by different species in each of these geographically distant areas (Buchy *et al.*, 2006b, 2013; Pol and Gasparini, 2009; Young *et al.*, 2012b; Herrera, 2015; Herrera *et al.*, 2021a). In addition, it seems that the Late Jurassic marine reptiles of the Mexican Gulf are represented by species that differ from the coeval European and South American fauna, with the notable exception of one specimen of *Ophtalmosaurus* (Buchy *et al.*, 2006a; Buchy, 2007).

Acknowledgements

The authors would like to thank the Paleontology A16 team for the discovery and initial surface preparation of the specimen, Renaud Roch (Jurassica Museum) for his skillful complete extraction of the bones from the matrix, and Davit Vasilyan (Jurassica Museum) for the acquisition of the images from the digital microscope. We would also like to thank Corentin Jouault (Muséum National d'Histoire Naturelle) for his help with setting up Bayesian analysis and Mark Young (University of Edinburgh) for giving access to the character matrix and TNT script as well as for editing the manuscript. We thanks the reviewers Pascal Abel (University of Tuebingen), Sven Sachs (Naturkunde-Museum Bielefeld) and Davide Foffa (Virginia Tech) for their comments that helped improve the quality of the manuscript. We also thank the Willi Hennig Society for making TNT freely available.

References

Abel, P., Sachs, S., Young, M.T., 2020. Metriorhynchid crocodylomorphs from the lower Kimmeridgian of Southern Germany: evidence for a new large-bodied geosaurin lineage in Europe. Alcheringa: An Australasian Journal of Palaeontology 44(2), p. 312- 326.

Aiglstorfer, M., Havlik, P., & Herrera, Y., 2020. The first metriorhynchoid crocodyliform from the Aalenian (Middle Jurassic) of Germany, with implications for the evolution of Metriorhynchoidea. Zoological Journal of the Linnean Society, 188(2), 522-551.

Andrade, M.B., Young, M.T., Desojo, J.B., Brusatte, S.L., 2010. The evolution of extreme hypercarnivory in Metriorhynchidae (Mesoeucrocodylia: Thalattosuchia) based on evidence from microscopic denticle morphology. Journal of Vertebrate Paleontology 30(5), p. 1451-1465.

Andrews, C.W., 1909. On some new steneosaurs from the Oxford Clay of Peterborough. Annals and Magazine of Natural History 3, p. 299-308.

Andrews, C.W., 1913. A descriptive catalogue of marine reptiles of the oxford clay. Based on the Leeds collection in The British Museum (Natural History), London. Part II.

Barrientos-Lara, J.I., Herrera, Y., Fernández, M.S., Alvarado-Ortega, J., 2016. Occurrence of *Torvoneustes* (Crocodylomorpha, Metriorhynchidae) in marine Jurassic deposits of Oaxaca, Mexico. Revista Brasileira de Paleontologia 19(3), p. 415-424.

Brochu, C.A., 1996. Closure of neurocentral sutures during crocodilian ontogeny: Implications for maturity assessment in fossil archosaurs. Journal of Vertebrate Paleontology 16, 49–62.

Buchy, M.-C., 2008. New occurrence of the genus *Dakosaurus* (Reptilia, Thalattosuchia) in the Upper Jurassic of north-eastern Mexico, with comments upon skull architecture of Dakosaurus and Geosaurus. Neues Jahrbuch für Geologie und Paläontologie - Abhandlungen 249(1), p.1-8.

Buchy, M.-C., 2007. Mesozoic marine reptiles from northeast Mexico: description, systematics, assemblages and palaeobiogeography. Unpublished PhD thesis, University of Karlsruhe, 98 pp.

Buchy, M.-C., Frey, E., Stinnesbeck, W., López, J.G., 2006a. An annotated catalogue of the Upper Jurassic (Kimmeridgian and Tithonian) marine reptiles in the collections of the Universidad Autónoma de Nuevo León, Facultad de Ciencias de la Tiersra, Linares, Mexico. ORYCTOS 6, 19p.

Buchy, M.-C., Vignaud, P., Frey, E., Stinnesbeck, W., González, A.H.G., 2006b. A new thalattosuchian crocodyliform from the Tithonian (Upper Jurassic) of northeastern Mexico. Comptes Rendus Palevol 5, p. 785–794.

Buchy, M.-C., Young, M.T., Andrade, M.B., 2013. A new specimen of *Cricosaurus saltillensis* (Crocodylomorpha: Metriorhynchidae) from the Upper Jurassic of Mexico: evidence for craniofacial convergence within Metriorhynchidae. ORYCTOS 10, p. 9-21

Cau, A., Fanti, F., 2011. The oldest known metriorhynchid crocodylian from the Middle Jurassic of North-eastern Italy: *Neptunidraco ammoniticus* gen. et sp. nov. Gondwana Research 19, p. 550–565.

1312 Chiarenza, A.A., Foffa, D., Young, M.T., Insacco, G., Cau, A., Carnevale, G., Catanzariti, R.,
1313 2015. The youngest record of metriorhynchid crocodylomorphs, with implications for the
1314 extinction of Thalattosuchia. Cretaceous Research 9.
1315 Clarac, F., De Buffrénil, V., Brochu, C., Cubo, J., 2017. The evolution of bone ornamentation in
1316 Pseudosuchia: morphological constraints versus ecological adaptation. Biological Journal of the
1317 Linnean Society 121, 395–408. https://doi.org/10.1093/biolinnean/blw034
1318 Colombié, C., Strasser, A., 2005. Facies, cycles, and controls on the evolution of a keep-up
1319 carbonate platform (Kimmeridgian, Swiss Jura): Evolution of a keep-up carbonate platform.
1320 Sedimentology 52, 1207–1227. https://doi.org/10.1111/j.1365-3091.2005.00736.x
1321 Comment, G., Lefort, A., Koppka, J., Hantzpergue, P., 2015. Le Kimméridgien D'Ajoie (Jura,
1322 Suisse) : Lithostratigraphie Et Biostratigraphie De La Formation De Reuchenette.
1323 https://doi.org/10.5281/ZENODO.34341
1324 de Buffrenil, V., 1982. Morphogenesis of bone ornamentation in extant and extinct crocodilians.
1325 Zoomorphology 99, 155–166.
1326 de Buffrénil, V., Clarac, F., Fau, M., Martin, S., Martin, B., Pellé, E., Laurin, M., 2015.
1327 Differentiation and growth of bone ornamentation in vertebrates: A comparative histological
1328 study among the Crocodylomorpha: Development of Bone Ornamentation In The
1329 Crocodylomorpha. J. Morphol. 276, 425–445. https://doi.org/10.1002/jmor.20351
1330 De sousa oliveira S., Girard L., Raselli I., Anquetin J. In Press. Virtual reconstruction of a Late
1331 Jurassic metriorhynchid skull from Switzerland and its use for scientific illustration and paleoart.
1332 MorphoMuseuM
1333 Fara, E., Ouaja, M., Buffetaut, E., Srarfi, D., 2002. First occurrences of thalattosuchian
1334 crocodiles in the Middle and Upper Jurassic of Tunisia. Neues Jahrbuch fur Geologie und
1335 Palaontologie - Monatshefte. 8. 465-476. 10.1127/njgpm/2002/2002/465.
1336 Fitzinger, L. J. F. J. 1843. Systema Reptilium. Fasciculus Primus, Amblyglossae. Braumüller et
1337 Seidel, Vienna, 134 p.
1338 Foffa, D., Young, M.T., 2014. The cranial osteology of *Tyrannoneustes lythrodectikos*
1339 (Crocodylomorpha: Metriorhynchidae) from the Middle Jurassic of Europe. PeerJ 2, e608.
1340 Foffa, D., Young, M.T., Brusatte, S.L., Graham, M.R., Steel, L., 2018a. A new metriorhynchid
1341 crocodylomorph from the Oxford Clay Formation (Middle Jurassic) of England, with
1342 implications for the origin and diversification of Geosaurini. Journal of Systematic
1343 Palaeontology 16, p. 1123–1143.
1344 Foffa, D., Young, M.T., Brusatte, S.L., 2018b. Filling the Corallian gap: New information on
1345 Late Jurassic marine reptile faunas from England. Acta Palaeontologica Polonica. 63.
1346 10.4202/app.00455.2018.
1347 Foffa, D., Young, M.T., Stubbs, T.L., Dexter, K.G., Brusatte, S.L., 2018c. The long-term
1348 ecology and evolution of marine reptiles in a Jurassic seaway. Nature Ecology & Evolution 2,
1349 1548–1555. https://doi.org/10.1038/s41559-018-0656-6

Foffa, D., Johnson, M. M., Young, M. T., Steel, L., & Brusatte, S. L., 2019. Revision of the Late Jurassic deep-water teleosauroid crocodylomorph *Teleosaurus megarhinus* Hulke, 1871 and evidence of pelagic adaptations in Teleosauroidea. PeerJ, 7, e6646.
Fraas, E., 1901. Die Meerkrokodile (Thalattosuchia n. g.) eine neue Sauriergruppe der Juraformation. Ahreshefte des Vereins für vaterländische Naturkunde in Württemberg 57, p. 409 - 418
Fraas, E., 1902. Die Meer-Crocodilier (Thalattosuchia) des oberen Jura unter specieller Berücksichtigung von *Dacosaurus* und *Geosaurus*. Palaeontographica 49, p. 1–71.
Frey, B., Buchy M-C, Stinnesbeck W., Guadalupe López-Oliva J., 2002. *Geosaurus vignaudi* n.sp. (Crocodyliformes: Thalattosuchia), first evidence of metriorhynchid crocodilians in the Late Jurassic (Tithonian) of central-east Mexico (State of Puebla). Canadian Journal of Earth Sciences. 39(10): 1467-1483. https://doi.org/10.1139/e02-060
Gandola, R., Buffetaut, E., Monaghan, N., Dyke, G., 2006. Salt glands in the fossil crocodile Metriorhynchus. Journal of Vertebrate Paleontology 26, p. 1009–1010.
Gasparini, Z., Iturralde-Vinent, M., 2001. Metriorhynchid crocodiles (Crocodyliformes) from the Oxfordian of Western Cuba. Neues Jahrbuch fur Geologie und Palaontologie - Monatshefte. 2001. 534-542. 10.1127/njgpm/2001/2001/534.
Geoffroy Saint-Hilaire, E. 1831. Recherches sur de grands sauriens trouvés à l'état fossile aux confins maritimes de la Basse-Normandie, attribués d'abord au Crocodile, puis déterminés sous les noms de *Teleosaurus* et *Steneosaurus*. Mémoires de l'Academie des sciences 12, p. 1138
George, I.D., Holliday, C.M., 2013. Trigeminal nerve morphology in *Alligator mississippiensis* and Its significance for Crocodyliform facial sensation and evolution. The Anatomical Record 296, p. 670–680.
Goloboff, P.A., Catalano, S.A., 2016. TNT version 1.5, including a full implementation of phylogenetic morphometrics. Cladistics 32, 221–238.
Goloboff, P.A., Farris, J.S., Nixon, K.C., 2008. TNT, a free program for phylogenetic analysis Cladistics 24, p. 774–786.
Gower, D. J. 1999. The cranial and mandibular osteology of a new rauisuchian archosaur from the Middle Triassic of southern Germany. Stuttgarter Beiträge zur Naturkunde Serie B (Geologie und Paläontologie) 280, p. 1-49
Grange, D.R., Benton, M.J., 1996. Kimmeridgian metriorhynchid crocodiles from England. Palaeontology. 39, p. 497-514
Grigg, Gordon, Kirshner, D., 2015. Biology and Evolution of Crocodylians. CSIRO Publishing. 672 p.
Guignard. J.-P. & Weidmann. M., 1977. Nouveaux gisements de crocodiliens dans le Malm du Jura. Bulletin de la Société Vaudoise des Sciences Naturelles. 73. 297-308
Hay, O. P., 1930. Second Bibliography and Catalogue of the Fossil Vertebrata of North America, Vol II. Carnegie Institution of Washington Publication No. 390, Carnegie Institution of Washington, Washington, DC, 1074 p.

1389 Herrera Y., 2015. Metriorhynchidae (Crocodylomorpha: Thalattosuchia) from Upper Jurassic–
1390 Lower Cretaceous of Neuquén Basin (Argentina), with comments on the natural casts of the
1391 brain. In: M. Fernández, Y. Herrera (Eds.) Reptiles Extintos - Volumen en Homenaje a Zulma
1392 Gasparini. Publicación Electrónica de la Asociación Paleontológica Argentina 15(1), p. 159–171.
1393 Herrera, Y., Fernández, M.S., Gasparini, Z., 2013. Postcranial skeleton *of Cricosaurus*
1394 *araucanensis* (Crocodyliformes: Thalattosuchia): morphology and palaeobiological insights
1395 15.Herrera, Y., Gasparini, Z., & Fernández, M. S. 2015a. *Purranisaurus potens* Rusconi, an
1396 enigmatic metriorhynchid from the Late Jurassic–Early Cretaceous of the Neuquén Basin.
1397 Journal of Vertebrate Paleontology, 35(2), e904790.
1398 Herrera, Y., Fernández, M.S., Lamas, S.G., Campos, L., Talevi, M., Gasparini, Z., 2015b.
1399 Morphology of the sacral region and reproductive strategies of Metriorhynchidae: a counter-
1400 inductive approach. Earth and Environmental Science Transactions of The Royal Society of
1401 Edinburgh 106, 247–255. https://doi.org/10.1017/S1755691016000165 Herrera, Y., Aiglstorfer,
1402 M., Bronzati, M., 2021a. A new species of *Cricosaurus* (Thalattosuchia: Crocodylomorpha)
1403 from southern Germany: the first three dimensionally preserved *Cricosaurus* skull from the
1404 Solnhofen Archipelago. Journal of Systematic Palaeontology 19(2), p. 145-167
1405 Herrera, Y., Fernández, M.S., Vennari, V.V., 2021b. *Cricosaurus* (Thalattosuchia,
1406 Metriorhynchidae) survival across the J/K boundary in the High Andes (Mendoza Province,
1407 Argentina). Cretaceous Research 118, 104673. https://doi.org/10.1016/j.cretres.2020.104673
1408 Holliday, C.M., Witmer, L.M., 2007. Archosaur adductor chamber evolution: Integration of
1409 musculoskeletal and topological criteria in jaw muscle homology. Journal of Morphology 268, p.
1410 457–484. https://doi.org/10.1002/jmor.10524
1411 Holliday, C.M., Witmer, L.M., 2009. The epipterygoid of crocodyliforms and its significance for
1412 the evolution of the orbitotemporal region of eusuchians, Journal of Vertebrate Paleontology,
1413 29:3, 715-733, DOI: 10.1671/039.029.0330
1414 Iordansky, N.N., 1973. The skull of the Crocodilia. In Biology of the Reptilia Volume 4. (Eds C
1415 Gans and TS Parsons) pp. 201–260. Academic Press, New York
1416 Johnson, M., Young, M.T.,Steel, L., Foffa, D., Smith, A., Hua, S., Havlik, P., Howlett, E., Dyke,
1417 G., 2017. Re-description of '*Steneosaurus*' *obtusidens* Andrews, 1909, an unusual macrophagous
1418 teleosaurid crocodylomorph from the Middle Jurassic of England. Zoological Journal of the
1419 Linnean Society. 182. 1-34. 10.1093/zoolinnean/zlx035.
1420 Johnson, M. M., Young, M. T., & Brusatte, S. L., 2020b. The phylogenetics of Teleosauroidea
1421 (Crocodylomorpha, Thalattosuchia) and implications for their ecology and evolution. PeerJ, 8,
1422 e9808.
1423 Krebs, B., 1967. Zwei Sieneosaurus-Wirbel aus den Birmenstorfer Schichten (Ober-Oxford) vom
1424 «Weissen Graben» bei Mönthal (Kt. Aargau). Eclogae Geologicae Helvetiae. 60. 689-695.
1425 Le Mort, J., Martin, J.E., Picot, L., Hua, S., 2022. First description of the most complete
1426 *Metriorhynchus* aff. *superciliosus* (Thalattosuchia) specimen from the Callovian of the Vaches-
1427 Noires cliffs (Normandy, France) and limitations in the classification of Metriorhynchidae. In
1428 Annales de Paléontologie (Vol. 108, No. 3, p. 102539). Elsevier Masson.

Leardi, J. M., Pol, D., & Clark, J. M., 2017. Detailed anatomy of the braincase of *Macelognathus vagans* Marsh, 1884 (Archosauria, Crocodylomorpha) using high resolution tomography and new insights on basal crocodylomorph phylogeny. PeerJ, 5, e2801. https://doi.org/10.7717/peerj.2801

Lepage, Y., Buffetaut, E., Hua, S., Martin, J.E., Tabouelle, J., 2008. Catalogue descriptif, anatomique, géologique et historique des fossiles présentés à l'exposition « Les Crocodiliens fossiles de Normandie » (6 novembre - 14 décembre 2008). Bulletin de la Société Géologique de Normandie et des Amis du Muséum du Havre, tome 95, fascicule 2, p. 5-152.

Lydekker, R., 1889. On the remains and affinities of five genera of Mesozoic reptiles. Quarterly Journal of the Geological Society, 45, p. 41-59.

Maddison, W. P. and D.R. Maddison. 2019. Mesquite: a modular system for evolutionary analysis. Version 3.61 http://www.mesquiteproject.org

Madzia, D., Sachs, S., Young, M. T., Lukeneder, A., Skupien, P., 2021. Evidence of two lineages of metriorhynchid crocodylomorphs in the Lower Cretaceous of the Czech Republic. Acta Palaeontologica Polonica 66(2).

Martin, J.E., Vincent, P., Falconnet, J., 2015. The taxonomic content of *Machimosaurus* (Crocodylomorpha, Thalattosuchia). Comptes Rendus Palevol 14, p. 305– 310. Meyer, H. von, 1845. System der fossilen Saurier [Taxonomy of fossil saurians]. Neues Jahrbuch für Mineralogie, Geognosie, Geologie und PetrefaktenKunde. p. 278-285

Martin, J. E. and Vincent, P., 2013. New remains of Machimosaurus hugii von Meyer, 1837 (Crocodilia, Thalattosuchia) from the Kimmeridgian of Germany, Fossil Record, 16, 179–196, https://doi.org/10.1002/mmng.201300009

Marty, D., Hug, W., Iberg, A., Cavin, L., Meyer, C., Lockley, M., 2003. Preliminary Report on the Courtedoux Dinosaur Tracksite from the Kimmeridgian of Switzerland. Ichnos 10, 209–219. https://doi.org/10.1080/10420940390256212

Massare, J.A., 1987. Tooth Morphology and Prey Preference of Mesozoic Marine Reptiles. Journal of Vertebrate Paleontology 7, 121–137.

Owen, R., 1883. On the Cranial and Vertebral characters of the Crocodilian Genus *Plesiosuchus*. Quarterly Journal of the Geological Society 40, p. 153-159

Parrilla-Bel, J., Young, M.T., Moreno-Azanza, M., Canudo, J. I., 2013. The first metriorhynchid crocodylomorph from the Middle Jurassic of Spain, with implications for evolution of the subclade Rhacheosaurini. PLoS ONE, 8:e54275. doi: 10.1371/journal.pone.0054275.

Parrilla-Bel, J., Canudo, J.I., 2015. Postcranial elements of "*Maledictosuchus riclaensis*" (Thalattosuchia) from the Middle Jurassic of Spain. Journal of Iberian Geology 41, 31–40. https://doi.org/10.5209/rev_JIGE.2015.v41.n1.48653

Pierce, S.E., Benton, M.J., 2006, *Pelagosaurus typus* Bronn, 1841 (Mesoeucrocodylia: Thalattosuchia) from the Upper Lias (Toarcian, Lower Jurassic) of Somerset, England, Journal of Vertebrate Paleontology, 26:3, 621-635, DOI: 10.1671/0272-4634(2006)26[621:PTBMTF]2.0.CO;2

1468 Pierce, S.E., Angielczyk, K.D. and Rayfield, E.J., 2009. Shape and mechanics in thalattosuchian
1469 (Crocodylomorpha) skulls: implications for feeding behaviour and niche partitioning. Journal of
1470 Anatomy, 215: 555-576. https://doi.org/10.1111/j.1469-7580.2009.01137.x
1471 Pochat-Cottilloux, Y., Martin, J. E., Amiot, R., Cubo, J., de Buffrénil, V., 2022. A survey of
1472 osteoderm histology and ornamentation among Crocodylomorpha: A new proxy to infer
1473 lifestyle? Journal of Morphology, 284, e21542. https://doi.org/10.1002/jmor.21542
1474 Pol, D., Gasparini, Z., 2009. Skull anatomy of *Dakosaurus andiniensis* (Thalattosuchia:
1475 Crocodylomorpha) and the phylogenetic position of Thalattosuchia. Journal of Systematic
1476 Palaeontology 7(2), p. 163–197.
1477 Prasad, G.V.R., de Lapparent de Broin, F., 2002. Late Cretaceous crocodile remains from Naskal
1478 (India): comparisons and biogeographic affinities. Annales de Paléontologie 88, 19–71.
1479 https://doi.org/10.1016/S0753-3969(02)01036-4
1480 Püntener C, Anquetin J, Billon-Bruyat J-P. 2020. New material of “Eurysternidae”
1481 (Thalassochelydia, Pan-Cryptodira) from the Kimmeridgian of the Swiss Jura Mountains.
1482 Palaeovertebrata 43:e2. DOI: 10.18563/pv.43.1.e2.
1483 Quenstedt, F. A., 1856. Sonst und jetzt: populäre Vorträge über Geologie. Laupp
1484 Rieppel, O., 1979. Ein *Geosaurus*-fragment (Reptilia, Thalattosuchia) aus dem oberen Malm von
1485 Evilard bei Biel.
1486 Rieppel, O., 1981. Fossile Krokodilier aus dem Schweizer Jura. Eclogae Geologicae Helvetiae.
1487 74/3. 735-751.
1488 Ronquist, F., Teslenko, M., van der Mark, P., Ayres, D.L., Darling, A., Höhna, S., Larget, B.,
1489 Liu, L., Suchard, M.A., Huelsenbeck, J.P., 2012. MrBayes 3.2: Efficient Bayesian phylogenetic
1490 inference and model choice across a large model space. Systematic Biology 61, p. 539–542.
1491 Ruebenstahl, A.A., Klein, M.D., Yi, H., Xu, X., & Clark, J.M., 2022. Anatomy and relationships
1492 of the early diverging Crocodylomorphs Junggarsuchus sloani and Dibothrosuchus elaphros. The
1493 Anatomical Record, 305(10), 2463– 2556. https://doi.org/10.1002/ar.24949
1494 Sachs, S., Young, M., Abel, P., Mallison, H., 2019. A new species of the metriorhynchid
1495 crocodylomorph *Cricosaurus* from the Upper Jurassic of southern Germany. Acta
1496 Palaeontologica Polonica 64. https://doi.org/10.4202/app.00541.2018
1497 Sachs, S., Young, M.T., Hornung, J.J., 2020. The enigma of *Enaliosuchus*, and a reassessment of
1498 the Lower Cretaceous fossil record of Metriorhynchidae, Cretaceous Research, Volume 114,
1499 104479, ISSN 0195-6671, https://doi.org/10.1016/j.cretres.2020.104479.
1500 Sachs, S., Young, M., Abel, P., Mallison, H., 2021. A new species of *Cricosaurus*
1501 (Thalattosuchia, Metriorhynchidae) based upon a remarkably well-preserved skeleton from the
1502 Upper Jurassic of Germany. Palaeontologia Electronica. https://doi.org/10.26879/928
1503 Schaefer, K., 2012. Variabilité de la morphologie dentaire des crocodiliens marins
1504 (Thalattosuchia) du Kimméridgien d’Ajoie (Jura, Suisse). Mémoire de Master (non-publié),
1505 Université de Fribourg. 111 p.
1506 Schaefer, K., Billon-Bruyat, J.-P., Hug, W.A., Friedli, V., Püntener, C., 2018. Vertébrés
1507 mésozoïques: crocodiliens. Catalogue du patrimoine paléontologique jurassien - A16. 188 p. .

Sebens, K.P., 1987. The Ecology of Indeterminate Growth in Animals 37.
Spindler, F., R. Lauer, H. Tischlinger, and M. Mäuser. 2021. The integument of pelagic crocodylomorphs (Thalattosuchia: Metriorhynchidae). Palaeontologia Electronica, 24:a25. doi: 10.26879/1099.
Vignaud, P. 1995. Les Thalattosuchia, crocodiles marins du Mesozoique: systematique phylogenetique, paleoecologie, biochronologie et implications paleogeographiques. Ph.D. dissertation, Universite de Poitiers, Poitiers, France,
Vignaud, P., 1997. La morphologie dentaire des thalattosuchia (Crocodylia, Mesosuchia).
von Arthaber, G., 1906. Beiträge zur kenntnis der organisation und der anpassungsercheinungen des genus *Metriorhynchus*.
Wagner, J. A., 1858. Neue Beiträge zur Kenntniss der urweltlichen Fauna des lithographischen Schiefers: Saurier (Vol. 8).
Waskow, K., Grzegorczyk, D., Sander, P.M., 2018. The first record of *Tyrannoneustes* (Thalattosuchia: Metriorhynchidae): a complete skull from the Callovian (late Middle Jurassic) of Germany. PalZ 92, p. 457–480.
Wilberg, E.W., 2012, Phylogenetic and morphometric assessment of the evolution of the longirostrine crocodylomorphs, The University of Iowa.
Wilberg, E.W., Godoy, P.L., Griffiths, E.F., Turner, A.H. Benson, R.B., 2022. A new early diverging thalattosuchian (Crocodylomorpha) from the Early Jurassic (Pliensbachian) of Dorset, UK and implications for the origin and evolution of the group. Journal of Vertebrate Paleontology, p.e2161909.
Wilkinson, L.E., Young, M.T., Benton, M.J., 2008. A new metriorhynchid crocodilian (Mesoeucrocodylia Thalattosuchia) from the Kimmeridgian (Upper Jurassic) of Wiltshire, UK. Palaeontology 51, p. 1307– 1333.
Young M.T., Hua S., Steel L., Foffa D., Brusatte S.L., Thüring S., Mateus O., Ruiz-Omeñaca J.I., Havlik P., Lepage Y., De Andrade M.B., 2014a. Revision of the Late Jurassic teleosaurid genus Machimosaurus (Crocodylomorpha, Thalattosuchia) Royal Society Open Science 1, 140222 140222 http://doi.org/10.1098/rsos.140222
Young, M.T., 2014b. Filling the 'Corallian Gap': re-description of a metriorhynchid crocodylomorph from the Oxfordian (Late Jurassic) of Headington, England. Historical Biology 26, p. 80–90.
Young, M.T., Andrade, M.B., 2009. What is *Geosaurus*? Redescription of *Geosaurus giganteus* (Thalattosuchia: Metriorhynchidae) from the Upper Jurassic of Bayern, Germany. Zoological Journal of the Linnean Society, 157, p. 551–585.
Young, M.T., Brusatte, S.L., Ruta, M., Andrade, M.B., 2010. The evolution of Metriorhynchoidea (Mesoeucrocodylia, Thalattosuchia): an integrated approach using geometric morphometrics, analysis of disparity, and biomechanics. Zoological Journal of the Linnean Society, 158, p. 801–859.
Young, M.T., Bell, M.A., Andrade, M.B., Brusatte, S.L., 2011. Body size estimation and evolution in metriorhynchid crocodylomorphs: implications for species diversification and niche

partitioning. Zoological Journal of the Linnean Society 163, 4, p. 1199–1216, https://doi.org/10.1111/j.1096-3642.2011.00734.x

Young, M.T., Brusatte, S.L., Beatty, B.L., Andrade, M.B., Desojo, J.B., 2012a. Tooth-on-tooth interlocking occlusion suggests macrophagy in the Mesozoic marine crocodylomorph *Dakosaurus*. The Anatomical Record 295, p. 1147–1158.

Young, M.T., Brusatte, S.L., Andrade, M.B., Desojo, J.B., Beatty, B.L., Steel, L., Schoch, R.R., 2012b. The cranial osteology and feeding ecology of the metriorhynchid crocodylomorph genera *Dakosaurus* and *Plesiosuchus* from the Late Jurassic of Europe. PLOS ONE 7, 42.

Young, M.T., Andrade, M.B., Brusatte, S.L., Sakamoto, M., Liston, J., 2013a. The oldest known metriorhynchid super-predator: a new genus and species from the Middle Jurassic of England, with implications for serration and mandibular evolution in predacious clades. Journal of Systematic Palaeontology 11, p. 475–513.

Young, M.T., Andrade, M.B., Etches, S., Beatty, B.L., 2013b. A new metriorhynchid crocodylomorph from the Lower Kimmeridge Clay Formation (Late Jurassic) of England, with implications for the evolution of dermatocranium ornamentation in Geosaurini. Zoological Journal of the Linnean Society. 169, p. 820–848.

Young, M.T., Steel, L., Brusatte, S.L., Foffa, D., Lepage, Y., 2014. Tooth serration morphologies in the genus *Machimosaurus* (Crocodylomorpha, Thalattosuchia) from the Late Jurassic of Europe. Royal Society Open Science. 1, 140269.

Young, M.T., Foffa, D., Steel, L., Etches, S., 2019. Macroevolutionary trends in the genus *Torvoneustes* (Crocodylomorpha: Metriorhynchidae) and discovery of a giant specimen from the Late Jurassic of Kimmeridge, UK. Zoological Journal of the Linnean Society 189(2), p. 483-493.

Young, M.T., Brignon, A., Sachs, S., Hornung, J.J., Foffa, D., Kitson, J.J.N., Johnson, M.M., Steel, L., 2020a. Cutting the Gordian knot: a historical and taxonomic revision of the Jurassic crocodylomorph *Metriorhynchus*. Zoological Journal of the Linnean Society 192(2), p. 510-553.

Young, M.T., Sachs, S., Abel, P., Foffa, D., Herrera, Y., Kitson, J.J.N., 2020b. Convergent evolution and possible constraint in the posterodorsal retraction of the external nares in pelagic crocodylomorphs. Zoological Journal of the Linnean Society 189, p. 494- 520.

Figure 1

Geographical map of the Ajoie region, Canton of Jura, Switzerland.

The excavation site of MJSN BSY008-465 (BSY, Courtedoux–Bois de Sylleux) is indicated along the A16 Transjurane highway (in grey).

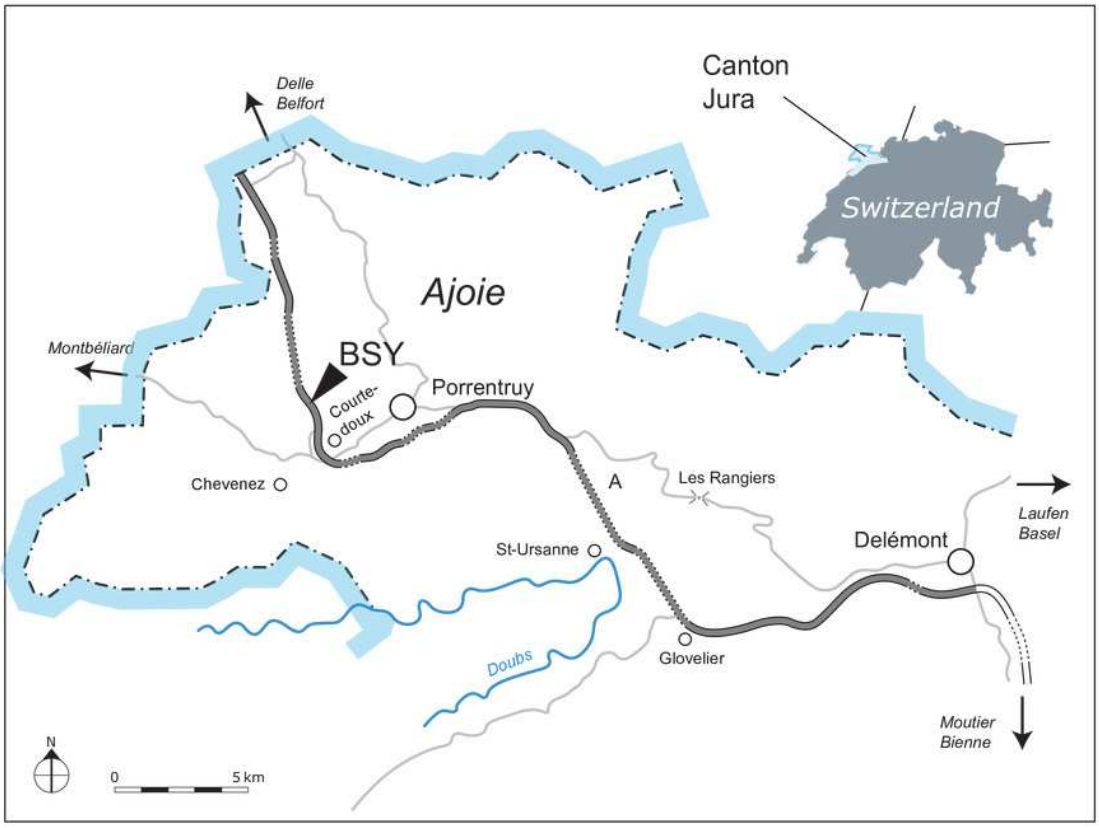

Figure 2

Taphonomical disposition of the metriorhynchid skeleton MJSN BSY008-465.

(a) photograph of the skeleton still embedded in the limestone block (see text); (b) drawing of the bones in their taphonomical position.

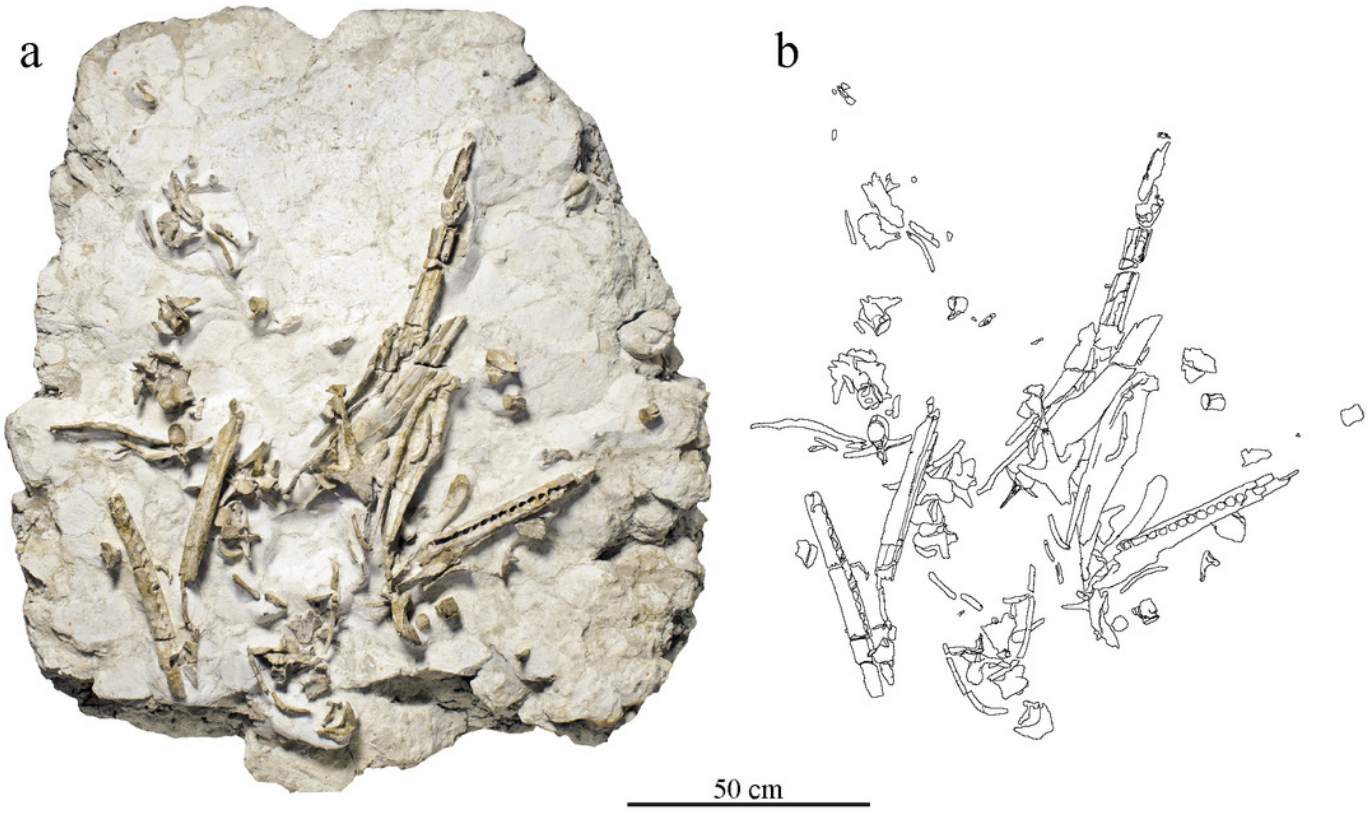

Figure 3

Stratigraphical section of the Reuchenette Formation in Ajoie, Canton of Jura, Switzerland, with a close-up on the Lower Virgula Marls.

MJSN BSY008-465 was found on the hardground level 4000 in the Lower Virgula Marls. The stratigraphical chart is derived from Comment *et al.* (2015) and Püntener *et al.* (2020).

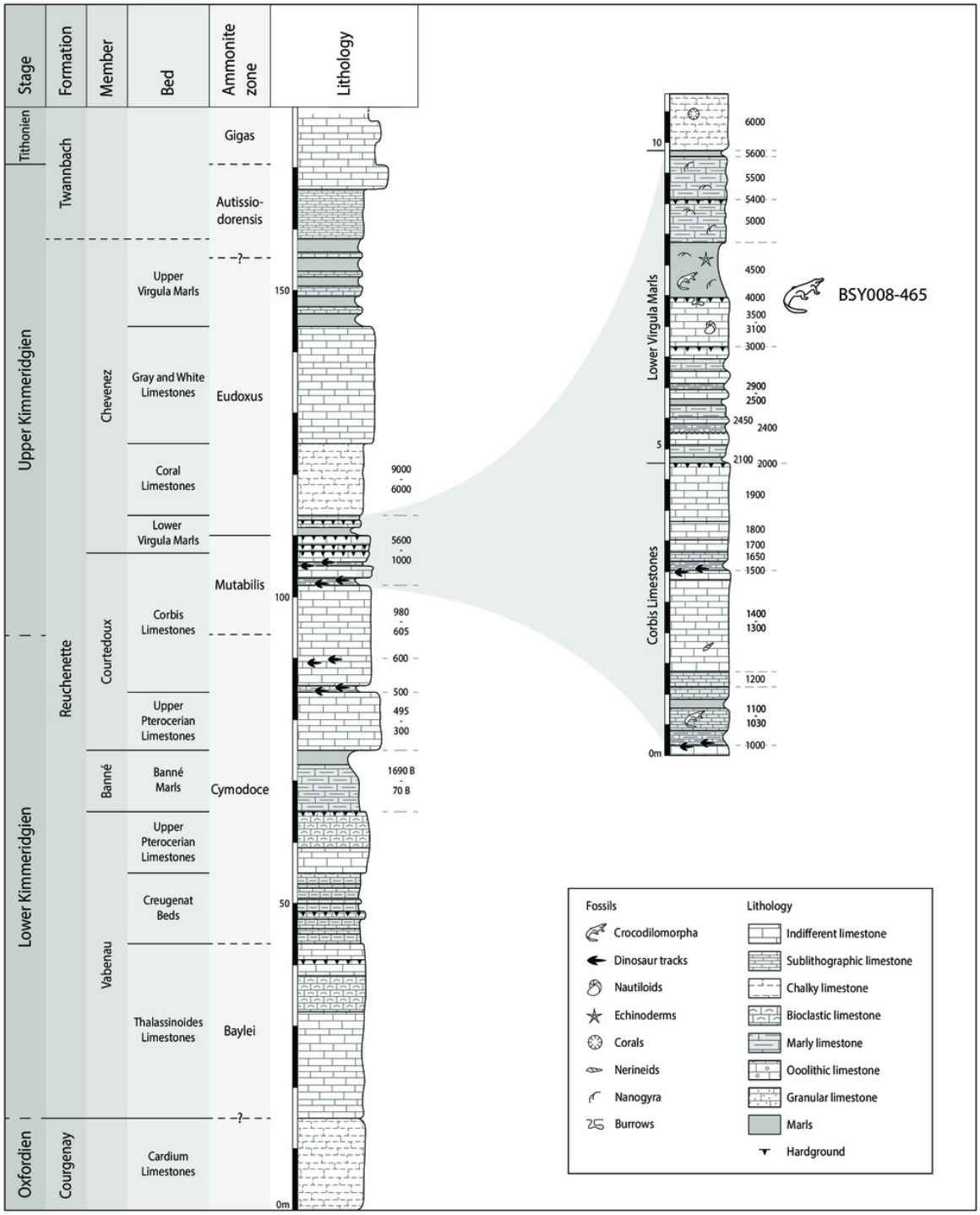
Stage
Formation
Member
Bed
Ammonite zone
Lithology
Tithonien
Upper Kimmeridgien
Lower Kimmeridgien
Oxfordien
Twannbach
Reuchenette
Courgenay
Chevenez
Courtedoux
Banné
Vabenau
Upper Virgula Marls
Gray and White Limestones
Coral Limestones
Lower Virgula Marls
Corbis Limestones
Upper Pterocerian Limestones
Banné Marls
Upper Pterocerian Limestones
Creugenat Beds
Thalassinoides Limestones
Cardium Limestones
Gigas
Autissio-dorensis
Eudoxus
Mutabilis
Cymodoce
Baylei
150
100
50
0m
9000
6000
5600
1000
980
605
600
500
495
300
1690 B
70 B
Lower Virgula Marls
Corbis Limestones
BSY008-465
10
5
0m
6000
5600
5500
5400
5000
4500
4000
3500
3100
3000
2900
2500
2450
2400
2100
2000
1900
1800
1700
1650
1500
1400
1300
1200
1100
1030
1000
Fossils
Crocodilomorpha
Dinosaur tracks
Nautiloids
Echinoderms
Corals
Nerineids
Nanogyra
Burrows
Lithology
Indifferent limestone
Sublithographic limestone
Chalky limestone
Bioclastic limestone
Marly limestone
Ooolithic limestone
Granular limestone
Marls
Hardground

Figure 4

MJSN BSY008-465, holotype of *Torvoneustes jurensis* (Kimmeridgian, Porrentruy, Switzerland).

Scientific drawings of the reconstructed skull (a) and mandible (b) in dorsal and (c) lateral views. the remaining matrix is represented in yellow. Anterior is to the right. Abbreviations: **al**, alveolus; **an**, angular; **art**, articular; **cp**, coronoid process; **den**, dentary; **fr**, frontal; **mx**, maxilla; **na**, nasal; **pa**, parietal; **pmx**, premaxilla; **po**, postorbital; **prf**, prefrontal; **san,** surangular; **sdg,** surangulodentary groove; **sq**, squamosal; **spl**, splenial; **tc**, tooth crown.

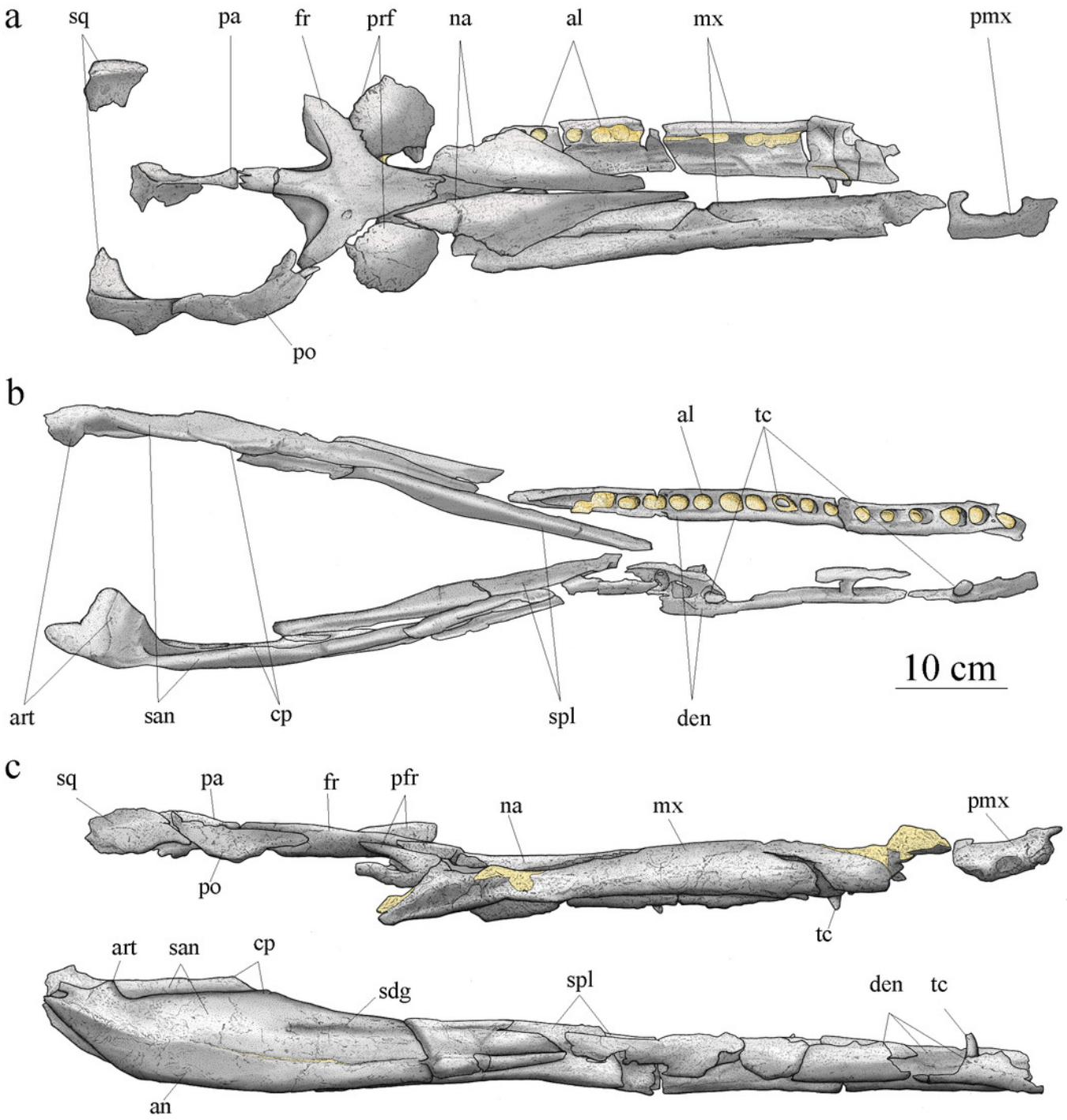
a
sq
pa
fr
prf
na
al
mx
pmx
po
b
al
tc
art
san
cp
spl
den
10 cm
c
sq
pa
fr
pfr
na
mx
pmx
po
tc
art
san
cp
sdg
spl
den
tc
an

Figure 5

MJSN BSY008-465, holotype of *Torvoneustes jurensis* (Kimmeridgian, Porrentruy, Switzerland).

(a) right premaxilla, (b) right prefrontal, (c) Left nasal, and (d) right nasal in dorsal views. Anterior is to the right.

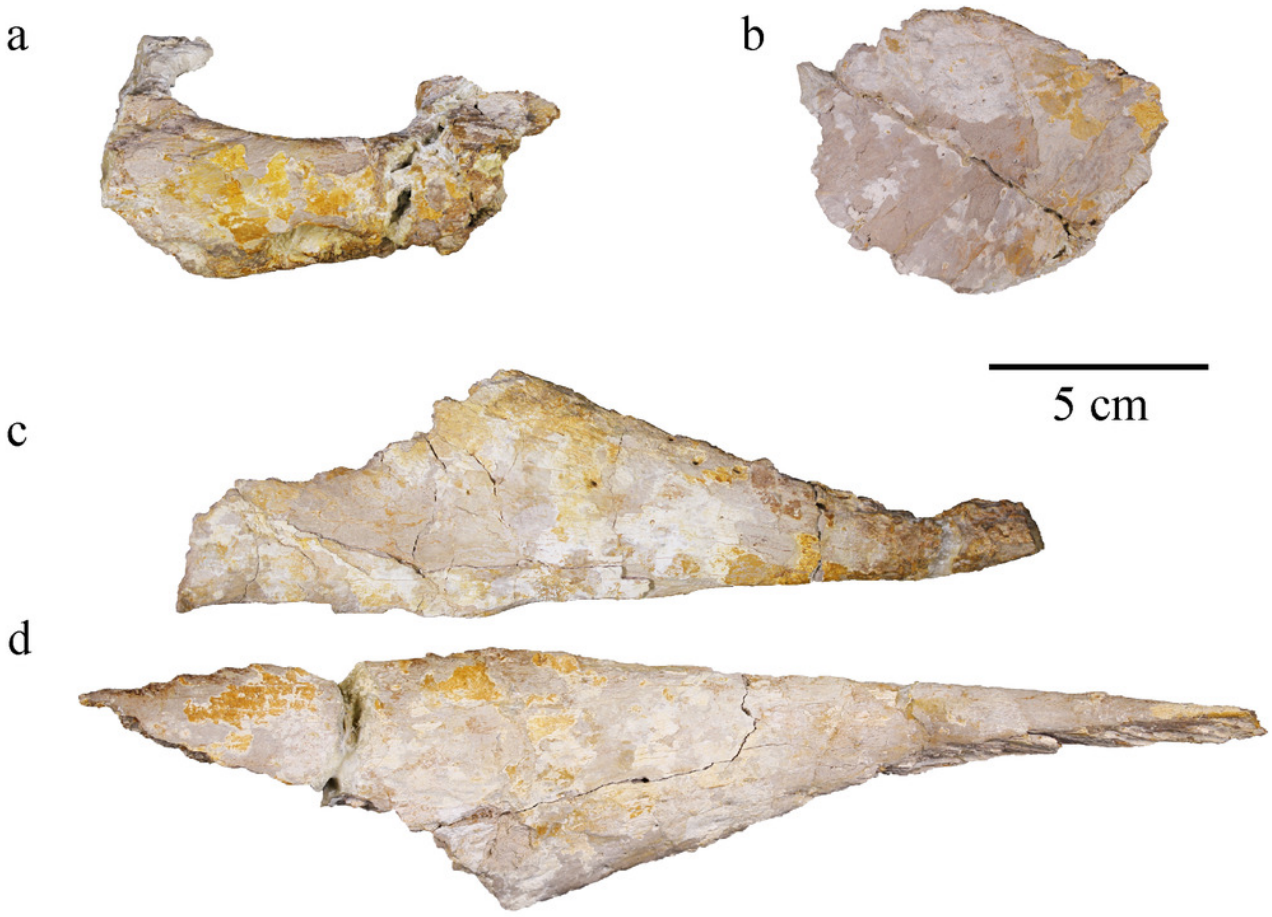

Figure 6

MJSN BSY008-465, holotype of *Torvoneustes jurensis* (Kimmeridgian, Porrentruy, Switzerland).

Photographs and scientific drawings of the right maxilla in (a, b) ventral and (c, d) lateral views. Anterior is to the right. Abbreviations: **al**, alveolus; **for**, foramen; **mx**, maxilla; **no**, notch; **pa**, palatine. Numbers indicate the preserved alveoli. Matrix is in yellow.

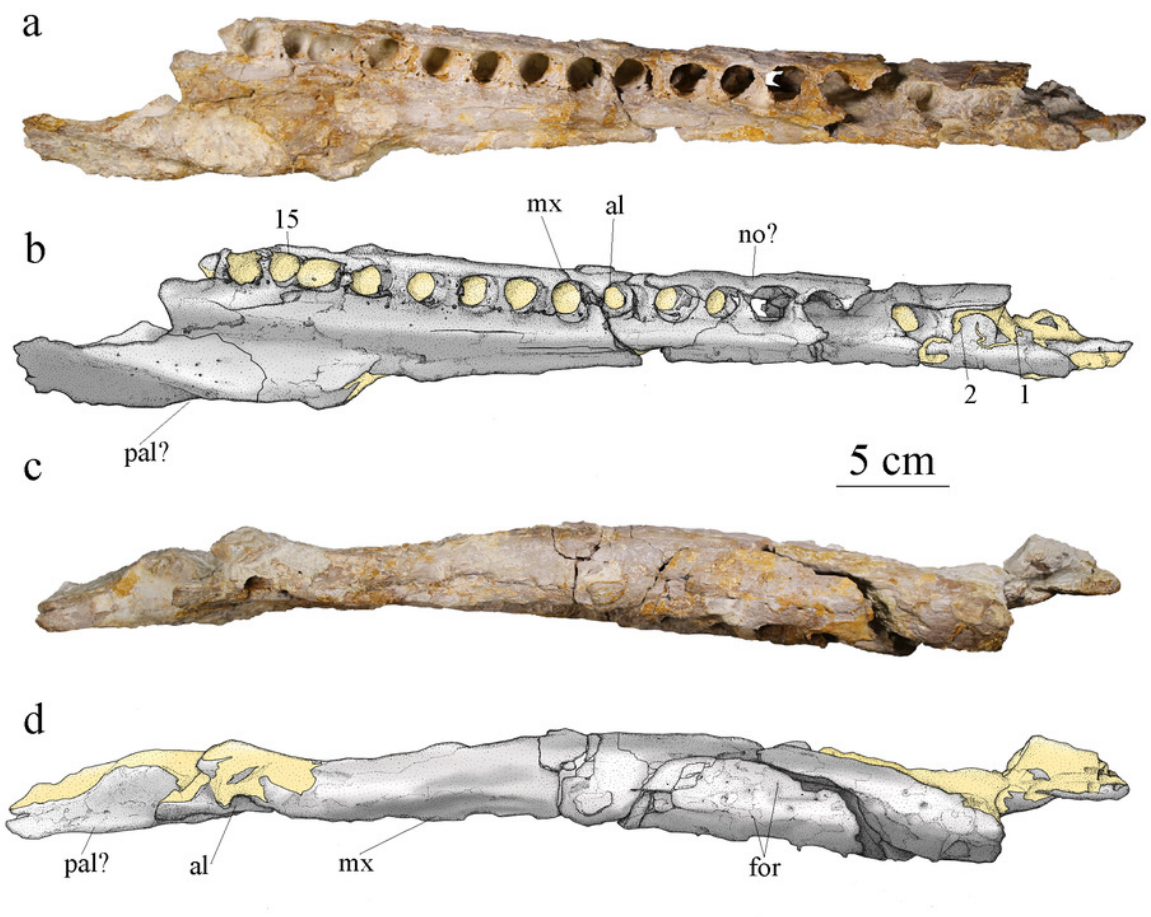

Figure 7

MJSN BSY008-465, holotype of *Torvoneustes jurensis* (Kimmeridgian, Porrentruy, Switzerland).

(a) Scientific drawing, (b) interpretative drawing and (c) photograph of the frontal and left prefrontal in dorsal view. The angle formed by the lateral contacts of the frontal with the prefrontal and nasal is indicated in (b). Abbreviation: **fr**, frontal; **if**, intertemporal flange; **prf**, prefrontal. Matrix is in yellow.

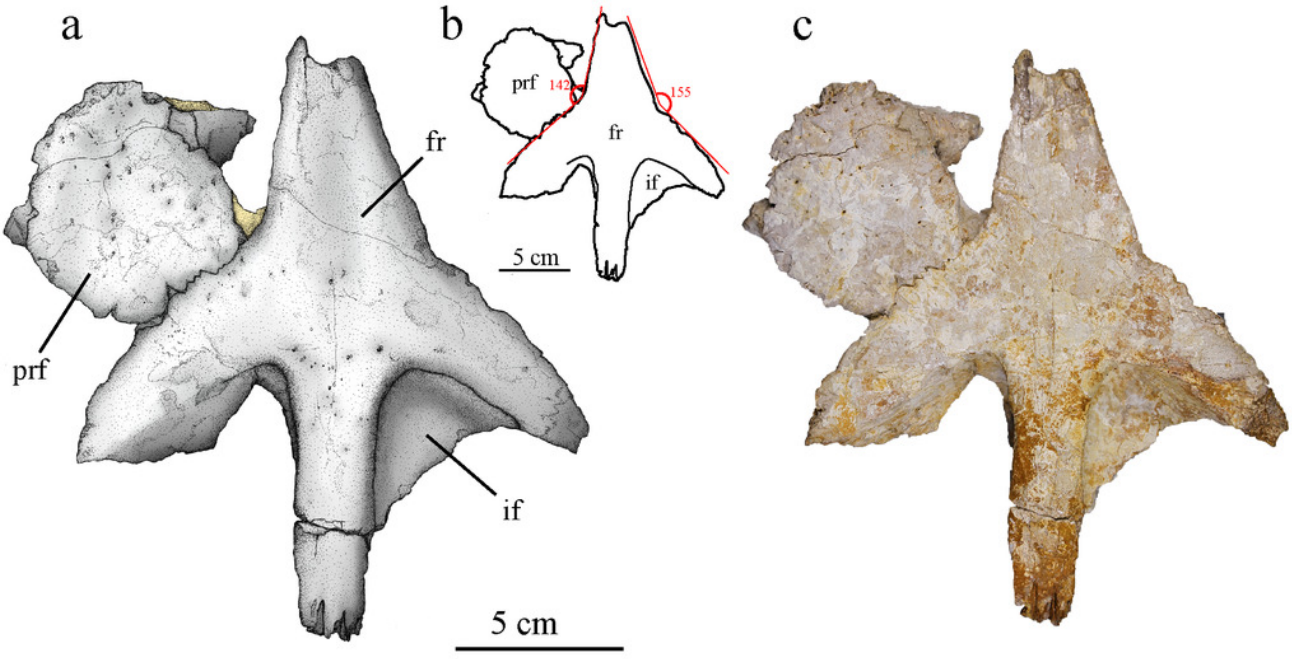

Figure 8

MJSN BSY008-465, holotype of *Torvoneustes jurensis* (Kimmeridgian, Porrentruy, Switzerland).

Posterior cranial elements with the right postorbital in (a) dorsal, (b) medial, and (c) lateral views; the parietal in (d) right lateral and (e) dorsal view; and the right squamosal in (f) dorsal view. Anterior to the right (except in b to the left). Abbreviations: **in**, incision; **sqfs**, squamosal flat surface.

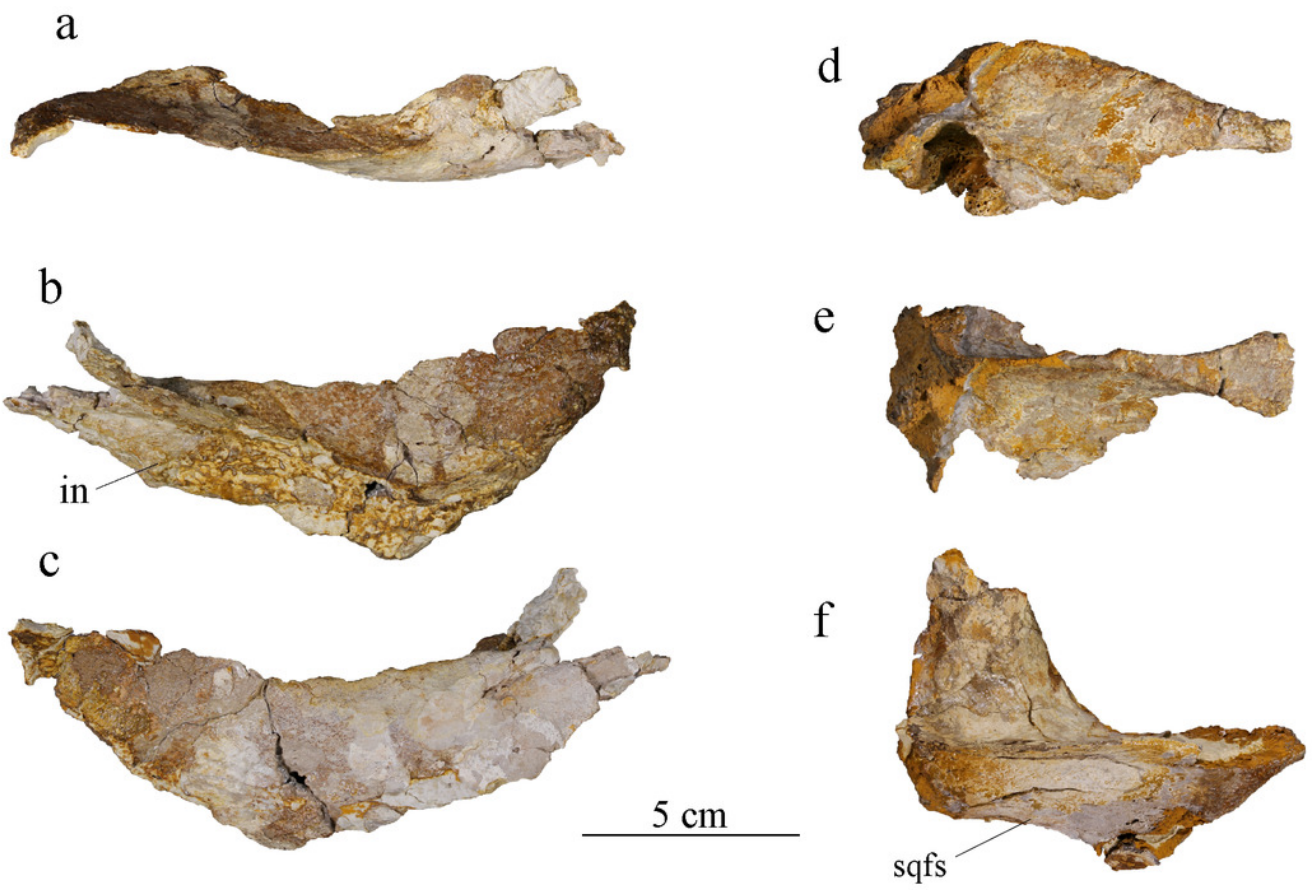

Figure 9

MJSN BSY008-465, holotype of *Torvoneustes jurensis* (Kimmeridgian, Porrentruy, Switzerland).

Photographs of the left dentary in (a) dorsal and (b) lateral views. Drawings of the left dentary in (c) dorsal and (d) lateral views. Anterior is to the left. Abbreviations: **al**, alveolus; **for**, foramen; **sdg**, surangulodentary groove; **tc**, tooth crown. Matrix is in yellow.

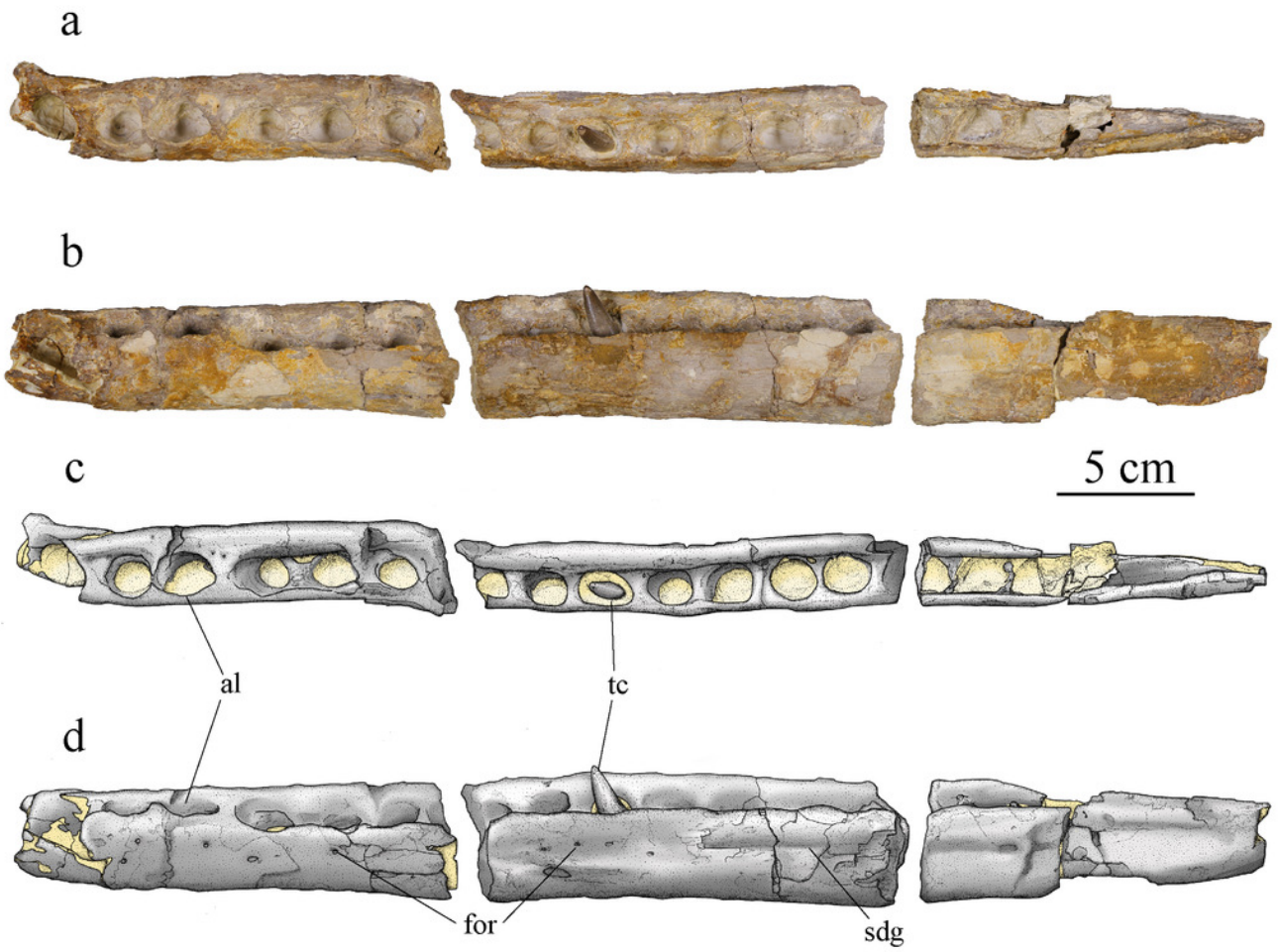

Figure 10

MJSN BSY008-465, holotype of *Torvoneustes jurensis* (Kimmeridgian, Porrentruy, Switzerland).

Photographs of the right splenial in (a) lateral, (b) medial, and (c) dorsal views. Photograph of the left splenial in (d) medial view. Abbreviations: **for**, foramen; **r**, ridge; **sym**, symphysis. Arrows point anteriorly and dashed lines show limits of the symphysis marks.

Figure 11

MJSN BSY008-465, holotype of *Torvoneustes jurensis* (Kimmeridgian, Porrentruy, Switzerland).

Photographs of the posterior part of the right ramus of the mandible in (a) medial, (b) dorsal, and (c) lateral views. Scientific drawings of the posterior part of the right ramus of the mandible in (d) medial, (e) dorsal, and (f) lateral views. Abbreviations: **an**, angular; **art**, articular; **cp**, coronoid process; **for**, foramen; **gf**, glenoid fossa; **pra**, prearticular; **ret**, retroarticular process; **san**, surangular; **sdg**, surangulodentary groove. Matrix is in yellow.

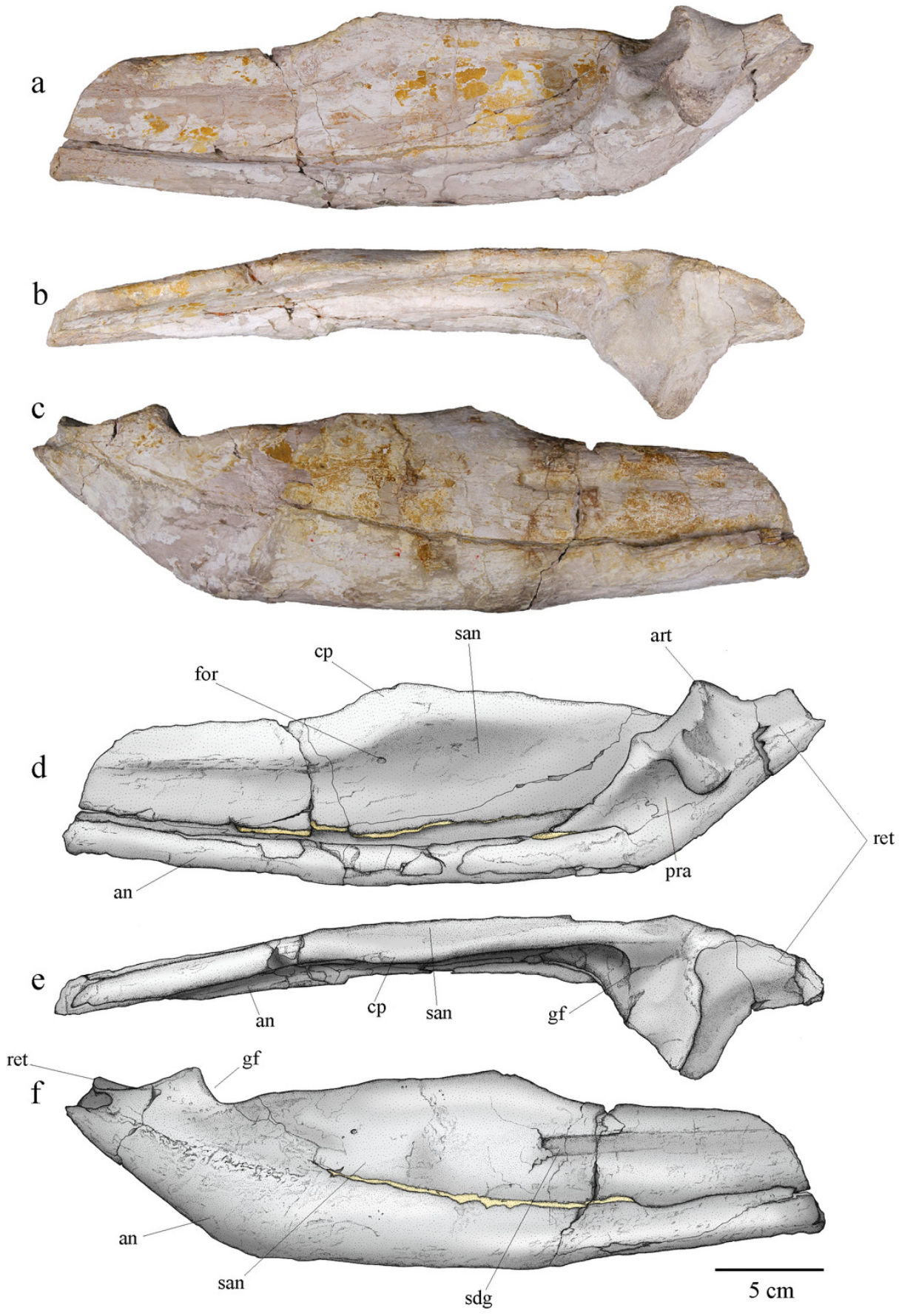
a
b
c
d
e
f
san
art
cp
for
ret
pra
an
cp
san
gf
an
ret
gf
san
sdg
5 cm

Figure 12

MJSN BSY008-465, holotype of *Torvoneustes jurensis* (Kimmeridgian, Porrentruy, Switzerland).

Two of the best-preserved isolated teeth in (a) lateral and (b) probably anterior views.

Abbreviations: **c**, crown; **ca**, carina; **r**, root.

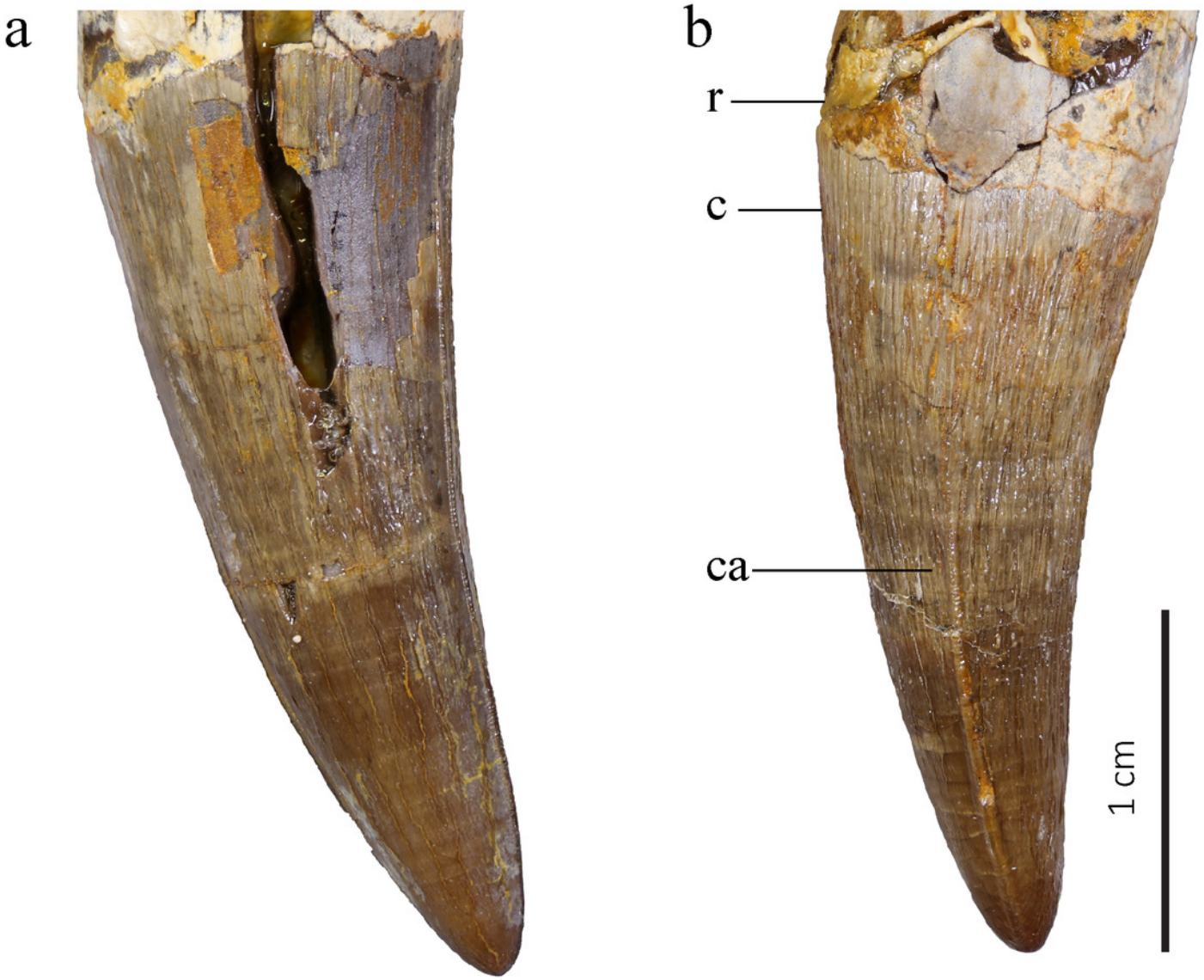

Figure 13

MJSN BSY008-465, holotype of *Torvoneustes jurensis* (Kimmeridgian, Porrentruy, Switzerland).

Microscopic photographs of MJSN BSY008-465 teeth. (a, b) mid-upper tooth crown; (c) tooth apex; (d) tooth base. **ib**, inflated base; **fd**, false denticle and **td**, true denticle.

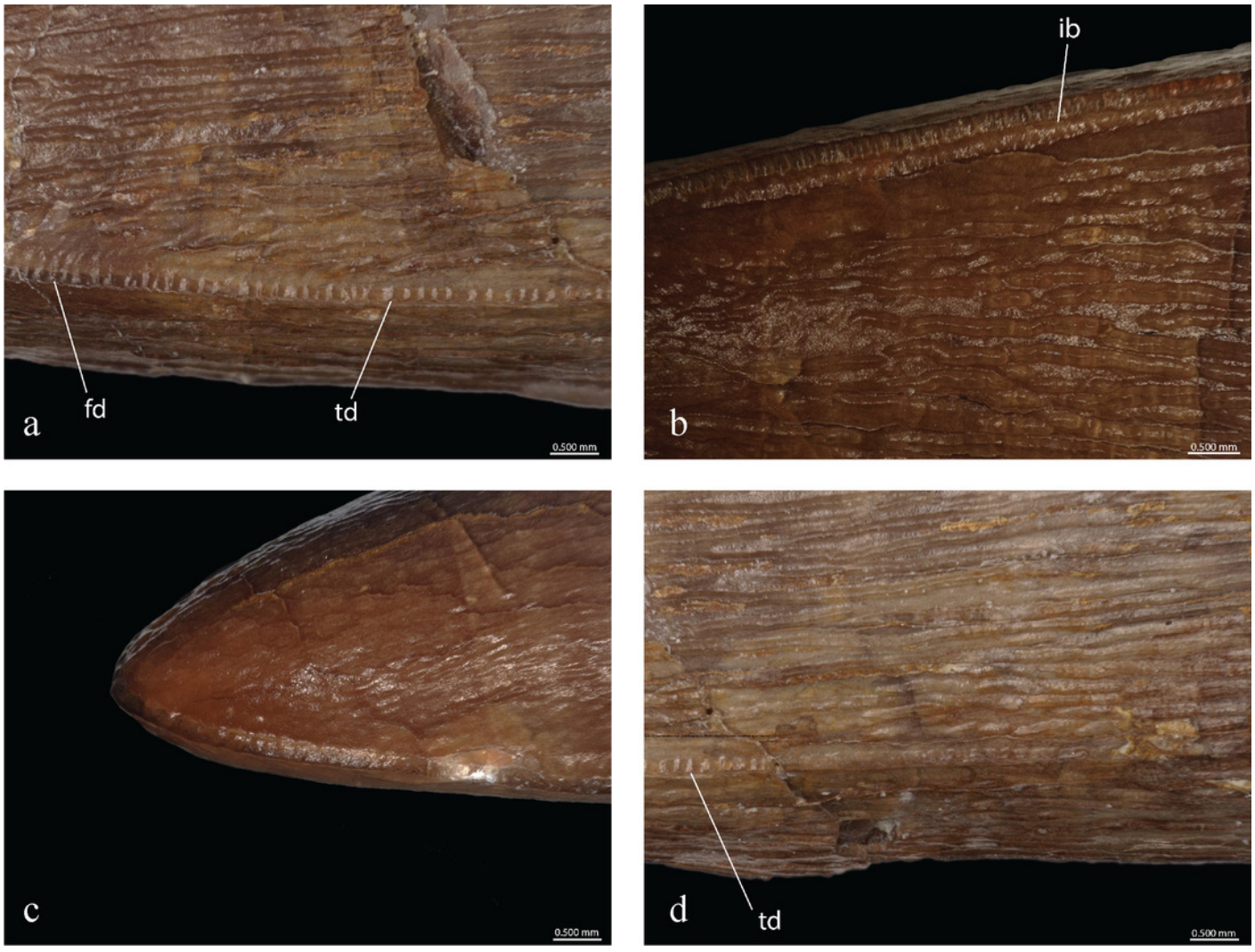

Figure 14

MJSN BSY008-465, holotype of *Torvoneustes jurensis* (Kimmeridgian, Porrentruy, Switzerland).

Cervical vertebra in (a) anterior and (b) right lateral views; dorsal vertebra in (c) anterior and (d) right lateral views; anterior caudal vertebra in (e) anterior and (f) right lateral views; Posterior caudal vertebrae in (g) anterior and (h) right lateral views. Abbreviations: **di**, diapophysis; **pa**, parapophysis; **prz**, prezygapophysis; **pz**, postzygapophysis.

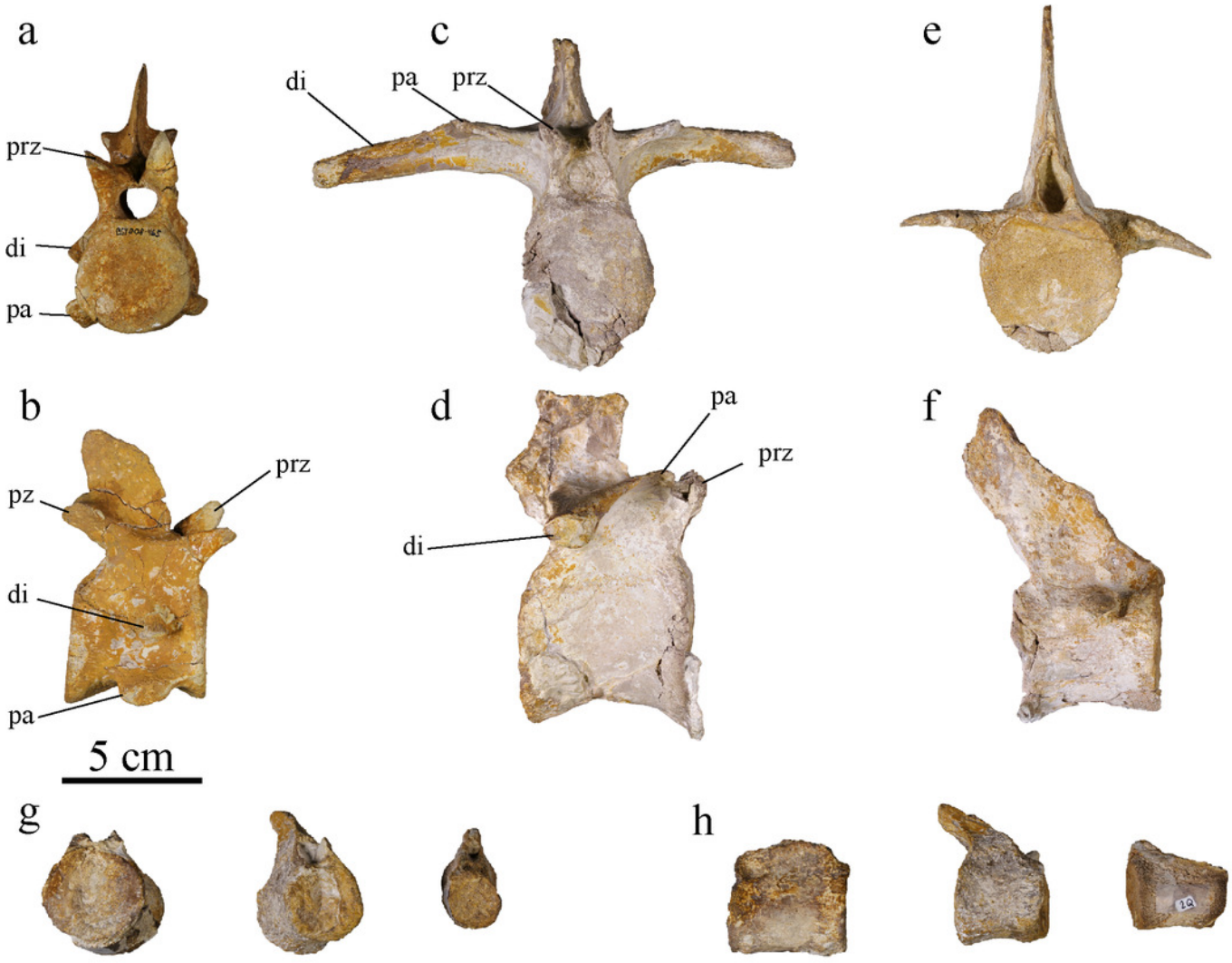

Figure 15

MJSN BSY008-465, holotype of *Torvoneustes jurensis* (Kimmeridgian, Porrentruy, Switzerland).

(a-c) cervical ribs, (d,e) dorsal ribs; chevron in (f) dorsal and (g) lateral views (anterior to the top).

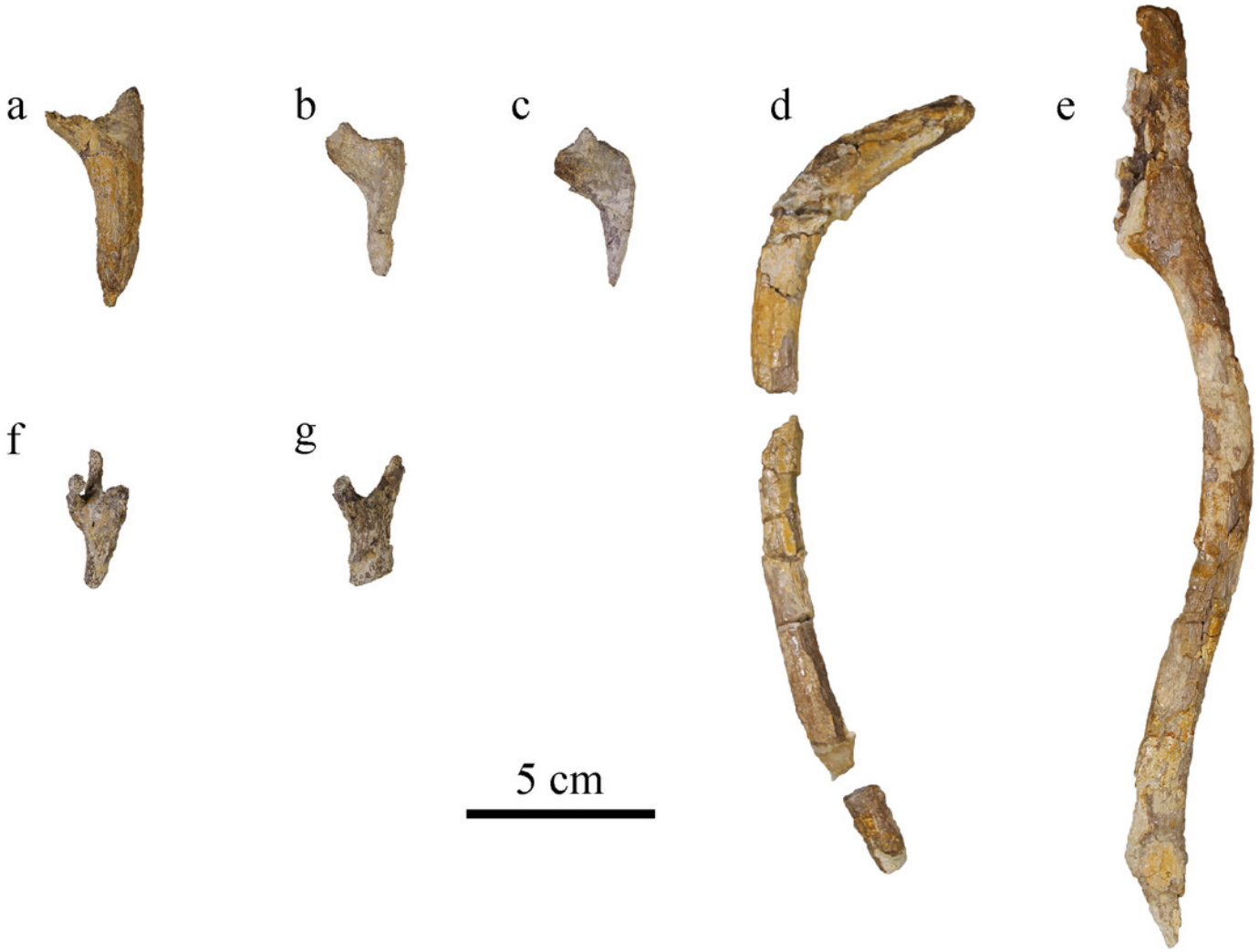

Figure 16

MJSN BSY008-465, holotype of *Torvoneustes jurensis* (Kimmeridgian, Porrentruy, Switzerland).

Right femur in (a) medial and (b) lateral views; (c) left ischium in lateral view; (d) right fibula in lateral view.

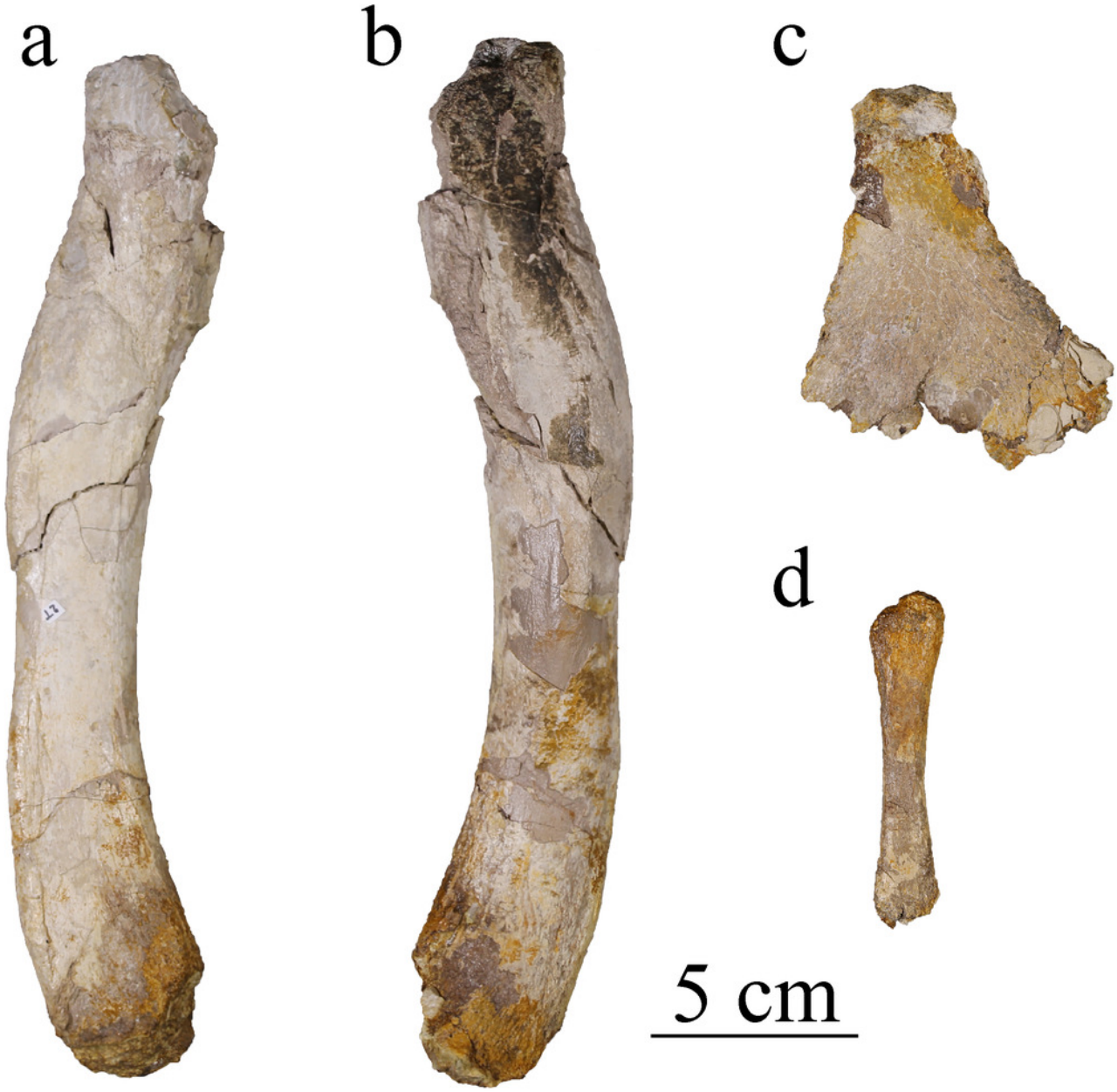
a
b
c
d
5 cm

Figure 17

Phylogenetic placement of MJSN BSY008-465 (*Torvoneustes jurensis* sp. nov.) within Geosaurinae in the parsimony analyses.

(a) strict consensus topology for the unweighted analysis; (b) strict consensus topology for the strongly downweighted analyses (k = 1 and k = 3), (c) strict consensus topology for the moderately downweighted analyses (k = 7 and k = 10); (d) strict consensus topology for the moderately to weakly downweighted analyses (k = 15, k = 20 and k = 50). Numbers indicate clades: 1. Geosaurinae, 2. Geosaurini, 3. E-clade. Complete strict consensus trees are provided in supplementary material S1.

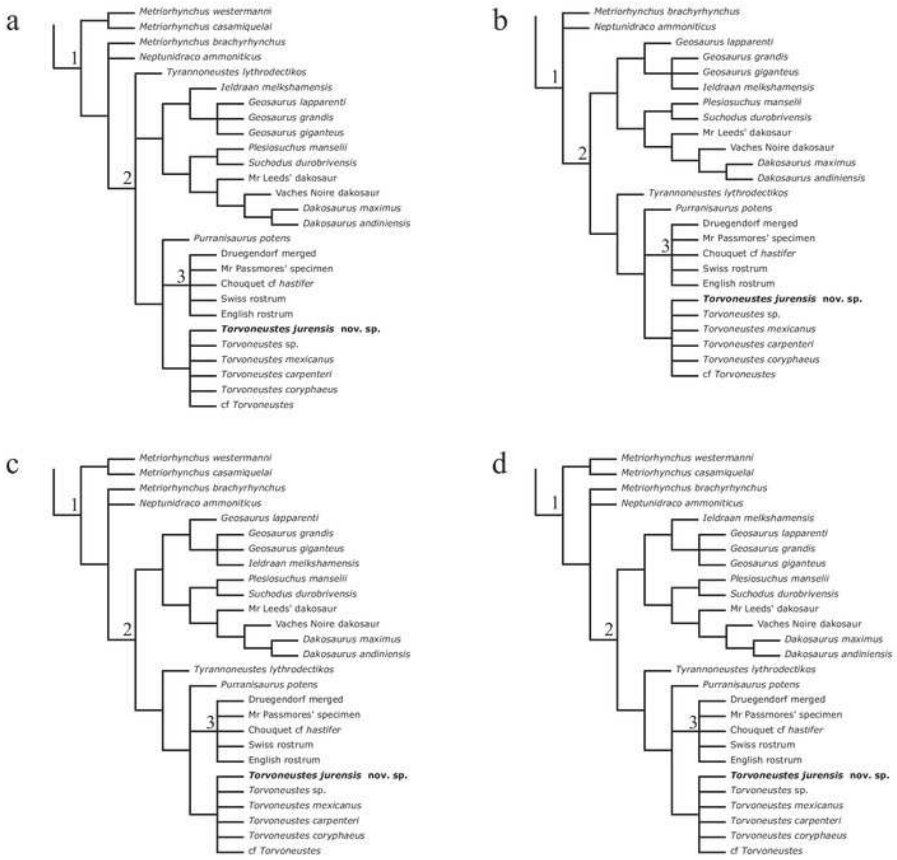
a
Metriorhynchus westermanni
Metriorhynchus casamiquelai
Metriorhynchus brachyrhynchus
Neptunidraco ammoniticus
Tyrannoneustes lythrodectikos
Ieldraan melkshamensis
Geosaurus lapparenti
Geosaurus grandis
Geosaurus giganteus
Plesiosuchus manselii
Suchodus durobrivensis
Mr Leeds' dakosaur
Vaches Noire dakosaur
Dakosaurus maximus
Dakosaurus andiniensis
Purranisaurus potens
Druegendorf merged
Mr Passmores' specimen
Chouquet cf hastifer
Swiss rostrum
English rostrum
Torvoneustes jurensis nov. sp.
Torvoneustes sp.
Torvoneustes mexicanus
Torvoneustes carpenteri
Torvoneustes coryphaeus
cf Torvoneustes
1
2
3
b
Metriorhynchus brachyrhynchus
Neptunidraco ammoniticus
Geosaurus lapparenti
Geosaurus grandis
Geosaurus giganteus
Ieldraan melkshamensis
Plesiosuchus manselii
Suchodus durobrivensis
Mr Leeds' dakosaur
Vaches Noire dakosaur
Dakosaurus maximus
Dakosaurus andiniensis
Tyrannoneustes lythrodectikos
Purranisaurus potens
Druegendorf merged
Mr Passmores' specimen
Chouquet cf hastifer
Swiss rostrum
English rostrum
Torvoneustes jurensis nov. sp.
Torvoneustes sp.
Torvoneustes mexicanus
Torvoneustes carpenteri
Torvoneustes coryphaeus
cf Torvoneustes
1
2
3
c
Metriorhynchus westermanni
Metriorhynchus casamiquelai
Metriorhynchus brachyrhynchus
Neptunidraco ammoniticus
Geosaurus lapparenti
Geosaurus grandis
Geosaurus giganteus
Ieldraan melkshamensis
Plesiosuchus manselii
Suchodus durobrivensis
Mr Leeds' dakosaur
Vaches Noire dakosaur
Dakosaurus maximus
Dakosaurus andiniensis
Tyrannoneustes lythrodectikos
Purranisaurus potens
Druegendorf merged
Mr Passmores' specimen
Chouquet cf hastifer
Swiss rostrum
English rostrum
Torvoneustes jurensis nov. sp.
Torvoneustes sp.
Torvoneustes mexicanus
Torvoneustes carpenteri
Torvoneustes coryphaeus
cf Torvoneustes
1
2
3
d
Metriorhynchus westermanni
Metriorhynchus casamiquelai
Metriorhynchus brachyrhynchus
Neptunidraco ammoniticus
Ieldraan melkshamensis
Geosaurus lapparenti
Geosaurus grandis
Geosaurus giganteus
Plesiosuchus manselii
Suchodus durobrivensis
Mr Leeds' dakosaur
Vaches Noire dakosaur
Dakosaurus maximus
Dakosaurus andiniensis
Tyrannoneustes lythrodectikos
Purranisaurus potens
Druegendorf merged
Mr Passmores' specimen
Chouquet cf hastifer
Swiss rostrum
English rostrum
Torvoneustes jurensis nov. sp.
Torvoneustes sp.
Torvoneustes mexicanus
Torvoneustes carpenteri
Torvoneustes coryphaeus
cf Torvoneustes
1
2
3

Figure 18

Phylogenetic placement of MJSN BSY008-465 (*Torvoneustes jurensis* sp. nov.) within Geosaurinae after pruning of unstable taxa.

(a) maximum agreement subtree for the unweighted analysis; (b) maximum agreement subtree for the strongly downweighted analyses (k = 1 and k = 3); (c) maximum agreement subtree for the moderately downweighted analyses (k = 7 and k = 10); (d) maximum agreement subtree for the moderately to weakly downweighted analyses (k = 15, k = 20 and k = 50). Numbers indicate clades: 1. Geosaurinae, 2. Geosaurini, 3. E- clade. Complete pruned consensus trees are provided in supplementary material S2

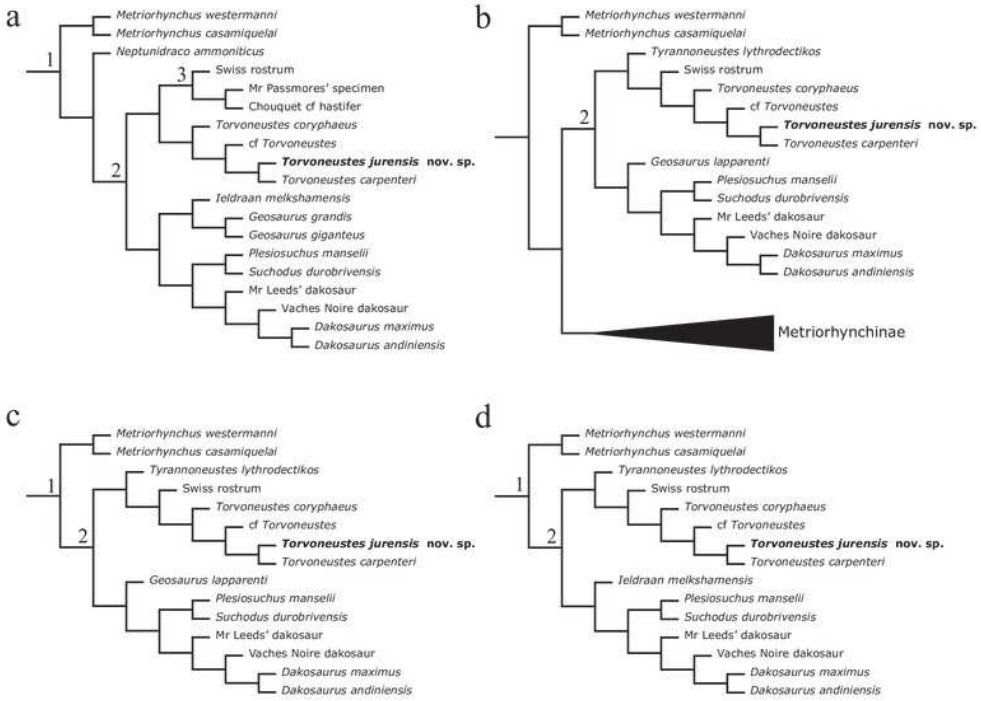
a
Metriorhynchus westermanni
Metriorhynchus casamiquelai
Neptunidraco ammoniticus
Swiss rostrum
Mr Passmores' specimen
Chouquet cf hastifer
Torvoneustes coryphaeus
cf Torvoneustes
Torvoneustes jurensis nov. sp.
Torvoneustes carpenteri
Ieldraan melkshamensis
Geosaurus grandis
Geosaurus giganteus
Plesiosuchus manselii
Suchodus durobrivensis
Mr Leeds' dakosaur
Vaches Noire dakosaur
Dakosaurus maximus
Dakosaurus andiniensis
1
2
3
b
Metriorhynchus westermanni
Metriorhynchus casamiquelai
Tyrannoneustes lythrodectikos
Swiss rostrum
Torvoneustes coryphaeus
cf Torvoneustes
Torvoneustes jurensis nov. sp.
Torvoneustes carpenteri
Geosaurus lapparenti
Plesiosuchus manselii
Suchodus durobrivensis
Mr Leeds' dakosaur
Vaches Noire dakosaur
Dakosaurus maximus
Dakosaurus andiniensis
Metriorhynchinae
2
c
Metriorhynchus westermanni
Metriorhynchus casamiquelai
Tyrannoneustes lythrodectikos
Swiss rostrum
Torvoneustes coryphaeus
cf Torvoneustes
Torvoneustes jurensis nov. sp.
Torvoneustes carpenteri
Geosaurus lapparenti
Plesiosuchus manselii
Suchodus durobrivensis
Mr Leeds' dakosaur
Vaches Noire dakosaur
Dakosaurus maximus
Dakosaurus andiniensis
1
2
d
Metriorhynchus westermanni
Metriorhynchus casamiquelai
Tyrannoneustes lythrodectikos
Swiss rostrum
Torvoneustes coryphaeus
cf Torvoneustes
Torvoneustes jurensis nov. sp.
Torvoneustes carpenteri
Ieldraan melkshamensis
Plesiosuchus manselii
Suchodus durobrivensis
Mr Leeds' dakosaur
Vaches Noire dakosaur
Dakosaurus maximus
Dakosaurus andiniensis
1
2

Figure 19

Phylogenetic placement of MJSN BSY008-465 (*Torvoneustes jurensis* sp. nov) within Metriorhynchidae in the Bayesian analysis

Numbers in red represent node support values. Numbers on the tree branches indicate clades: 1. Metriorhynchidae, 2. Geosaurinae and 3. Geosaurini. Complete tree is provided in supplementary material S3.

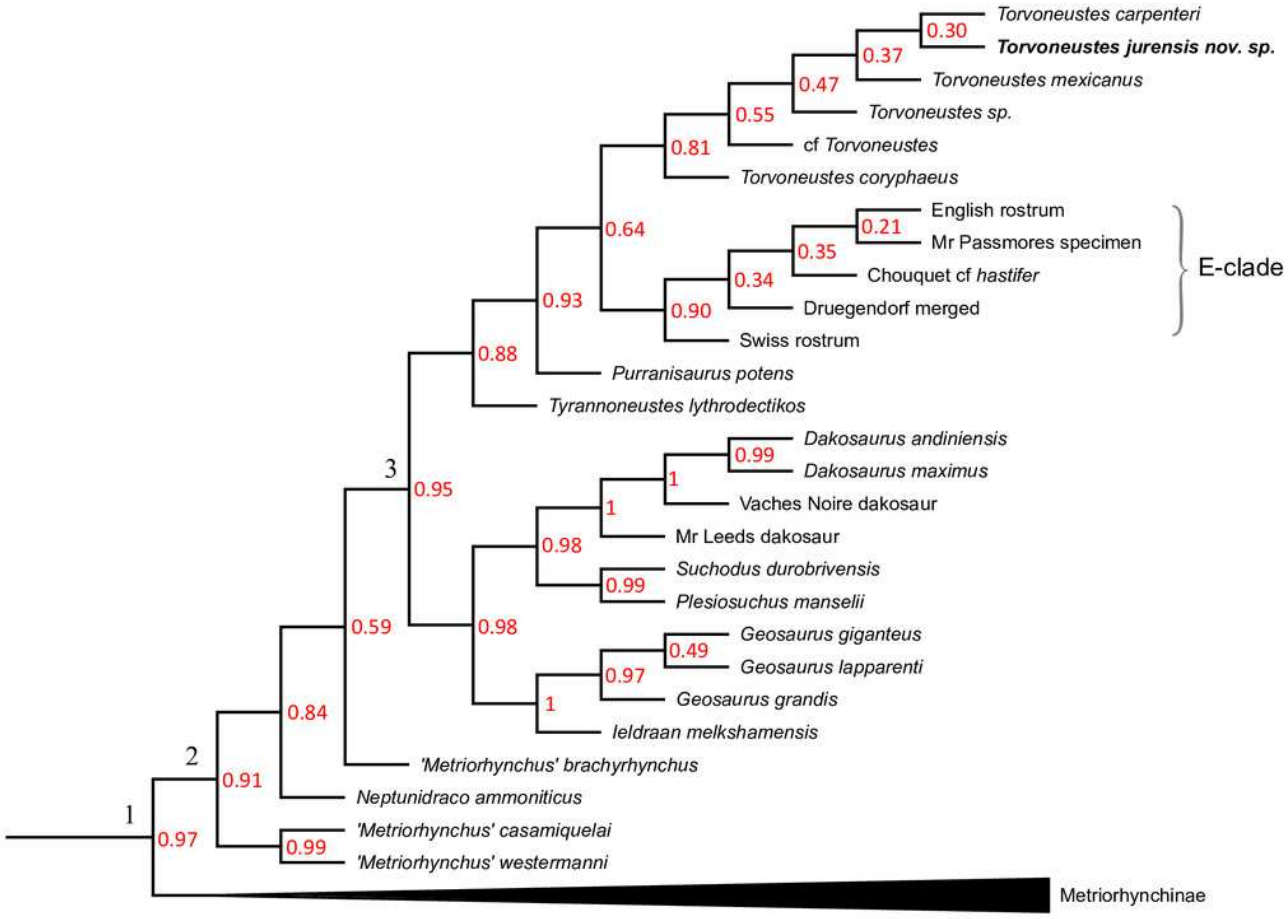

Figure 20

Life reconstruction of Torvoneustes jurensis MJSN BSY008-465 in its paleoenvironment.

Artwork by SDSO.

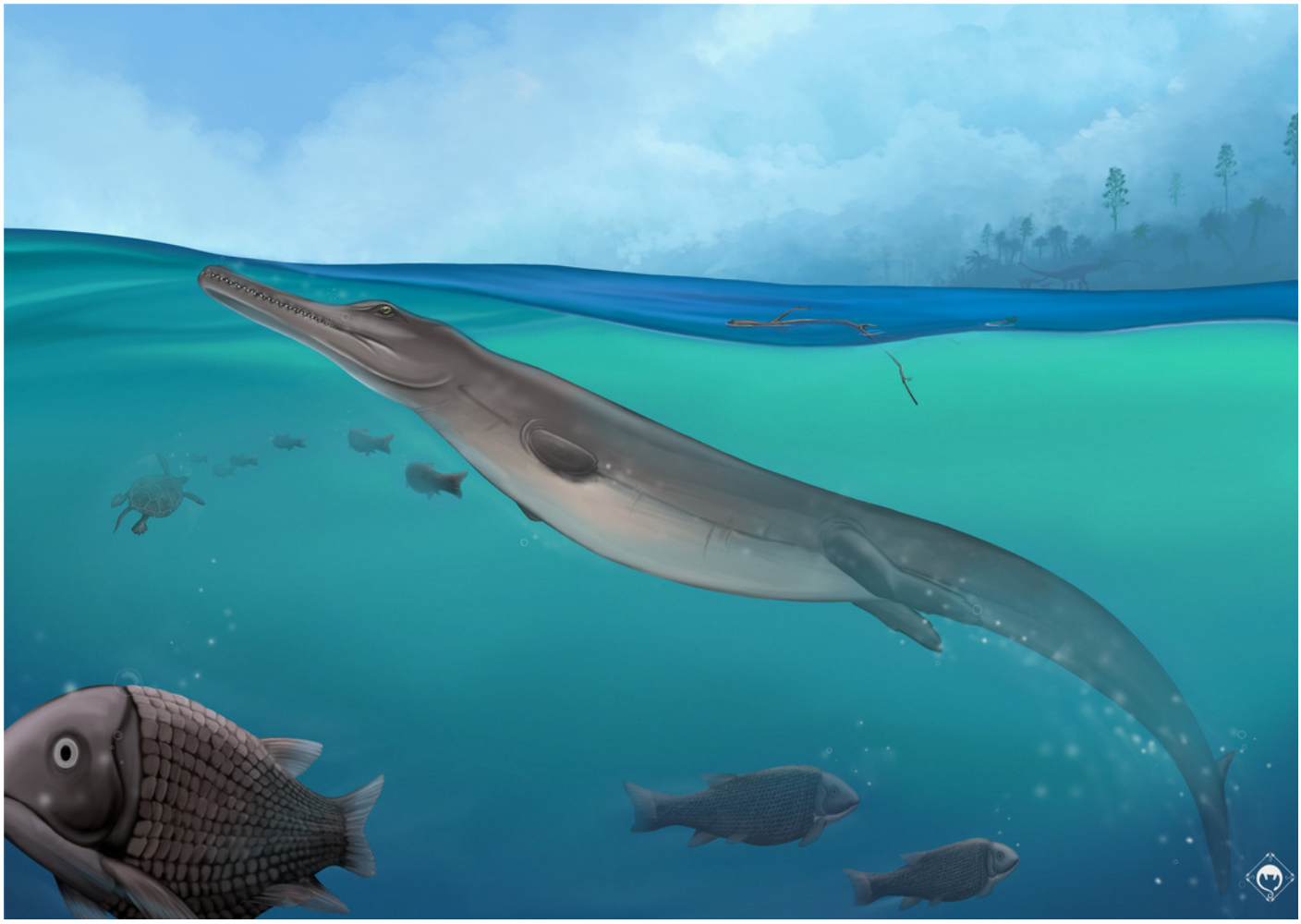

Table 1(on next page)

Overview of the Kimmeridgian-Lower Tithonian metriorhynchids species and a few of their dental characteristics.

Gracilineustes acutus is excluded from the table due to the lack of information. The specimen was lost during WW2, the same goes for Rhacheosaurus gracilis NHMUK PV R 3948 for whom the teeth or alveoli are indistinguishable, while Rhacheosaurus cf. gracilis LF 2426 skull is not entirely represented. Therein the distinction between "true ziphodont" and "false ziphodont" condition as defined by Andrade *et al.*, (2010) is not specified. The estimated tooth count is from the referred articles; the denticle density for Dakosaurus maximus and Geosaurus grandis from Andrade *et al*., (2010) and for Torvoneustes mexicanus from Barrientos-Lara *et al*., (2016).

Family	Metriorhynchinae									Geosaurinae								
Tribe	Rhacheosaurinae									Geosaurini								
Species	*Cricosaurus suevicus* (Fraas, 1901, 1902, SMNS 9808)	*Cricosaurus albersdoerferi* (Sachs *et al.*, 2021, BMMS-BK 1-2)	*Cricosaurus elegans* (Wagner, 1852, BSPG AS I 504)	*Cricosaurus bambergensis* (Sachs *et al.*, 2019, NKMB-P-Watt 14/274)	*Cricosaurus arauhuti* (Herrera *et al.*, 2021, SNSB-BSPG 1973 I 195)	*Maledictosuchus nuyiviianan* (Barrientos-Lara *et al.*, 2018, IGM 4863)	*Cricosaurus' saltillensis* (Buchy *et al.*, 2013, MUDECPC 487)	*Metriorhynchus paleobrosus* (Phillips, 1871, Grange & Benton, 1996, (OUMNHJ.29823)	Metriorhynchus Geoffroyii (Me. Brevirostris) (Young *et al.*, 2020; MHNGV-2232)	*Metriorhynchus' cf hastifer* (Chouquet cf '*hastifer*', Lepage *et al.*, 2008, Eudes-Deslongchamps, 1867)	*Dakosaurus maximus* (Young *et al.*, 2012, SMNS 8203)	*Plesiosuchus manselii* (Young *et al.*, 2012, NHMUK PV OR 40103)	*Geosaurus giganteus* (Young & Andrade, 2009, NHMR.12299, NHM3700	*Geosaurus grandis* (Young et al., 2012, BSPG AS-VI-1)	*Torvoneustes carpenteri* (Grange & Benton, 1996, BRSMG Ce17365)	*Torvoneustes* (Young *et al.*, 2013, MJML K1863)	*Torvoneustes coryphaeus* (Young *et al.*, 2013, MJML K1863)	*Torvoneustes mexicanus* (Barrientos-Lara *et al.*, 2016, IGM 9026)	MJSNBSY0 08-465

													20)					
Age	Upper Kimmeridgian	Upper Kimmeridgian	Lower Tithonian	Upper Kimmeridgian	Lower Tithonian	Kimmeridgian	Lower Tithonian	Lower Tithonian	Lower Kimmeridgian	Kimmeridgian	Upper Kimmeridgian	Upper Kimmeridgian	Lower Tithonian	Lower Tithonian	Upper Kimmeridgian	Lower Kimmeridgian	Kimmeridgian	Upper Kimmeridgian
Country	Germany	Germany	Germany	Germany	Germany	Mexico	Mexico	United Kingdom	France	France	Germany	United Kingdom	Germany	Germany	United Kingdom	United Kingdom	Mexico	Switzerland
Tethorna mentation	Smooth	Smooth	Smooth	Smooth	Well spaced, low long itudinal ridges	Smooth labial side. discontinuous low apicobasal ridges on	faint apicobasally aligned subparallel ridges	?	?	Conspicious apicobasal ridges	Overall smooth	Low relief apicobasal ridges	Overall smooth	Smooth	Conspicious apicobasal ridges	Conspicious apicobasal ridges	Conspicious apicobasal ridges	Conspicious apicobasal ridges

						the lingual surface												
Carinae	Yes, faint	Yes, faint	Yes, faint	Yes, faint	Yes, at least unicarenate	Yes	Yes, faint	?	?	Yes	Yes, prominent	Yes, prominent	Yes, prominent	Yes, prominent	Yes, prominent	Yes, prominent	Yes, prominent	Yes, prominent
Denticules	No	No	No	No	No	No	No	?	?	?	Yes	Yes	Yes	Yes	Yes	Yes	Yes	Yes
Ziphodonty	/	/		/	/	/	/	?	?	?	Macro	Micro	Micro	Micro	Micro	Micro	Micro	Micro
Denticules density (number of denticle/5mm)	/	/		/	/	/	/	?	?		16-18	?	?	28, 1	?	?	30	30-40

Maxillary tooth count (absolute)	26	23		23	/	17	12	25 (OUMNHJ.29823)-27	14	20?	13	14	12 (NHM37020)	14	11	11	5	15
Maxillary tooth count (estimated)		23+		23+	/	26?	17	/	20+? (half of the rostrum is easily missing)	20+?		14 to 18	12+		14	17-19		Up to 21
Dentary tooth count (absolute)	24	22		18+	/	/	15	14	/	/	12	13	7 (NHM37020)		/	/	4	16
Dentary tooth co		22+		18+	/	/	~15?	14+	/	/			7+		/	/		Up to 17

unt (estimated)																		
Taphonomic condition	Complete specimen in limestone	Complete specimen in limestone	Skull in limestone	Complete specimen in limestone	Incomplete skull	Incomplete skull	Disarticulated skull	Skull. No teeth remaining	Anterior half of the rostrum, no teeth remaining	complete skull	Incomplete skull	Incomplete skull	NHMR.12229: middle portion of the skull and mandible, deformed. NHM		Heavily crushed, incomplete skull	Incomplete skull, hlaf of the rostrum missing	Fragmentary rostrum	Disarticulated skull

													37020: skull and mandible in limestone.					

1

Table 2(on next page)

Descriptives statistics of the cladograms resulting from the parsimony analysis.

In the unwieghted analysis, the number of Most Parsimonious Cladograms is higher than the storage capicity (20 000).

K	Number of MPCs	Length	CI	RI	RC	HI
-		2417	0,334	0,803	0,268	0,666
1	297	2072	0,389	0,845	0,329	0,611
3	297	2065	0,391	0,846	0,331	0,609
7	99	2044	0,395	0,848	0,335	0,605
10	99	2044	0,395	0,848	0,335	0,605
15	33	2034	0,397	0,85	0,337	0,603
20	33	2033	0,397	0,85	0,337	0,603
50	33	2033	0,397	0,85	0,337	0,603

1